KU LEUVEN

Update on modern muonic x-ray experiments

PSI

Stella Vogiatzi

On behalf of the RefRadii & muX collaborations

26-30 May, 2025

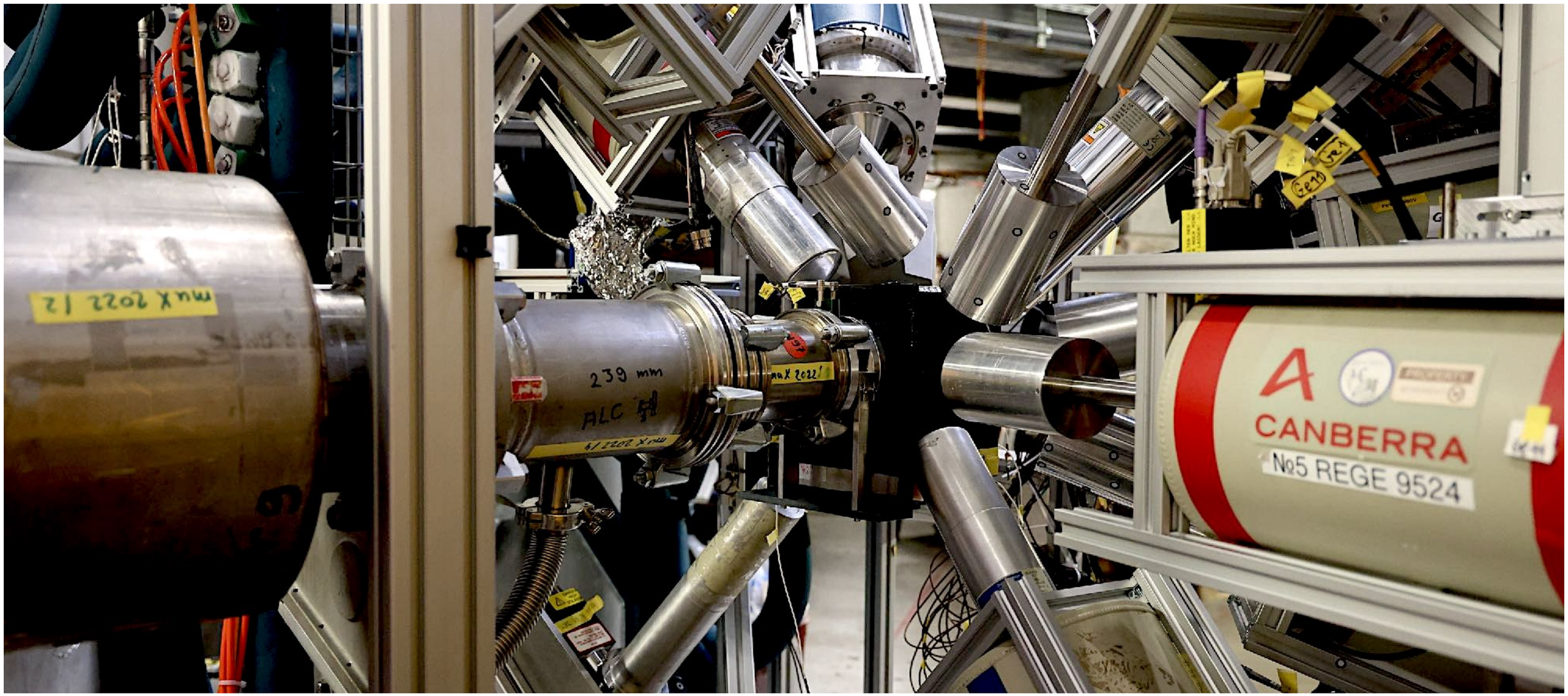

Our *exotic* muonic atom

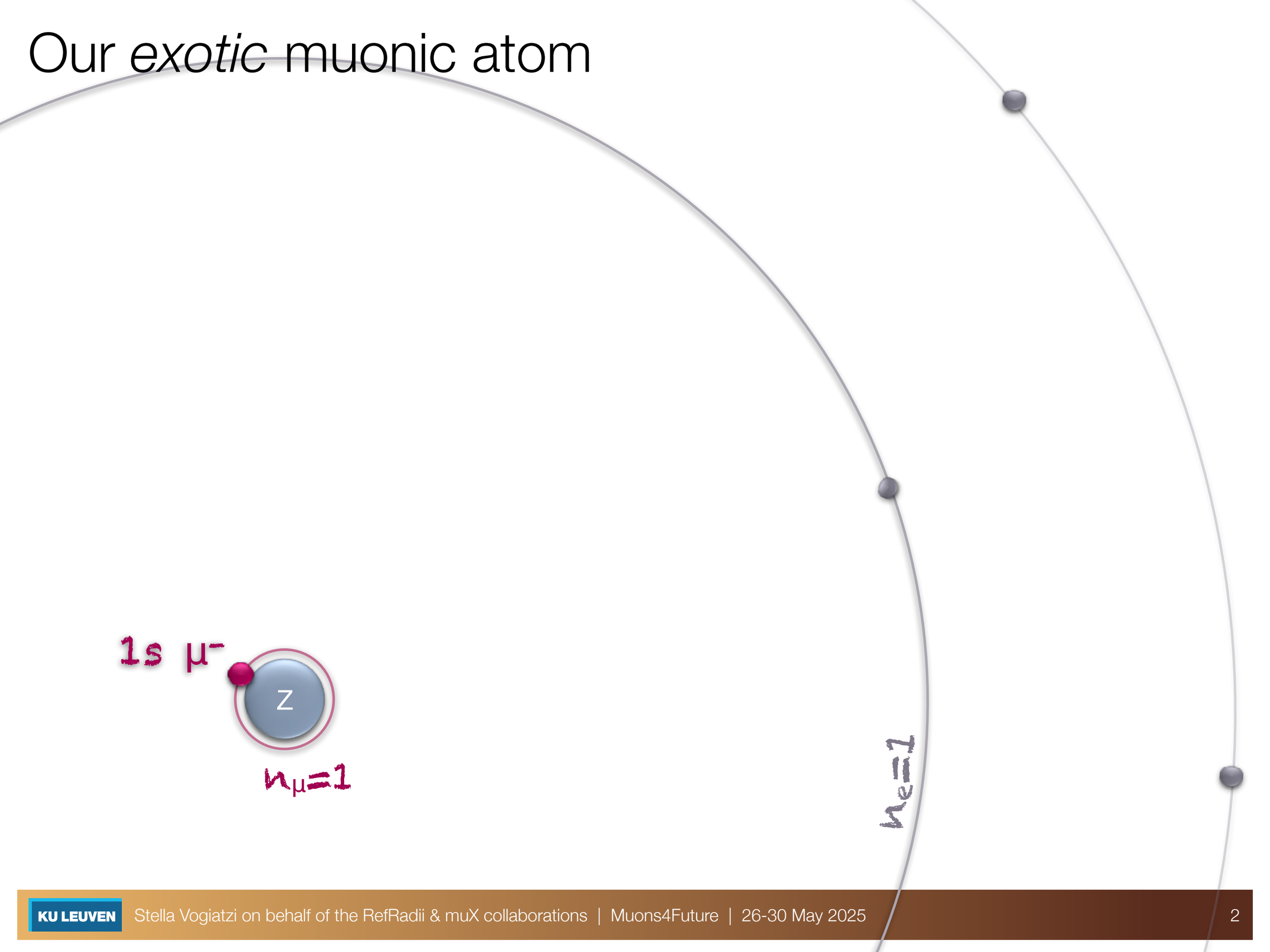

Our *exotic* muonic atom

Stopping negative muons **directly** to targets of >100 mg

Achtung! **...only when you have an abundant and stable target

From muon capture to the ground state

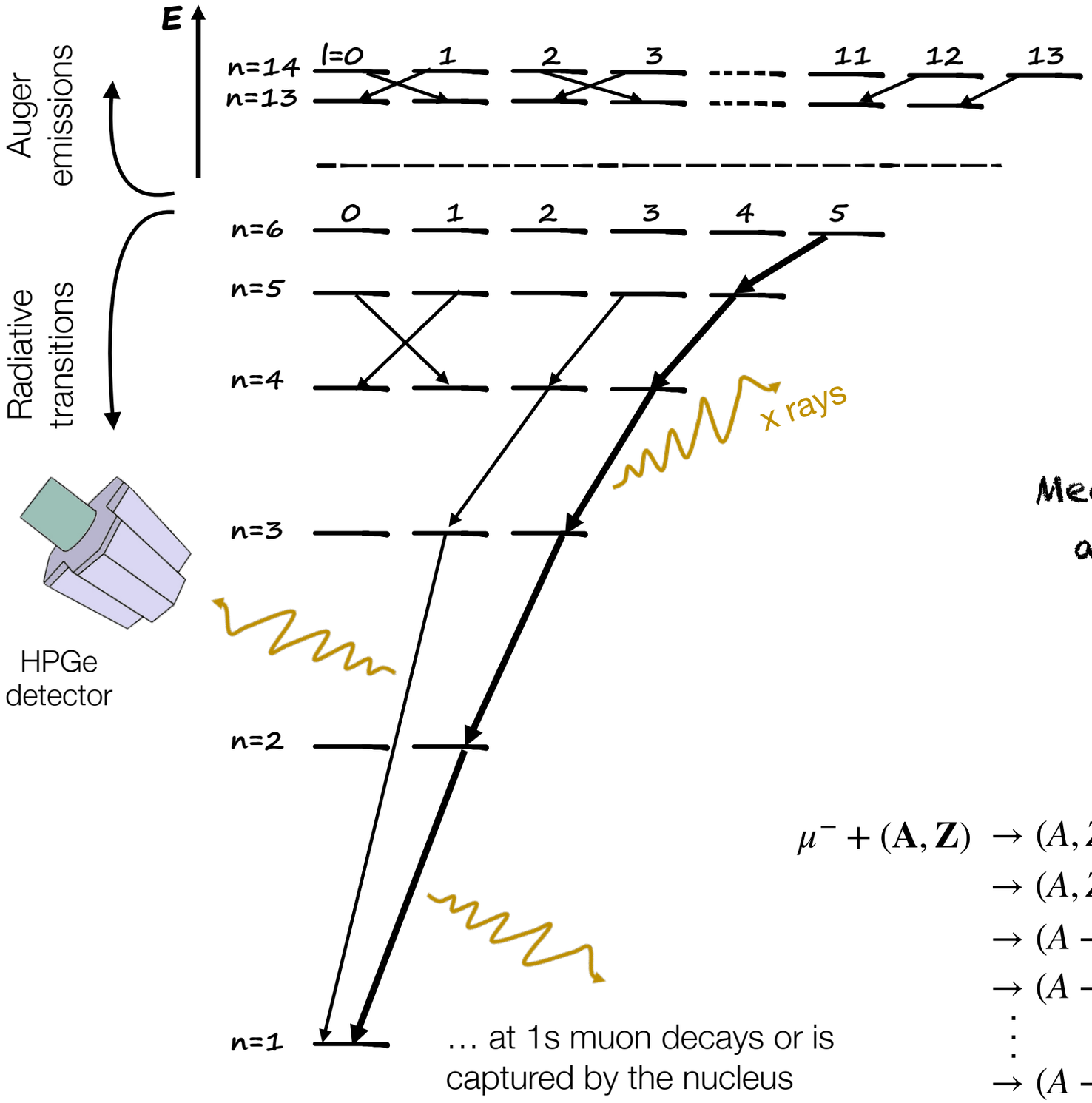

cascade starts at n~14

Measuring energies and intensities!

… at 1s muon decays or is captured by the nucleus

$$
\begin{aligned}
\mu^- + (\mathbf{A}, \mathbf{Z}) &\rightarrow (A, Z-1)^* + \nu_\mu \\
&\rightarrow (A, Z-1) + \gamma \\
&\rightarrow (A-1, Z-1) + \gamma + n \\
&\rightarrow (A-2, Z-1) + \gamma + 2n \\
&\vdots \\
&\rightarrow (A-2, Z-2) + \gamma + n + p
\end{aligned}
$$

Energy spectrum of a muonic atom
As seen by a HPGe detector

Eur. Phys. J. Plus 135, 777 (2020)

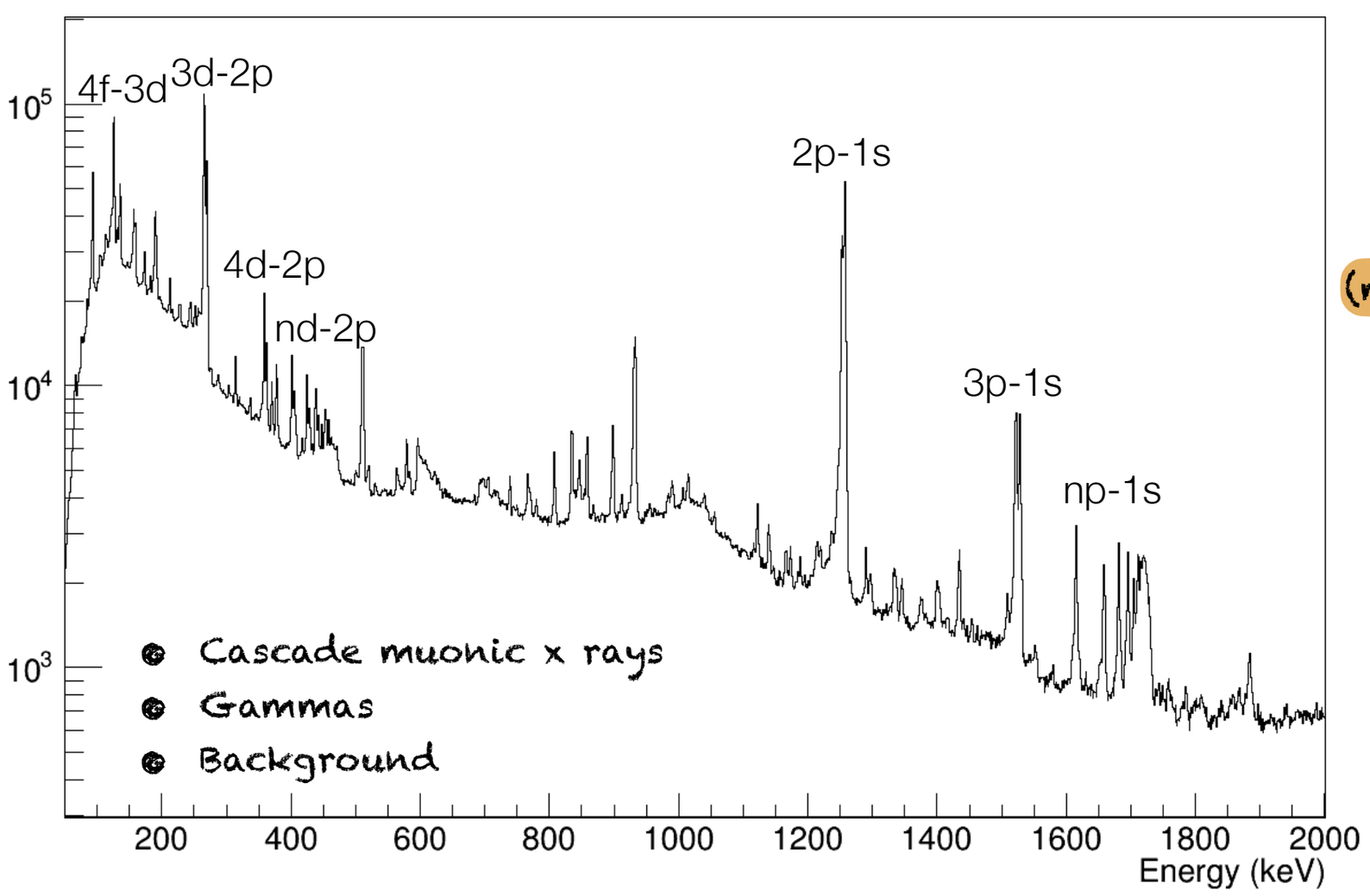

Muonic cascade intensities for elemental compositions (MIXE)

Muonic cascade energies for charge radii extraction (muX & Reference Radii & QUARTET)

mid- and heavy-isotopes (up to $_{96}$Cm) with HPGe

Low-masses ($_{3}$Li to $_{12}$Mg) with MMC

Nuclear capture gammas for capture rates (MONUMENT)

Science case

By measuring absolute nuclear charge radii…

- Benchmark laser spectroscopy results & challenge state-of-art nuclear models

- Provide better understanding of the underlying nuclear structure

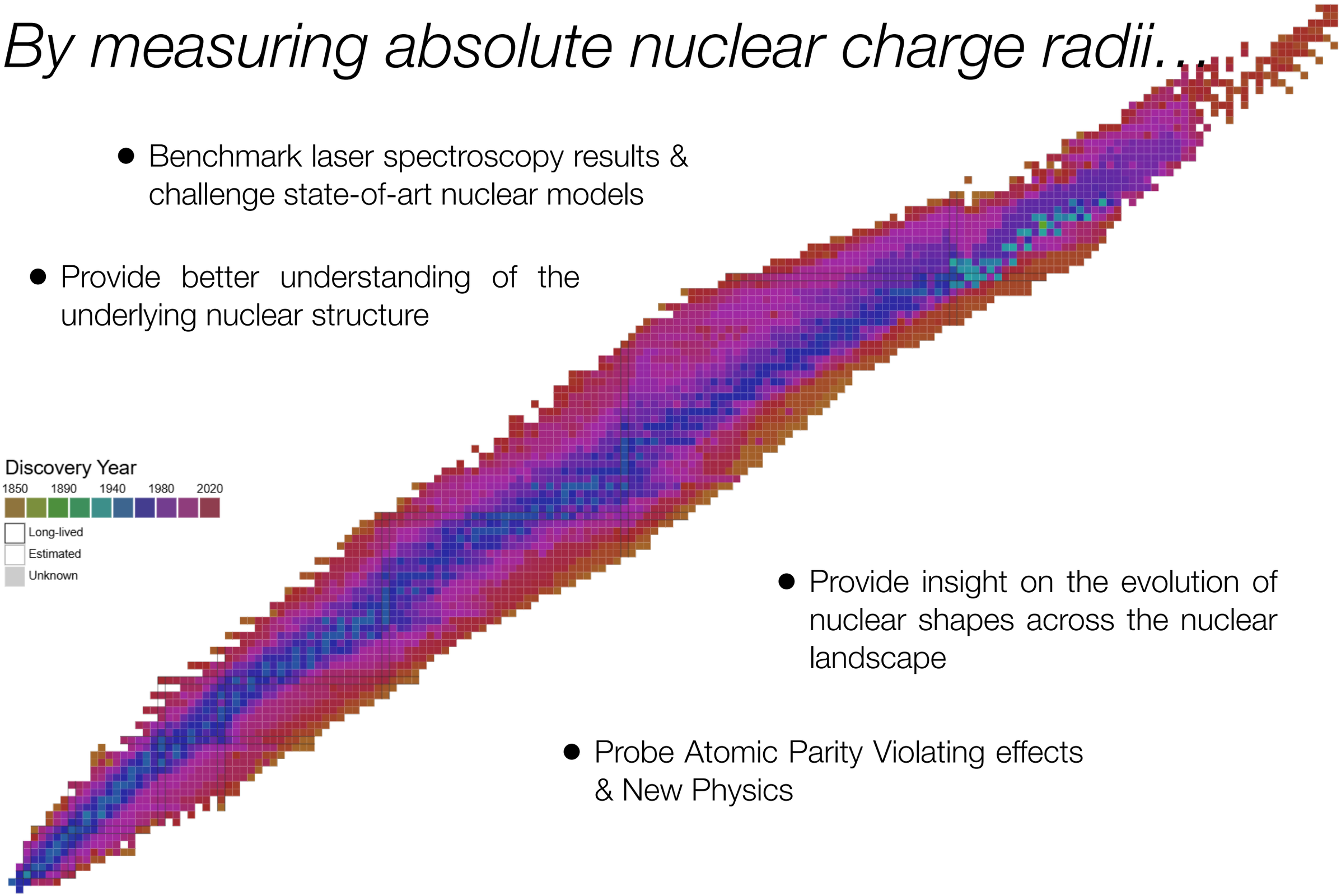

- Provide insight on the evolution of nuclear shapes across the nuclear landscape

- Probe Atomic Parity Violating effects & New Physics

Why not using electrons to probe charge radii?

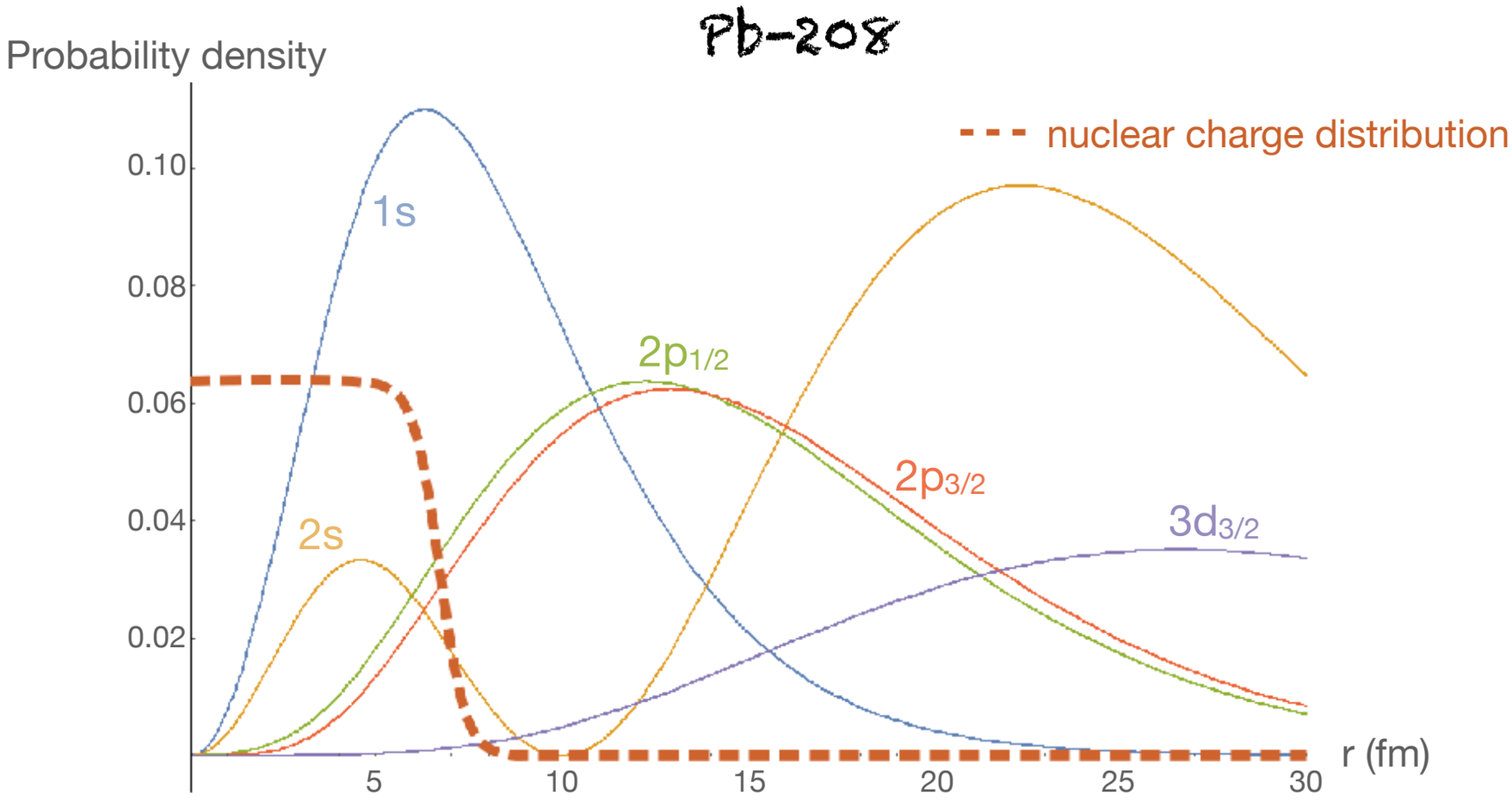

- Large overlap of the low-lying muonic states with the nuclear charge distribution.

- The measurement of the muonic energy levels allows to extract properties of the nucleus such as the charge radius

2p-1s transition most sensitive to R_N

$$R_N^2 = \langle r^2 \rangle = \frac{1}{Ze} \int d^3\vec{r}\, \rho(\vec{r})\, r^2$$

nuclear charge distribution

Back to the muonic cascade

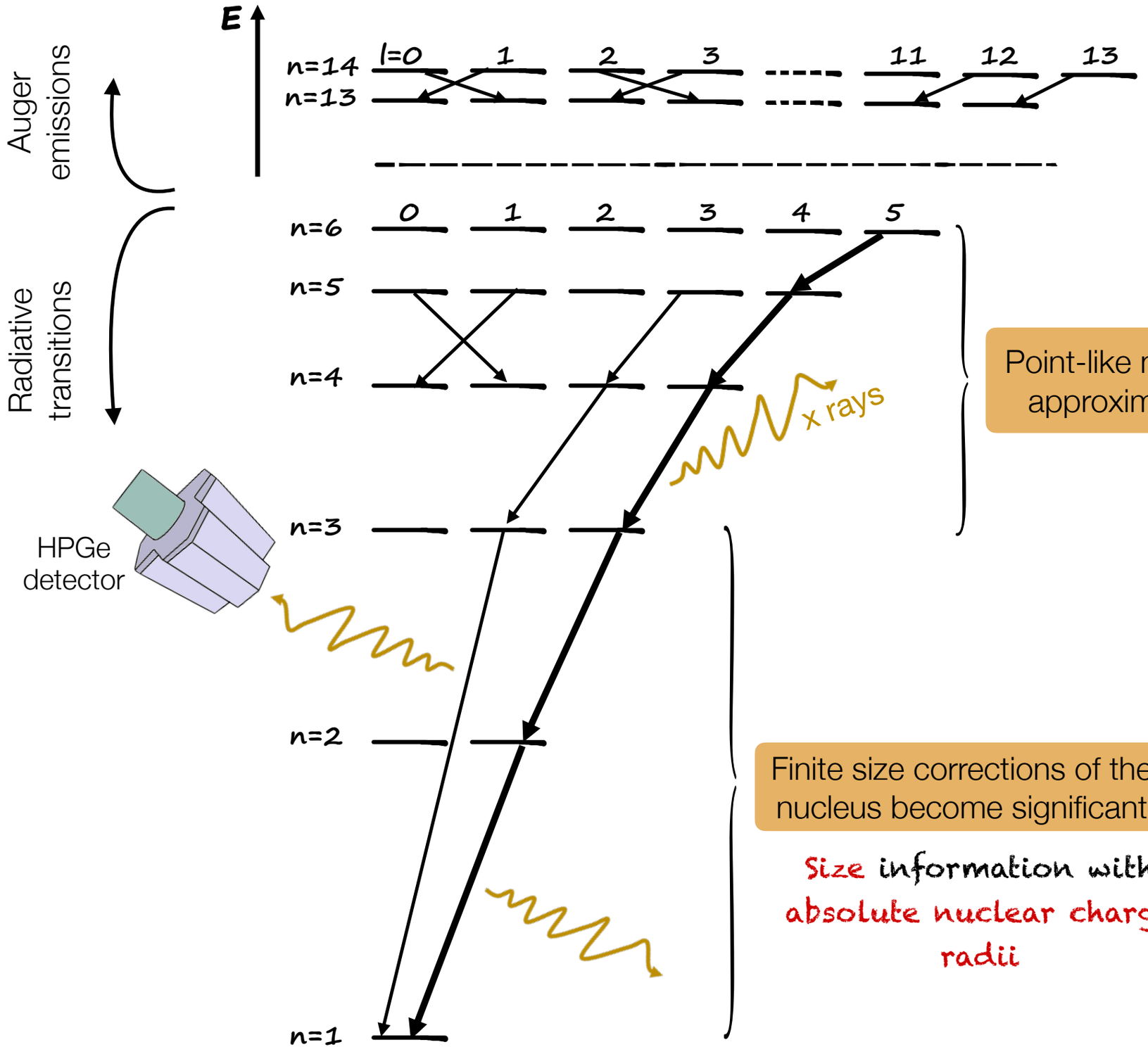

Point-like nucleus approximation

Finite size corrections of the nucleus become significant

Size information with absolute nuclear charge radii

Shape information with spectroscopic quadrupole moments

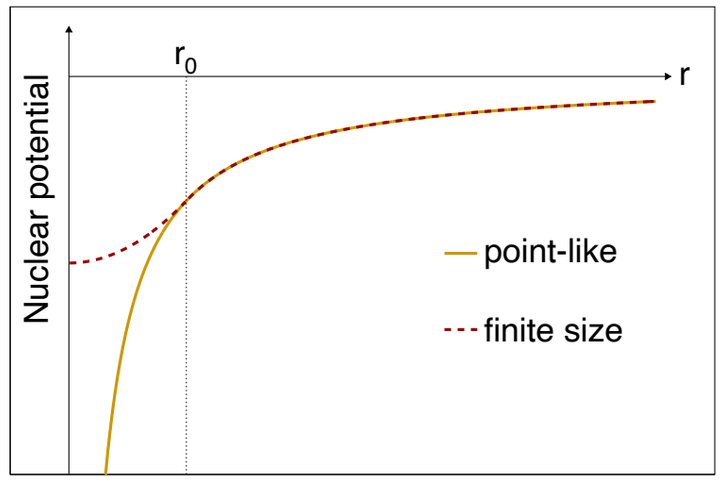

$E_{1s}(Z = 82) \sim 19\,\mathrm{MeV}$ (point nucleus)

$\sim 10.6\,\mathrm{MeV}$ (finite size)

Muonic atoms & Hyperfine Splitting

The bless and the curse

Fine splitting (FS): $\vec{J} = \vec{l} + \vec{s}$

Static hyperfine splitting (HFS): $\vec{F} = \vec{I} + \vec{J}$

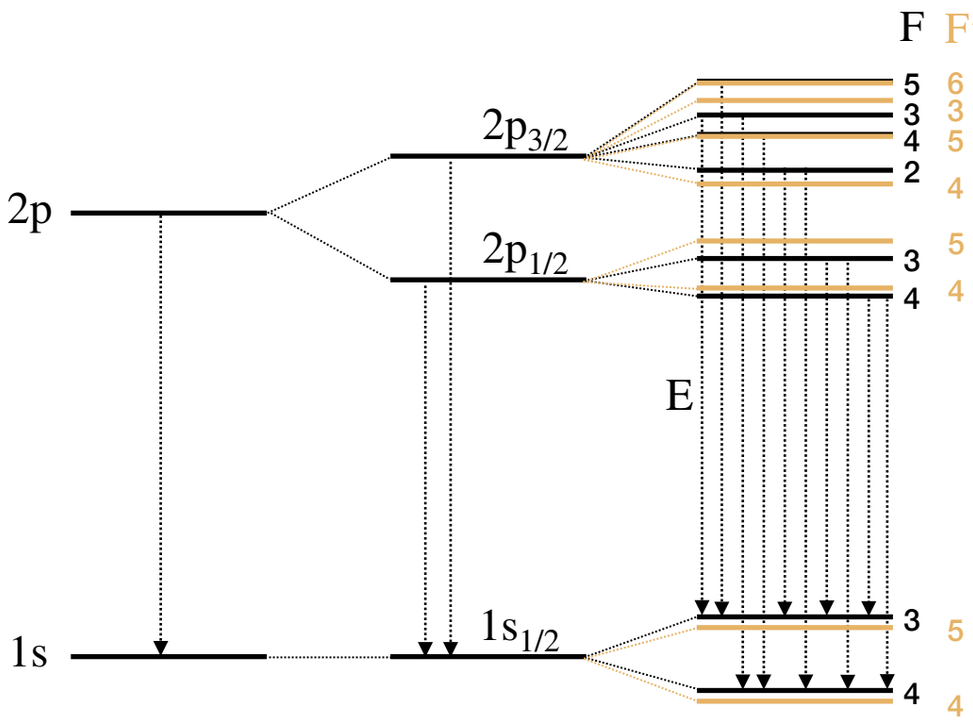

$$I_{ground} = \frac{7^+}{2} \quad I_{excited} = \frac{9^+}{2}$$

- Energy displacement due to the E2 and M1 interactions:

$$\Delta E_F(E2) = A_2\, 6 \frac{K(K+1) - 4/3\, I(I+1)J(J+1)}{4I(2I-1)J(2J-1)}$$

$$\Delta E_F(M1) = \frac{A_1}{2} \{F(F+1) - I(I+1) - J(J+1)\}$$

Dynamic HFS effect

- The hyperfine levels from ground and excited nuclear states are mixed due to the high energy of muonic transitions

- HFS also observed in even-even nuclei with zero spin in the ground state

How to extract nuclear charge parameters from measured muonic energies

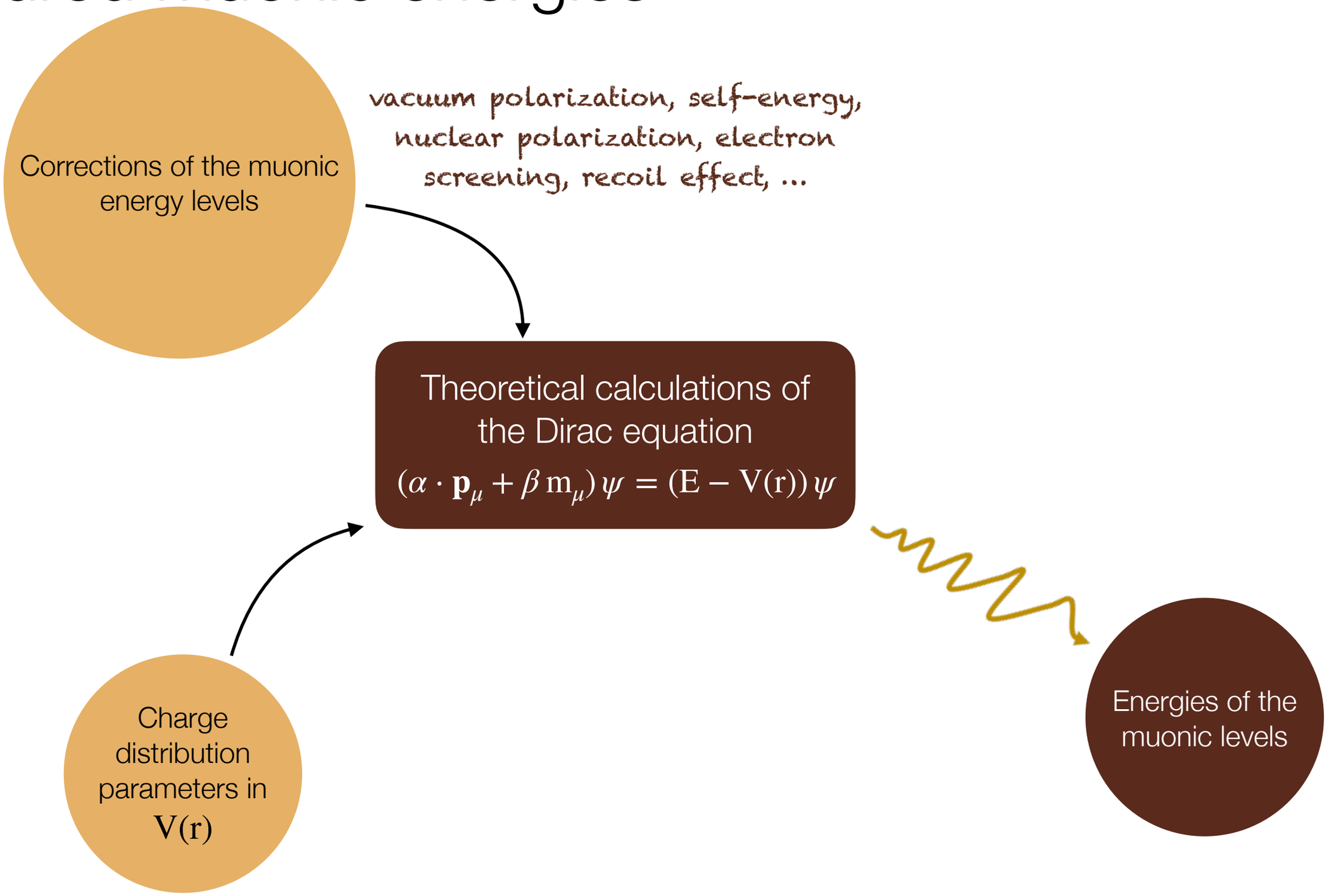

How to extract nuclear charge parameters from measured muonic energies

Corrections of the muonic energy levels

vacuum polarization, self-energy, nuclear polarization, electron screening, recoil effect, ...

Theoretical calculations of the Dirac equation

$$(\alpha \cdot \mathbf{p}_{\mu} + \beta\, \mathrm{m}_{\mu})\, \psi = (\mathrm{E} - \mathrm{V}(\mathrm{r}))\, \psi$$

Extract the charge distribution parameters

Measured energies by HPGe detectors

A technique used heavily in the past..

Angeli, I., & International Atomic Energy Agency, International Nuclear Data Committee, Vienna (Austria). (1999). Table of nuclear root mean square charge radii.

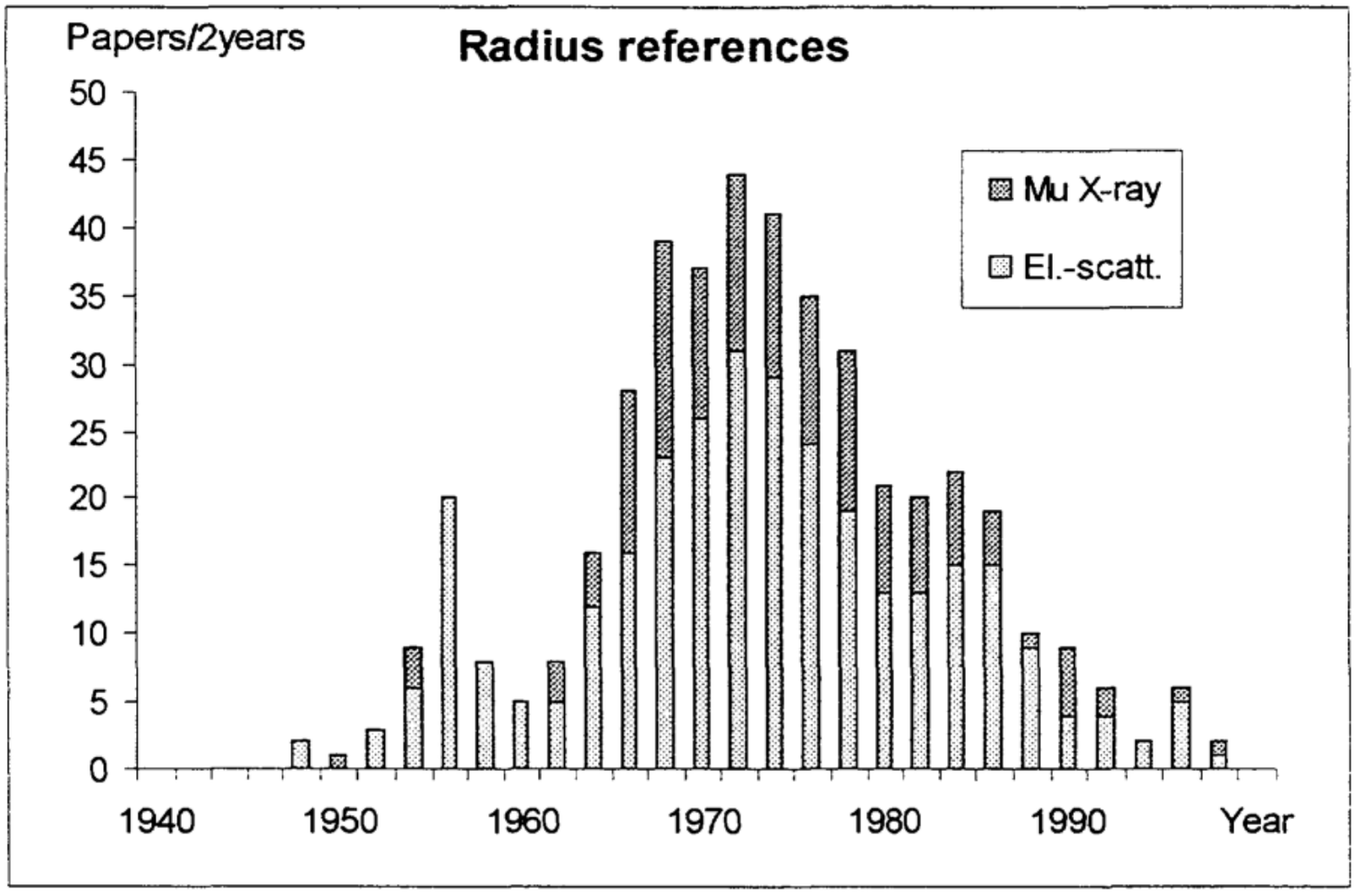

Down to a few microgram targets!!!

Extending measurements to rare and radioactive targets.

Paul Scherrer Institute

PSI

High Intensity Proton Accelerator (HIPA) facility at Paul Scherrer Institute

Detection system
Schematics

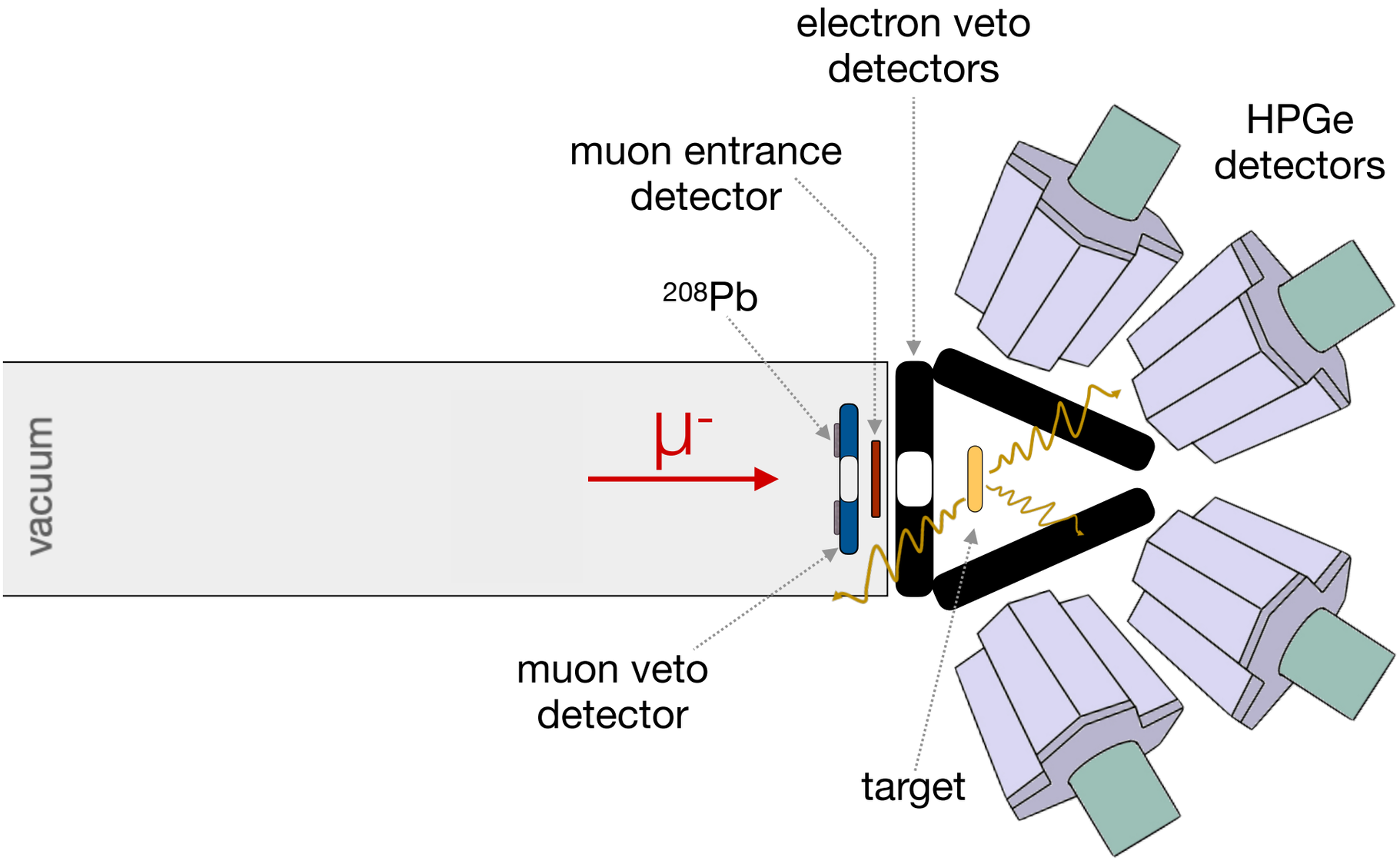

Macroscopic ^{28}Si target

Detection system
Muon-time correlated analysis

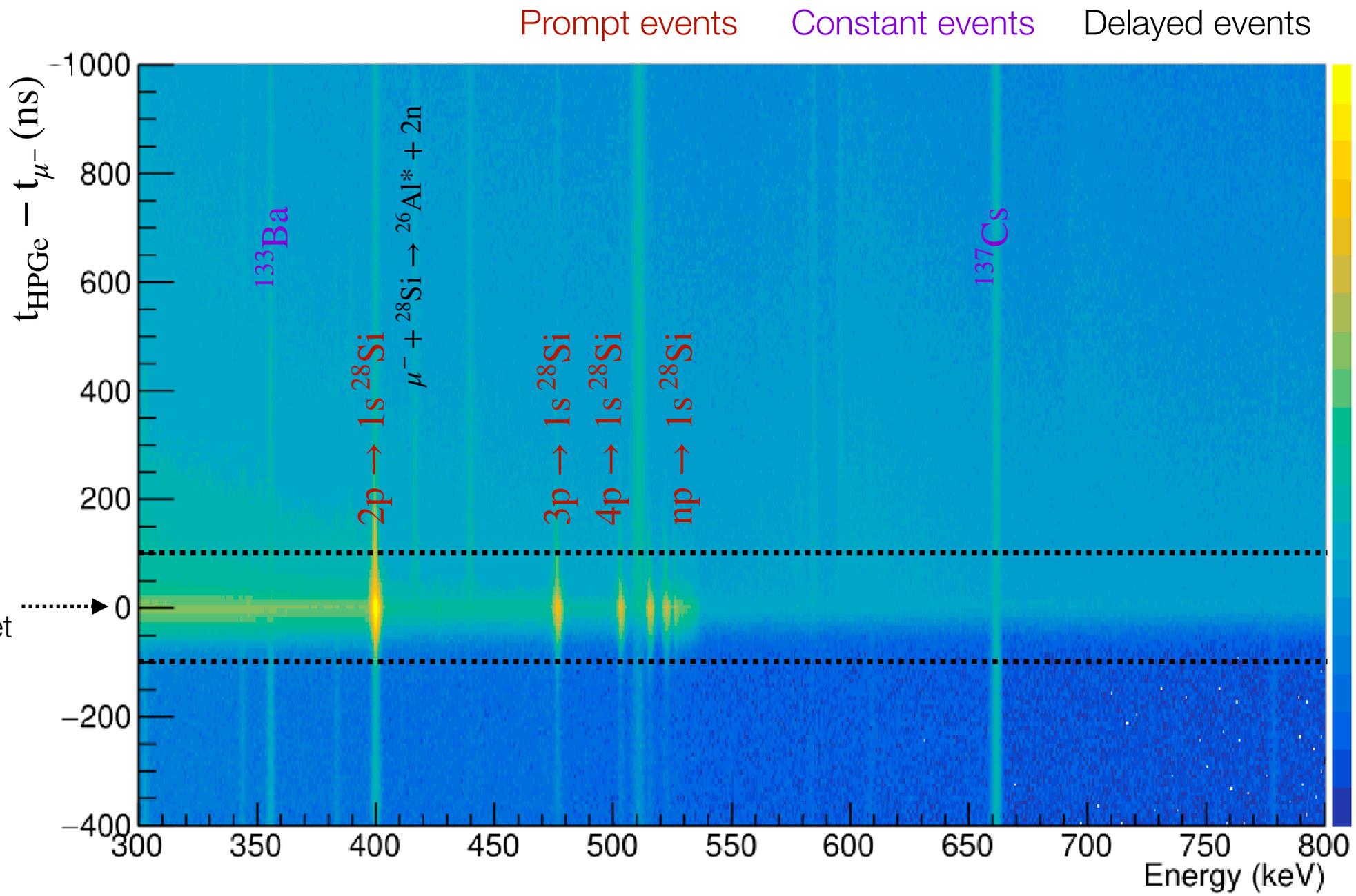

Time of the muon impinging on target

Detection system
Muon-time correlated analysis

After ELET : $FWHM_{dt} \sim 14$ nsec

Prompt events Constant events Delayed events

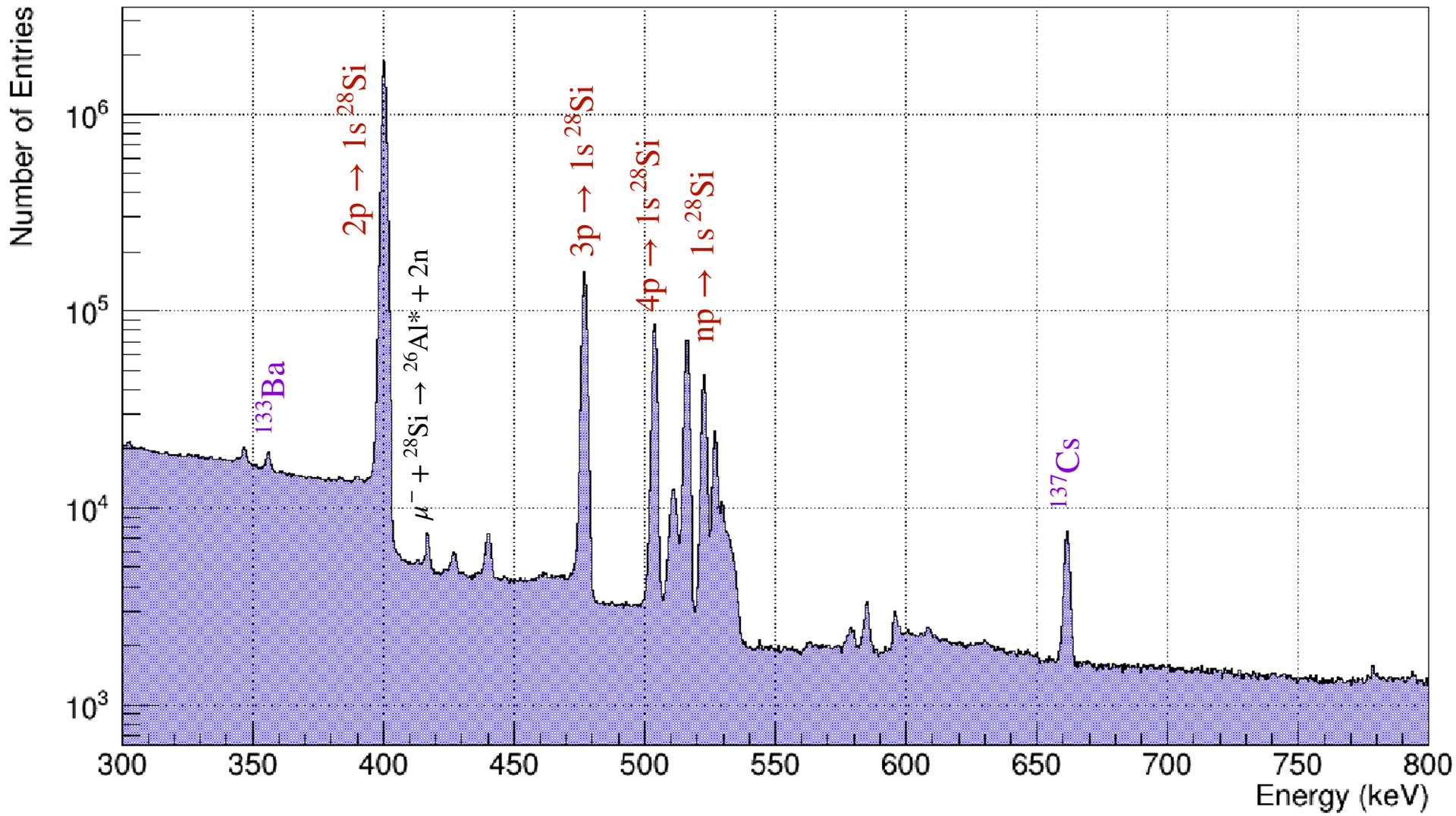

Experimental timeline

2016 — ^{185}Re and ^{187}Re (500 mg)

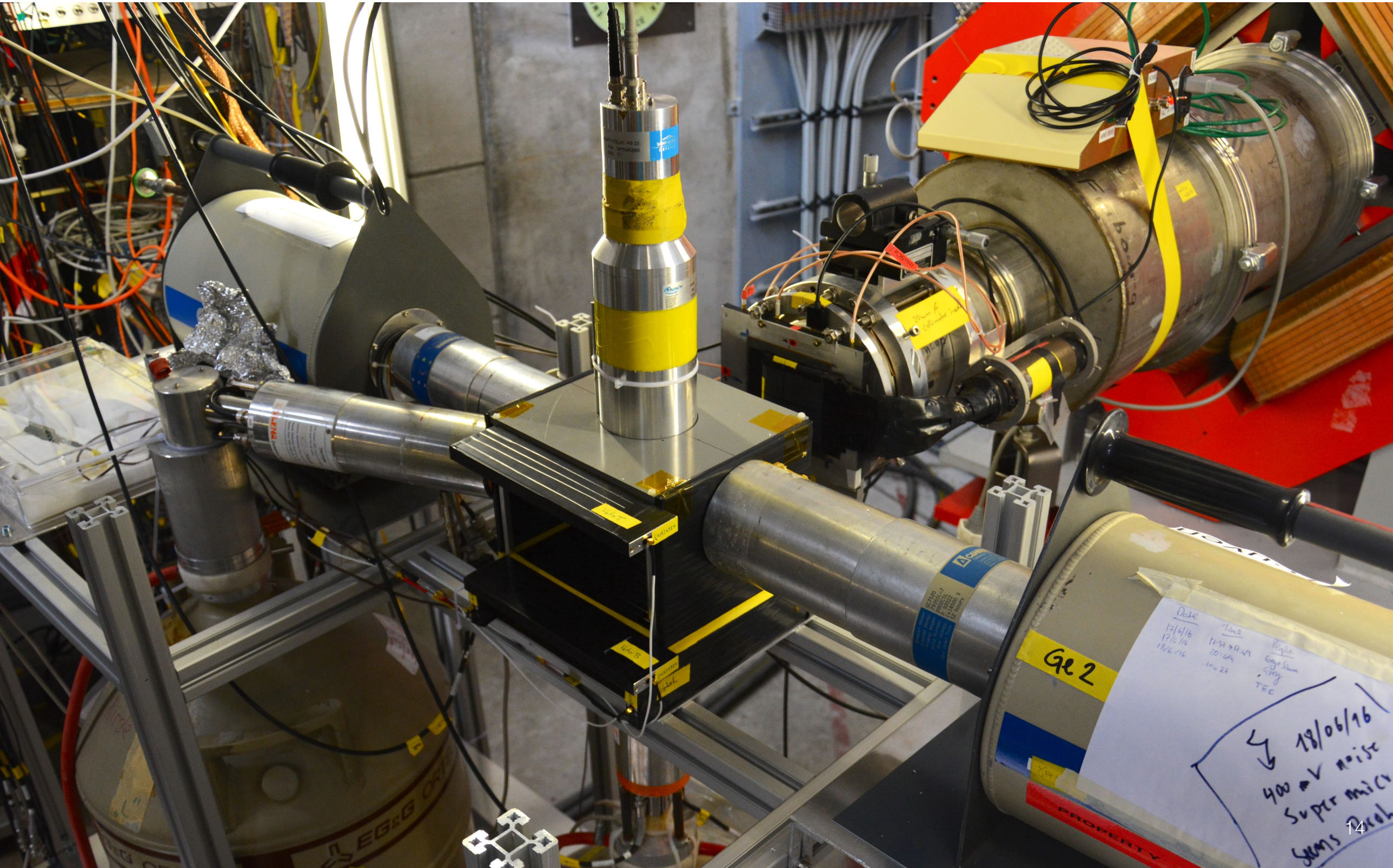

^{185}Re and ^{187}Re 5g4f analysis
Spectroscopic quadrupole moment

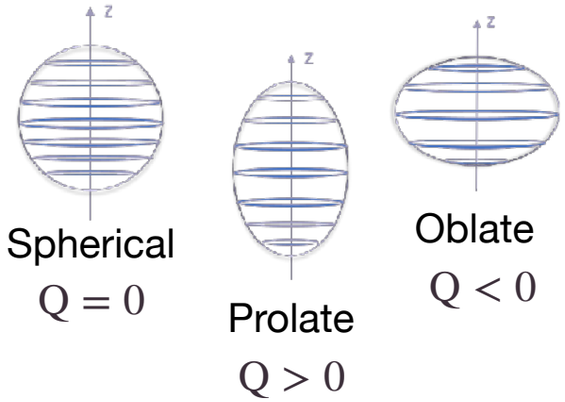

Phys. Rev. C 101, 054313 (2020)

Our first physics result

$$Q(^{185}\mathrm{Re}) = 2.07(5)\,\mathrm{b}$$

$$Q(^{187}\mathrm{Re}) = 1.94(5)\,\mathrm{b}$$

^{185}Re

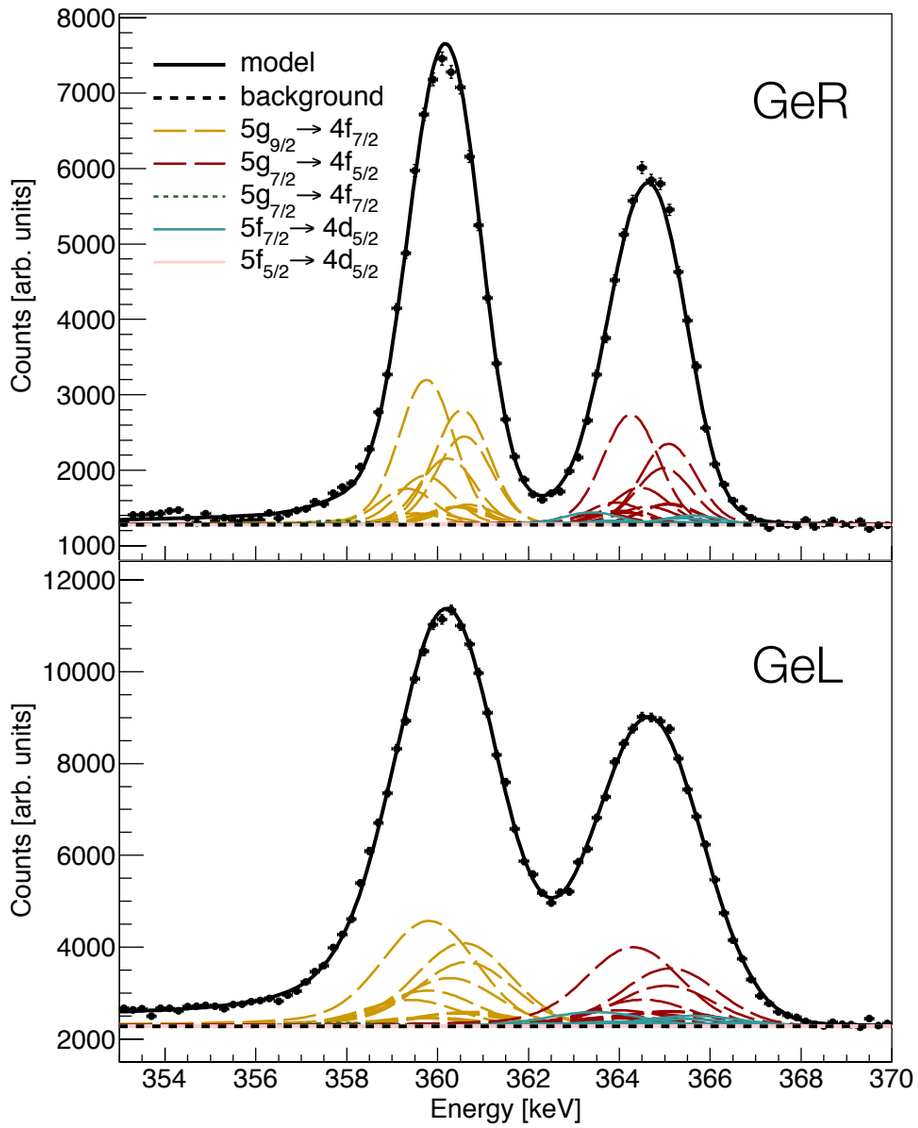

^{187}Re

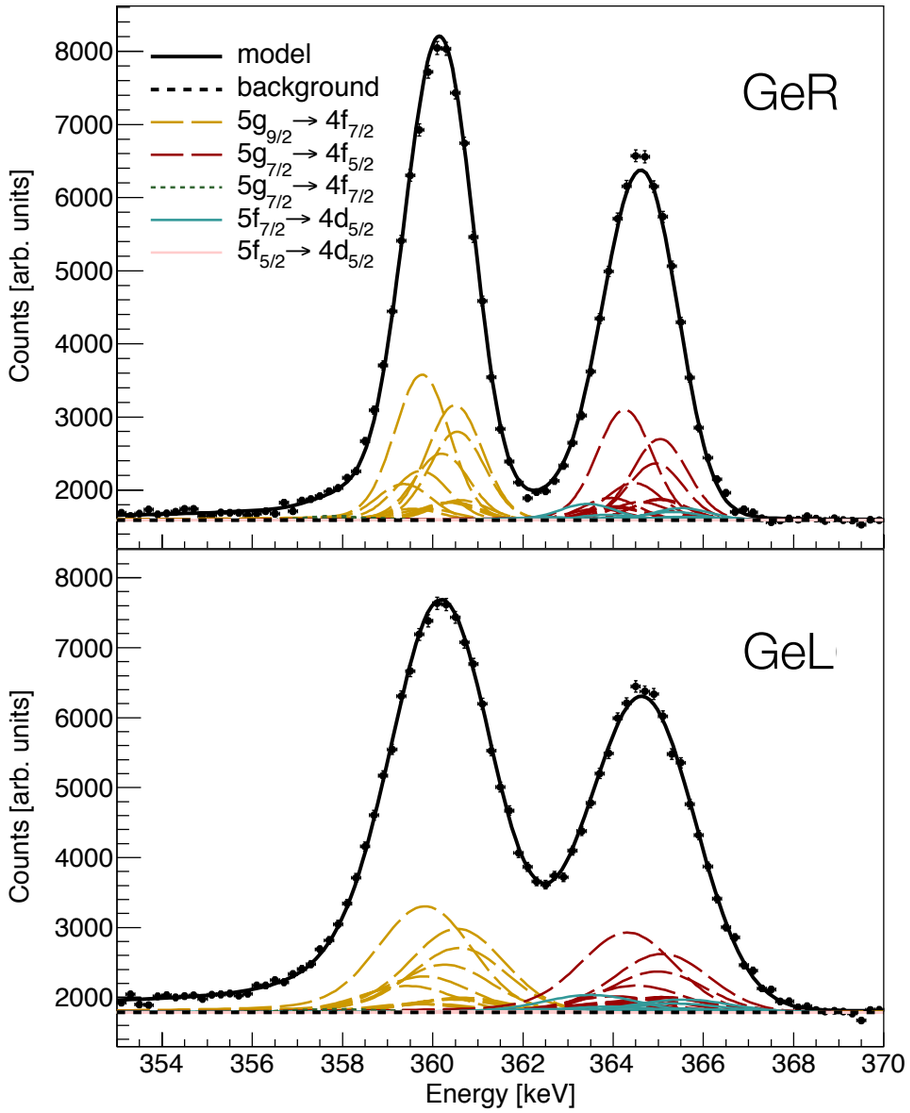

^{185}Re and ^{187}Re 2p1s analysis

Outlook: Nuclear charge radius

PhD thesis of S.M. Vogiatzi

- First time attempting to measure the last stable element with a non-measured absolute nuclear charge radius.

- Admixture of ground and excited hyperfine states due to the dynamic effect — very complicated muonic energy spectrum.

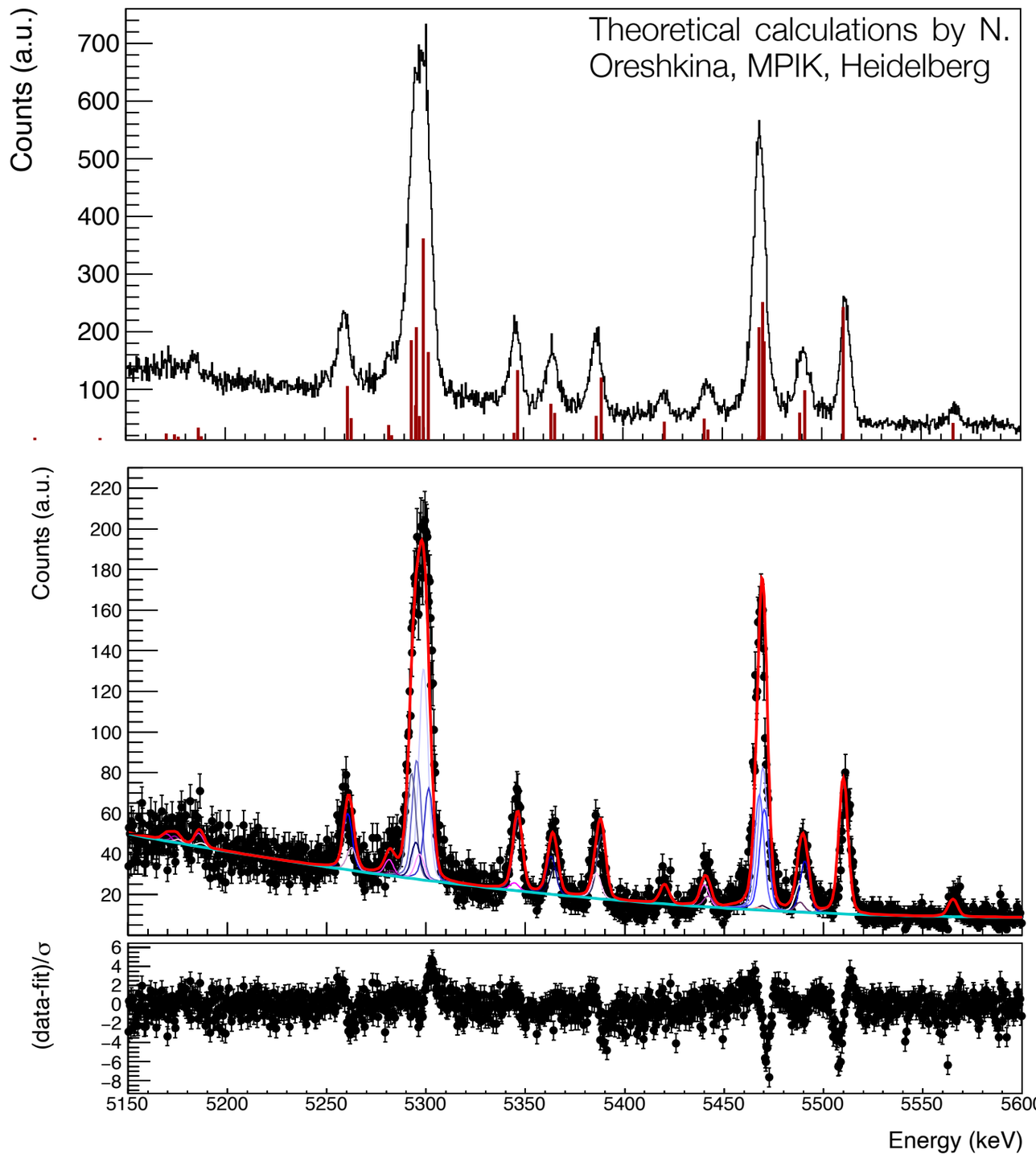

Experimental timeline
2017 — Towards microgram targets

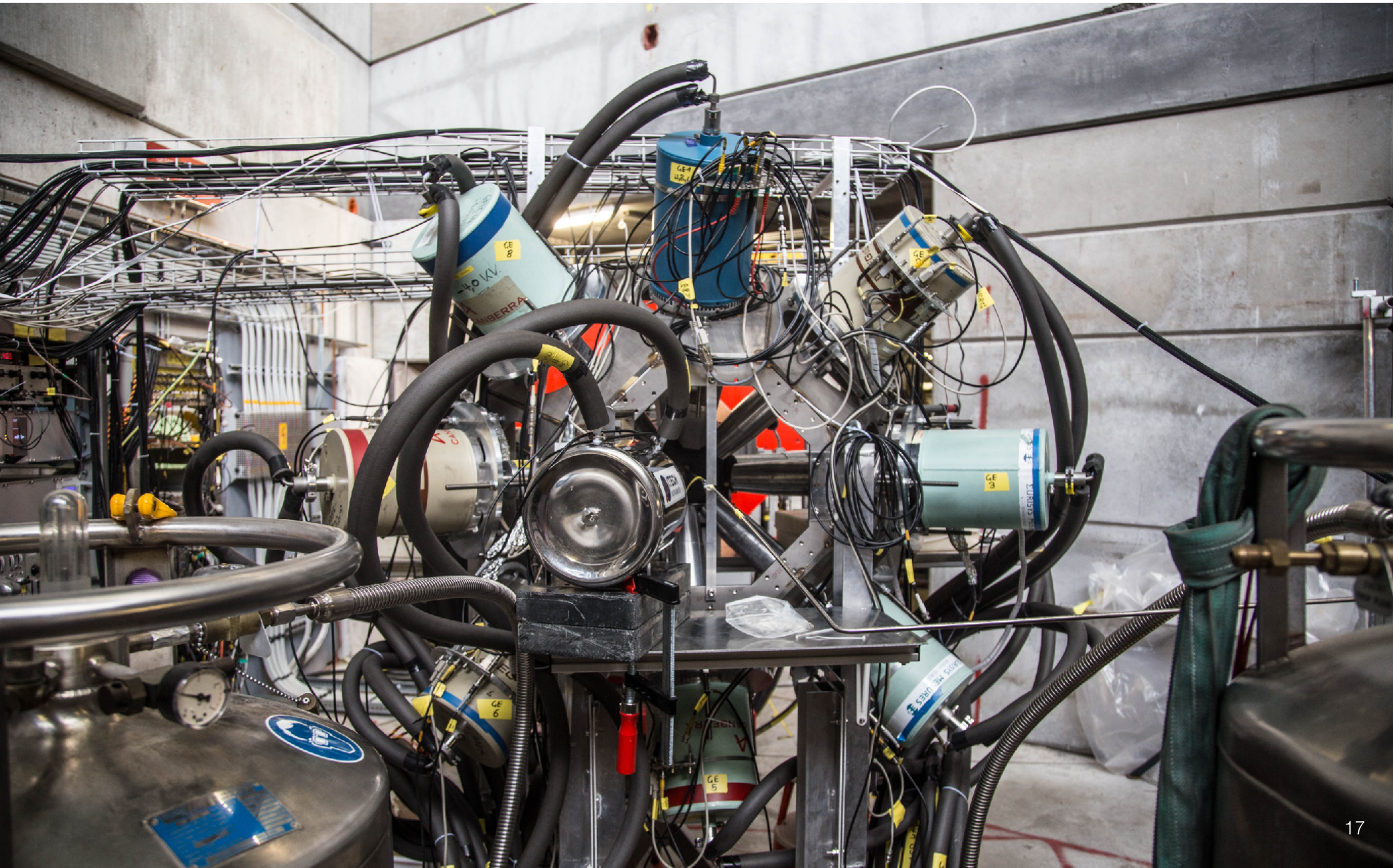

Muon transfer to microgram targets

Developed by the muX collaboration Eur. Phys. J. A 59, 15 (2023)

Inspired by the work of Strasser *et al.* and Kraiman *et al.*

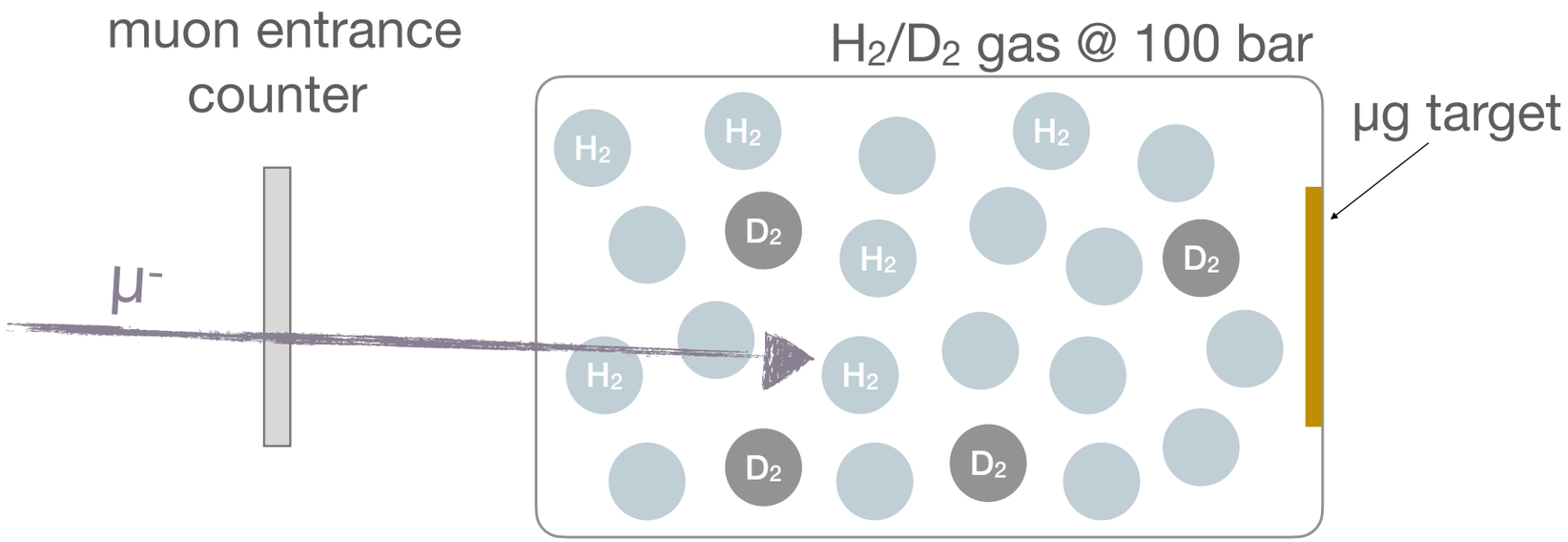

Muon transfer to microgram targets

Developed by the muX collaboration Eur. Phys. J. A 59, 15 (2023)

Inspired by the work of Strasser *et al.* and Kraiman *et al.*

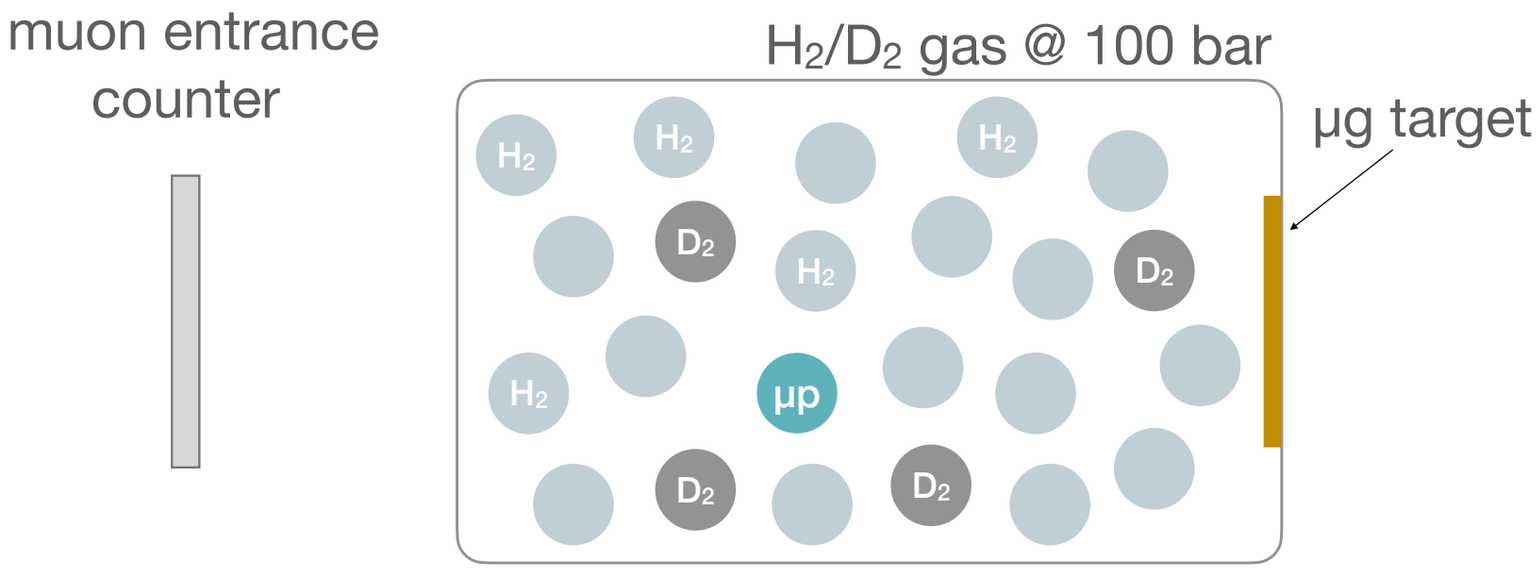

1. μ^- stops in 100 bar of H_2 + 0.25% D_2 & forms muonic hydrogen μp

Muon transfer to microgram targets

Developed by the muX collaboration Eur. Phys. J. A 59, 15 (2023)

Inspired by the work of Strasser *et al.* and Kraiman *et al.*

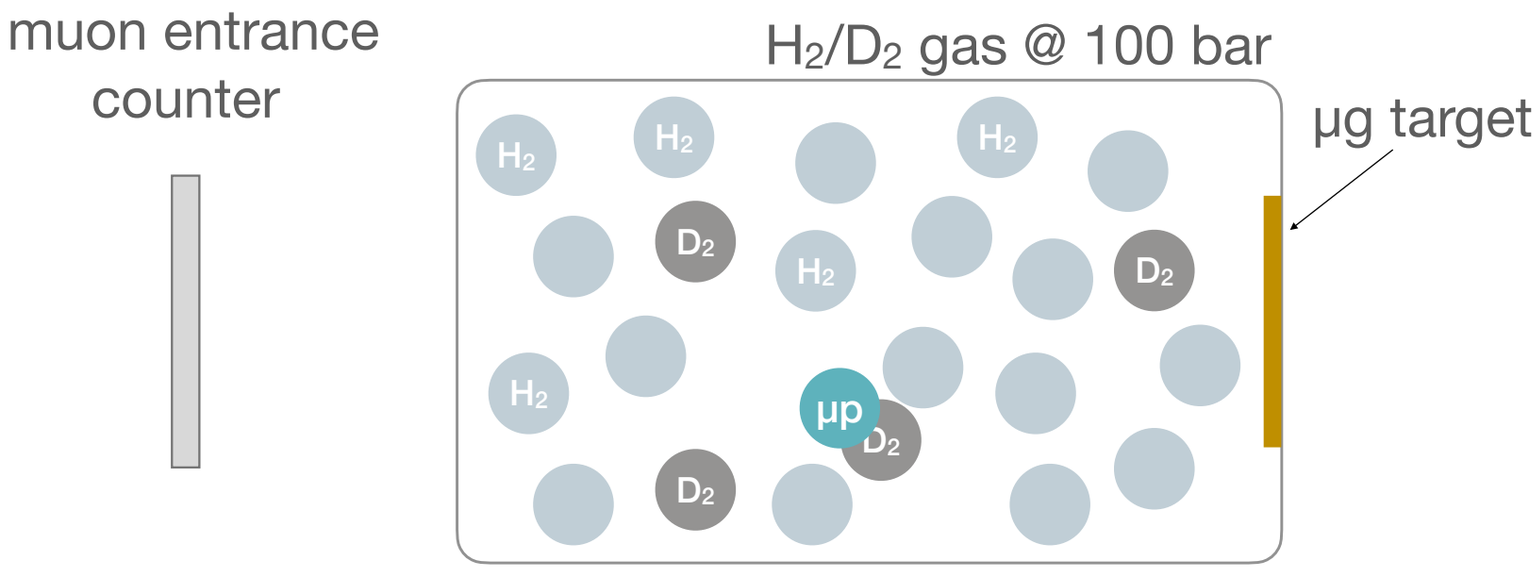

1. μ^- stops in 100 bar of H_2 + 0.25% D_2 & forms muonic hydrogen μp
2. transfer to deuterium μp → μd

Muon transfer to microgram targets

Developed by the muX collaboration Eur. Phys. J. A 59, 15 (2023)

Inspired by the work of Strasser *et al.* and Kraiman *et al.*

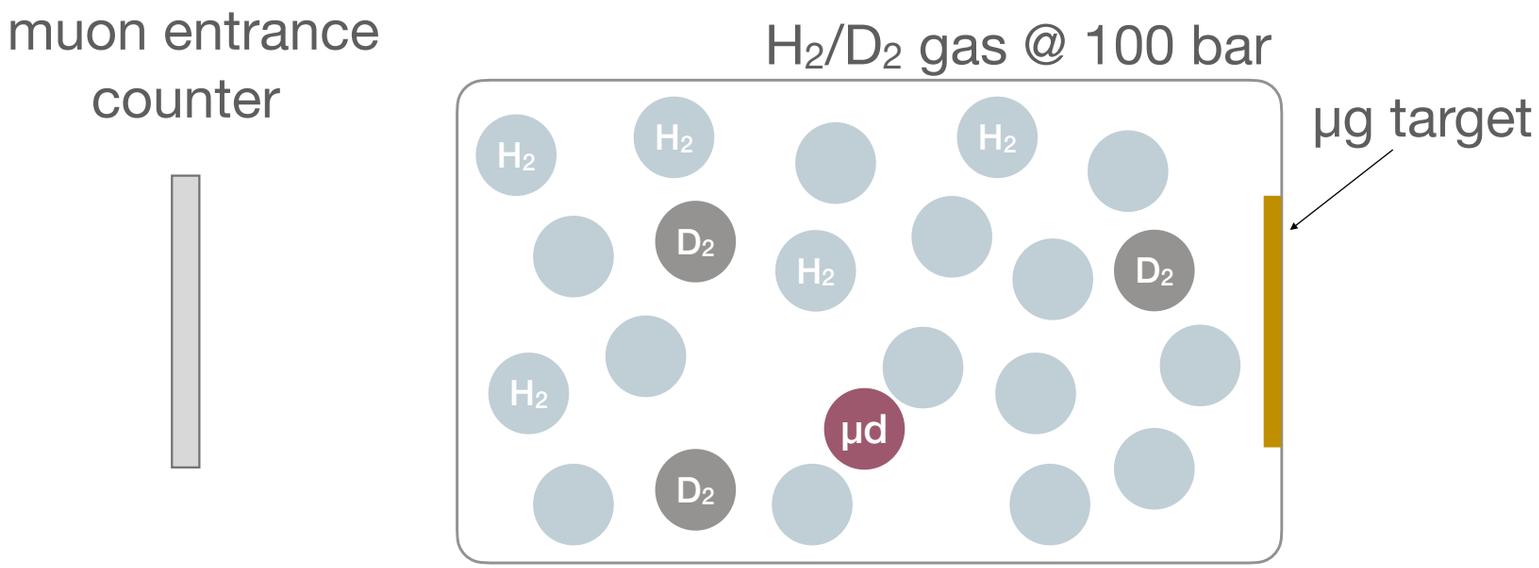

1. μ^- stops in 100 bar of H_2 + 0.25% D_2 & forms muonic hydrogen μp
2. transfer to deuterium μp → μd

Muon transfer to microgram targets

Developed by the muX collaboration Eur. Phys. J. A 59, 15 (2023)

Inspired by the work of Strasser *et al.* and Kraiman *et al.*

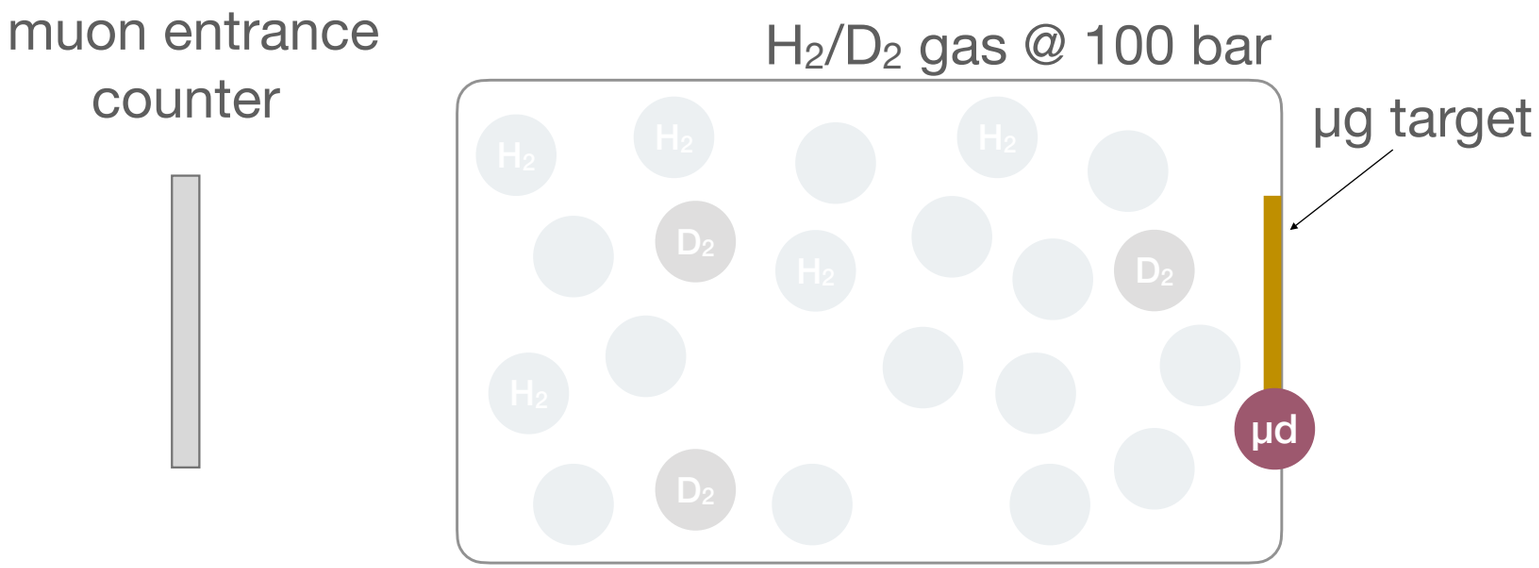

1. μ^- stops in 100 bar of H_2 + 0.25% D_2 & forms muonic hydrogen μp
2. transfer to deuterium μp → μd
3. μd moves almost freely in the H_2 gas

Physical Review A 73, 034501 (2006)

Muon transfer to microgram targets

Developed by the muX collaboration Eur. Phys. J. A 59, 15 (2023)

Inspired by the work of Strasser *et al.* and Kraiman *et al.*

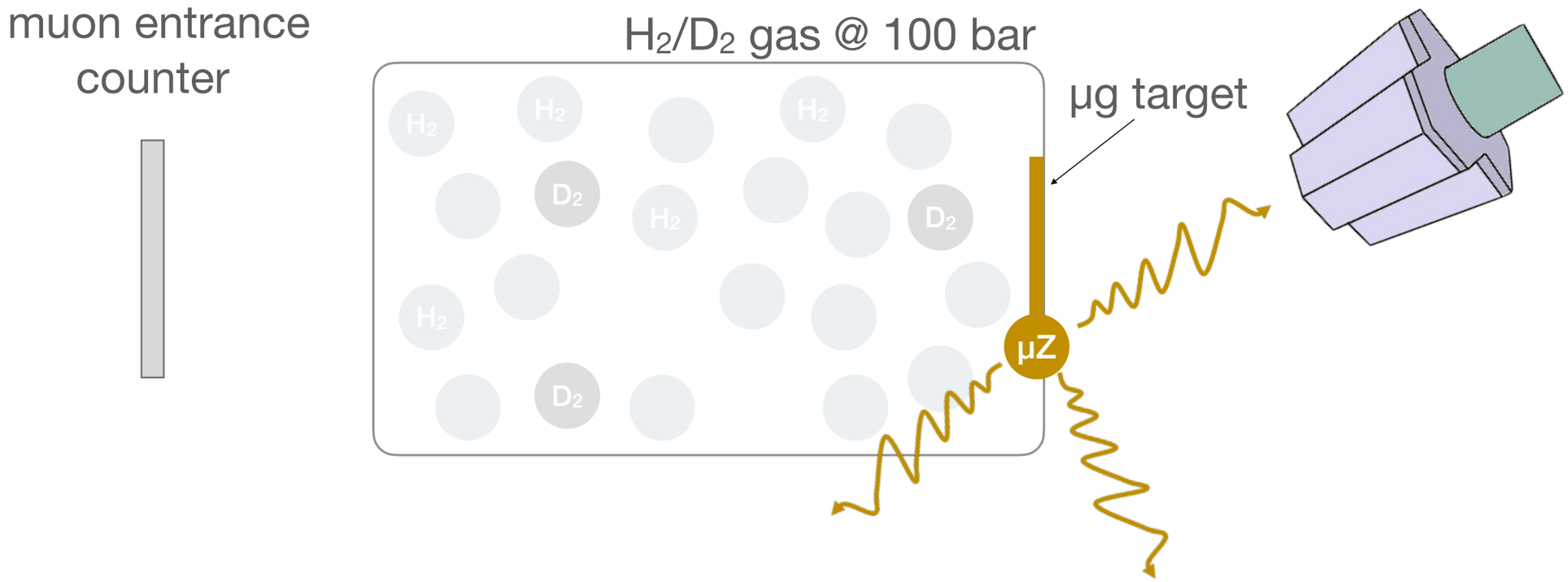

1. μ^- stops in 100 bar of H_2 + 0.25% D_2 & forms muonic hydrogen μp
2. transfer to deuterium μp → μd
3. μd moves almost freely in the H_2 gas Physical Review A 73, 034501 (2006)
4. transfer to high-Z element μd → μZ when hitting target & emission of x rays during the atomic cascade

Gas cell measurements

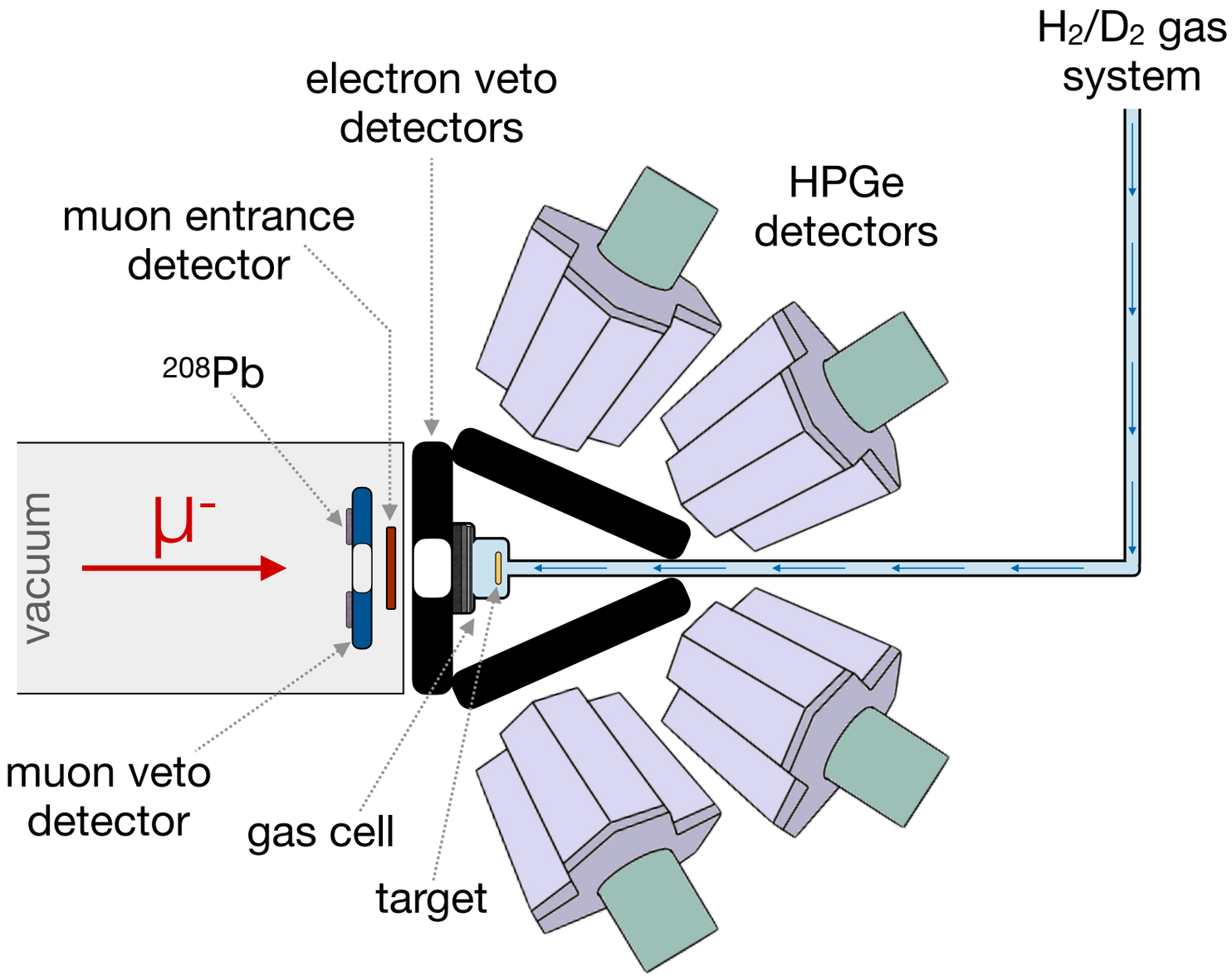

Gas cell measurements

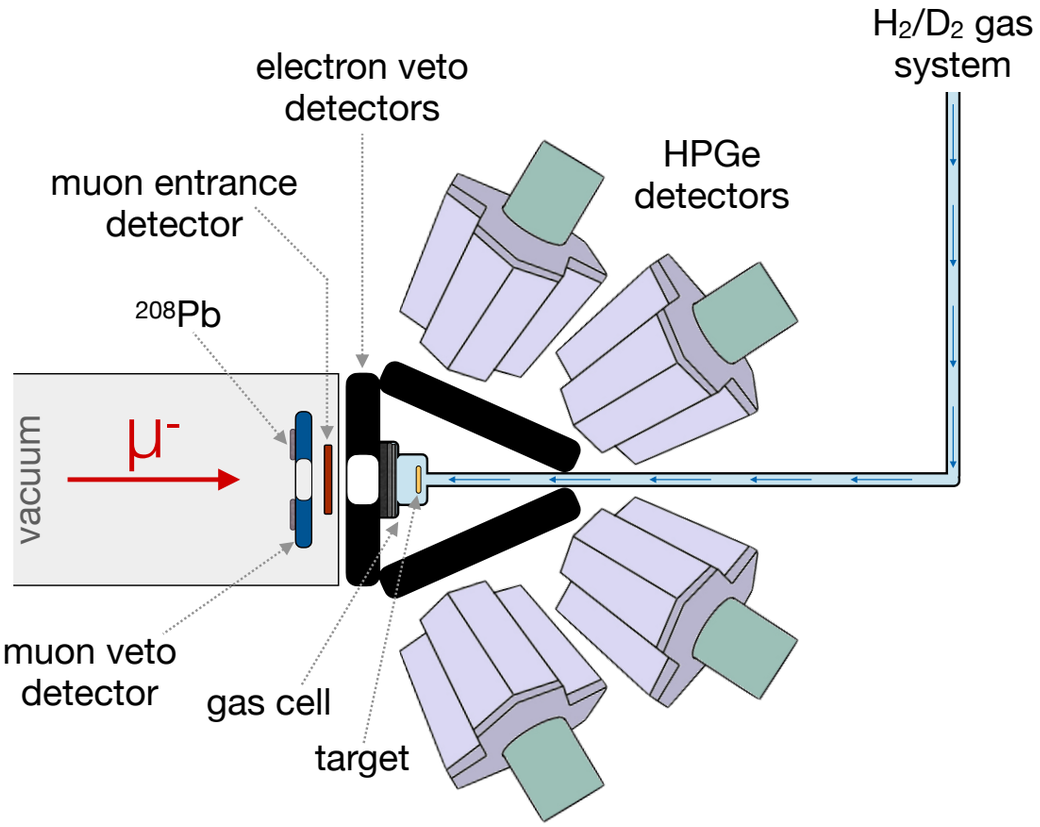

Schematics of detectors setup

Gas cell measurements

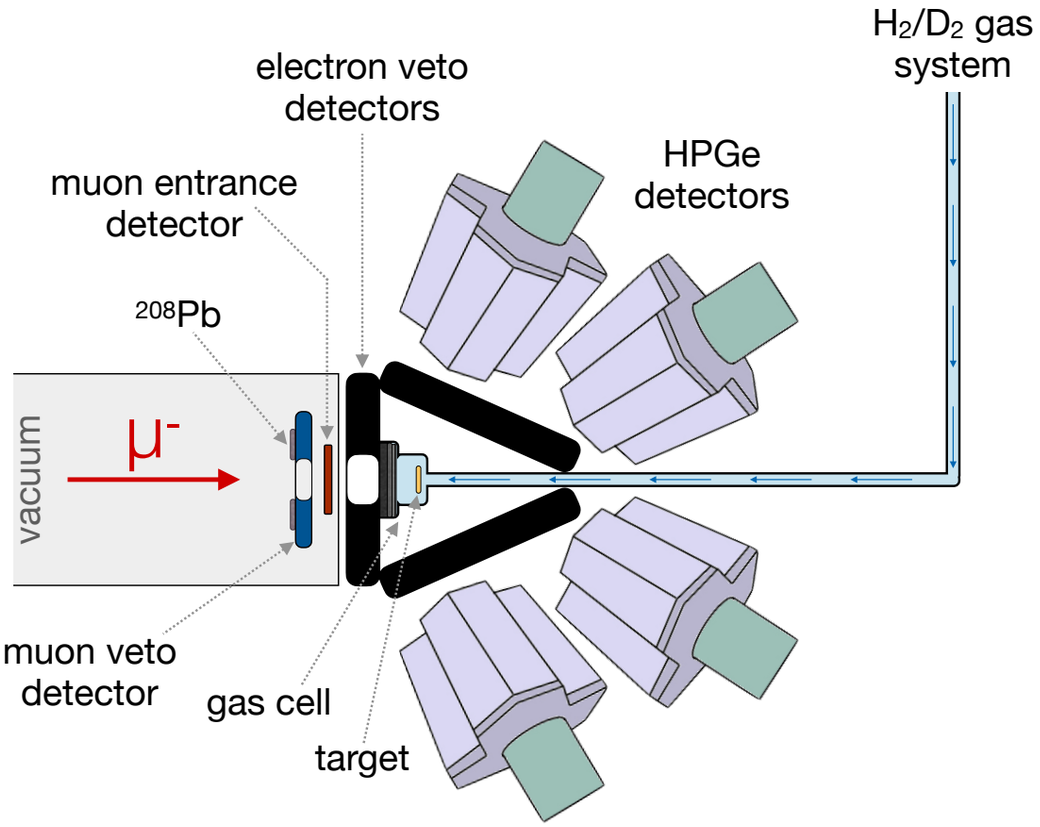

Schematics of detectors setup

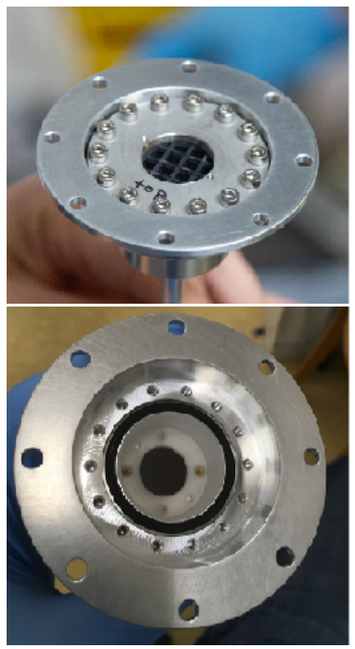

The gas cell

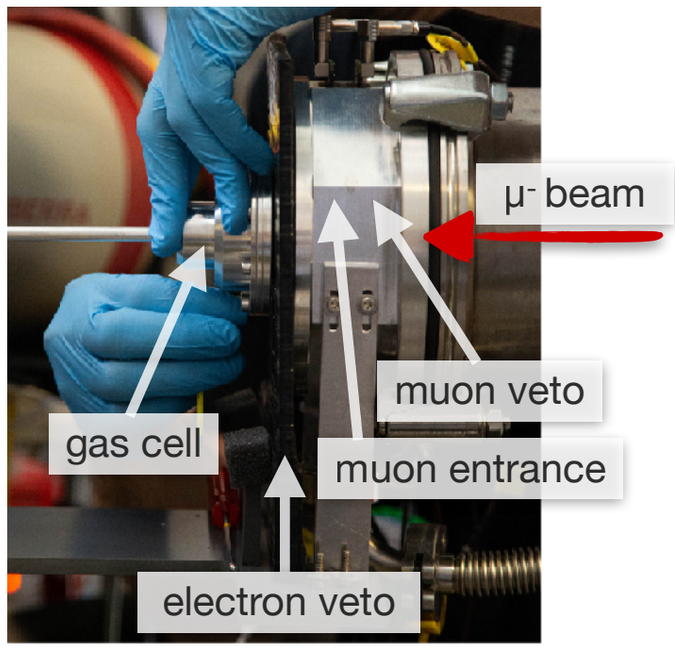

The muon and electron counters

Gas cell measurements

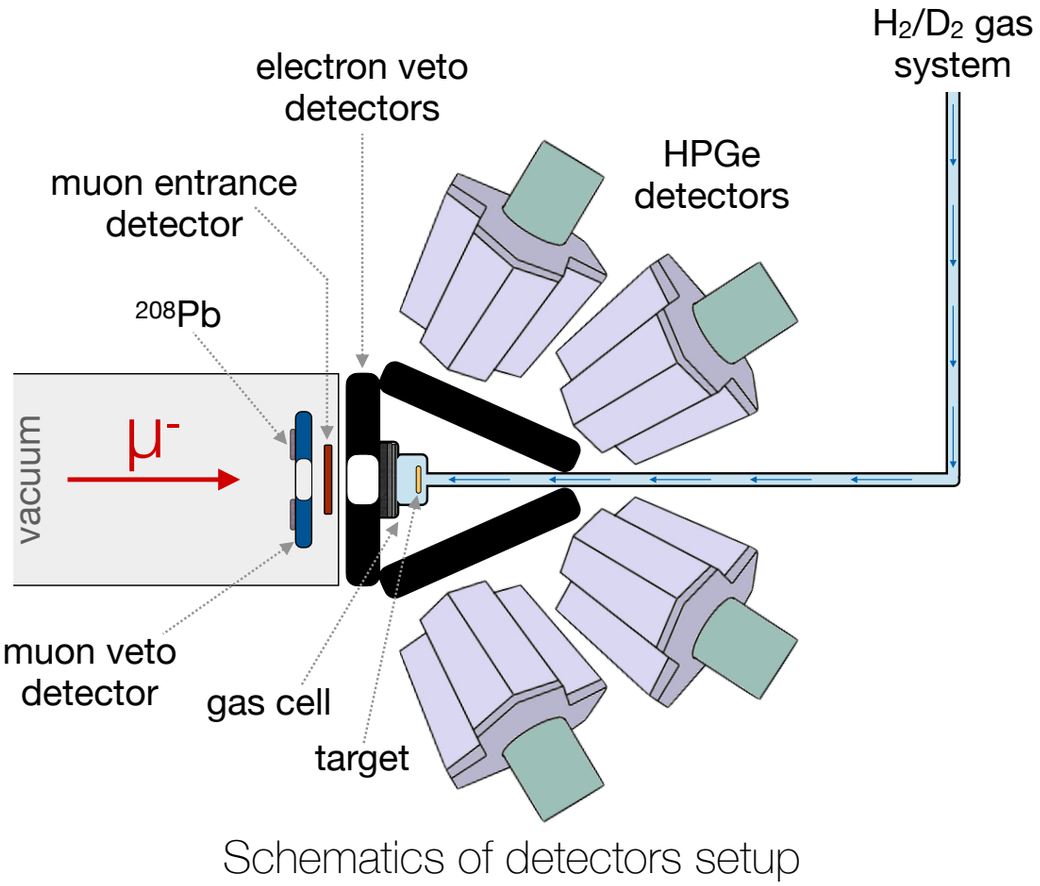

Schematics of detectors setup

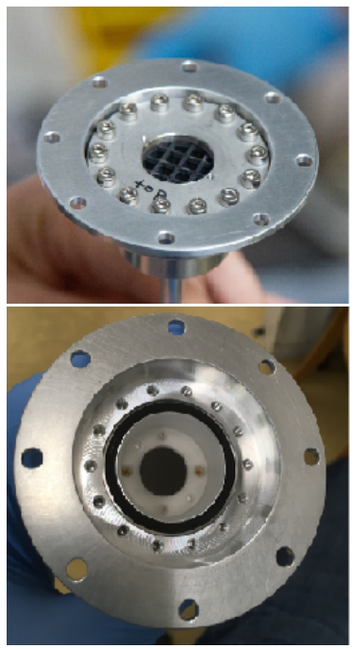

The gas cell

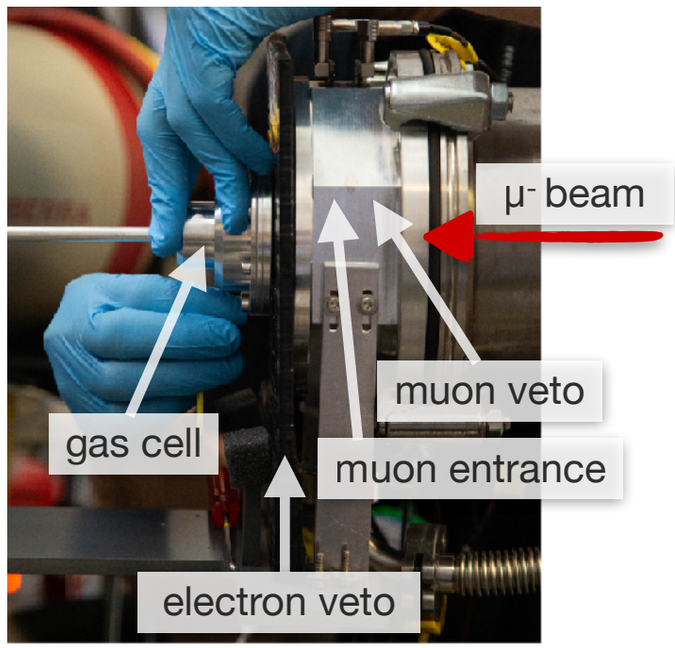

The muon and electron counters

Demonstration of principal in a 5 μg gold target in 2017, 18.5 h of measurement

the time the muon enters the gas cell

Eur. Phys. J. A 59, 15 (2023)

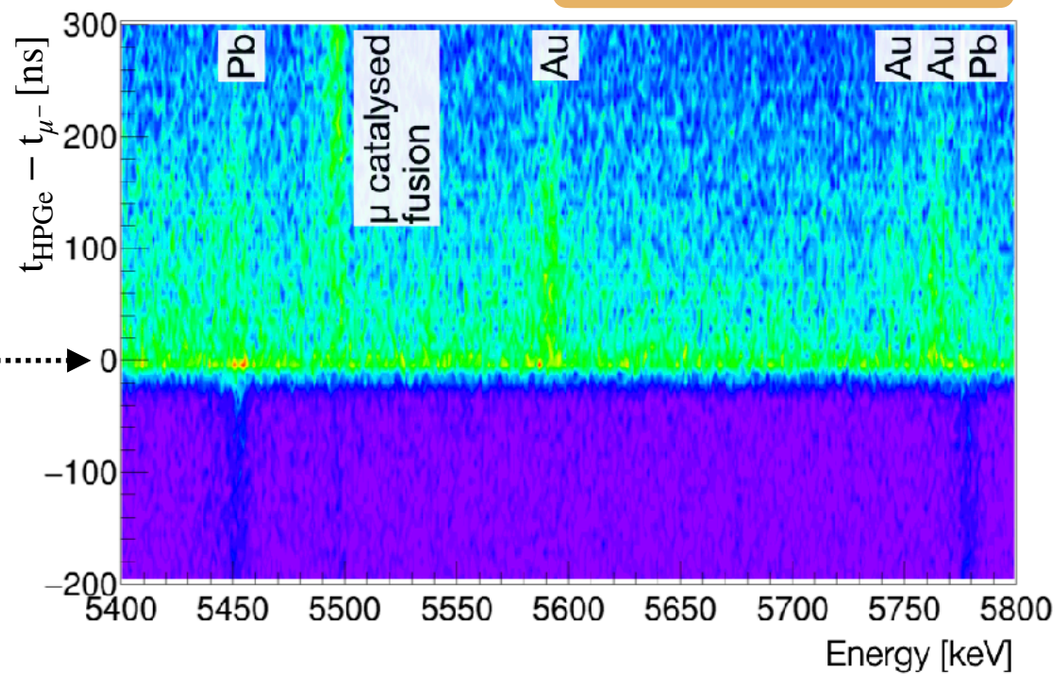

Experimental timeline

2019 — first radioactive targets ^{248}Cm & ^{226}Ra (5 µg)

Experimental timeline

2019 — Miniball clusters & frame @PSI during LS2

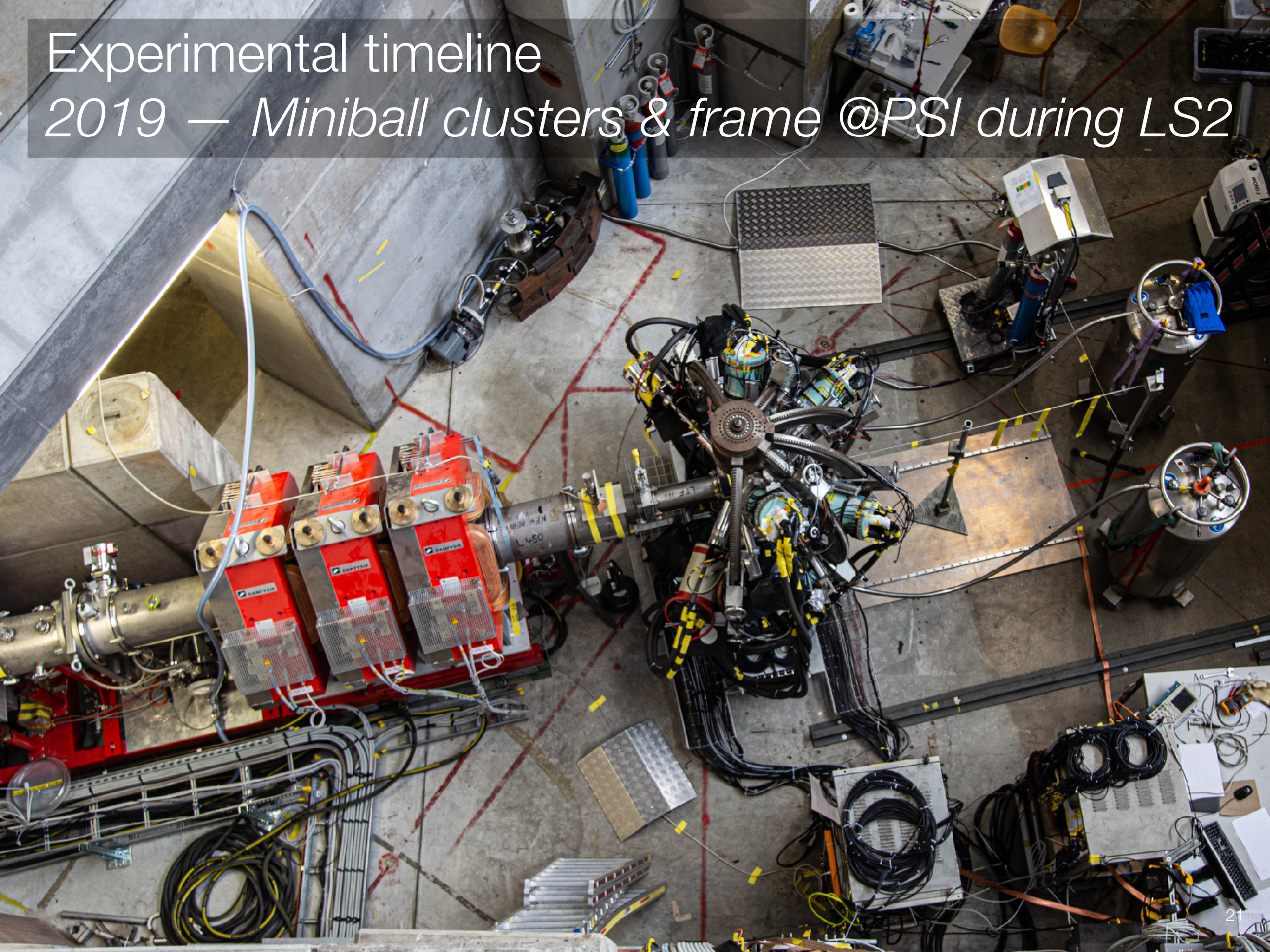

How to get to good S/B ratio at high energies?

- Electron veto cuts
- Addback
- Gain drift corrections
- Baseline correction

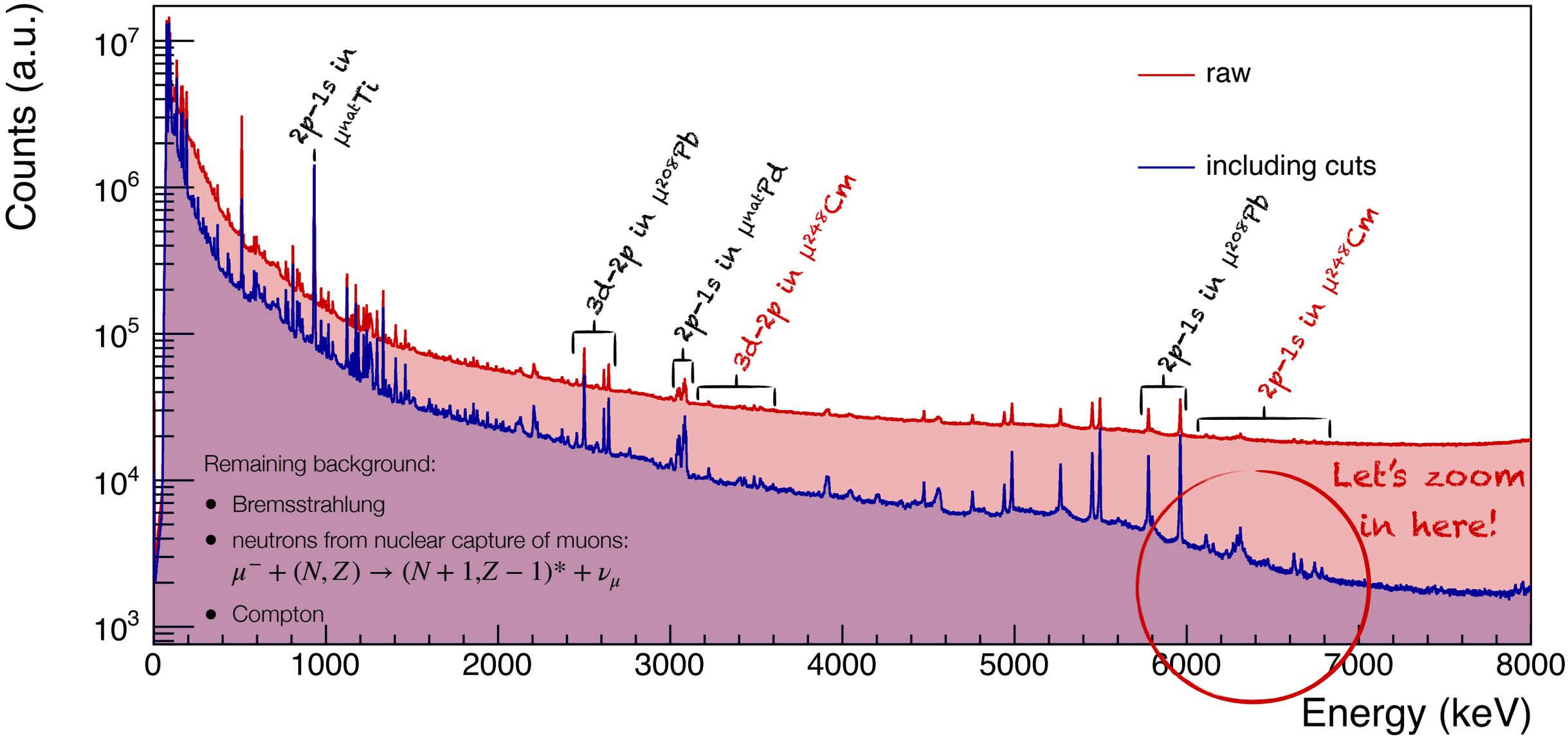

^{248}Cm 2p1s analysis

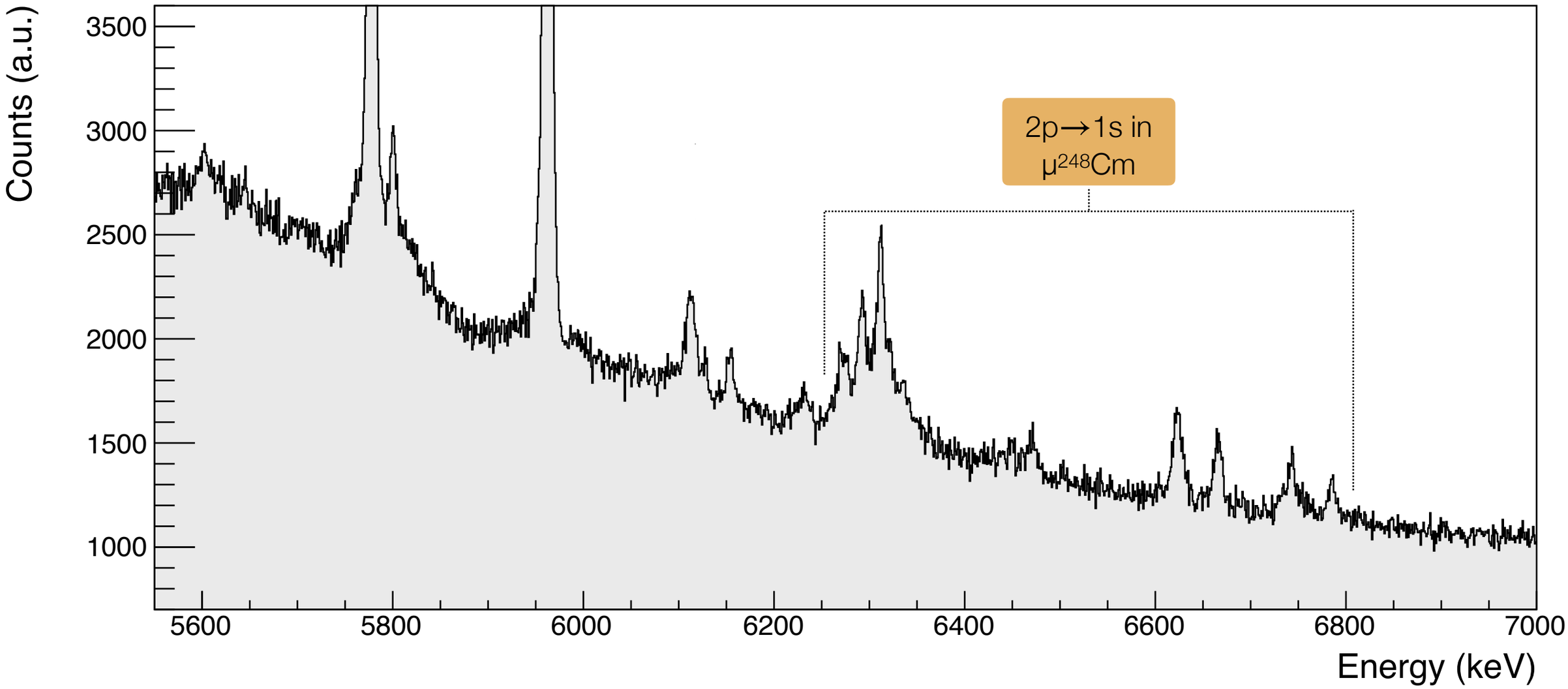

^{248}Cm 2p1s analysis

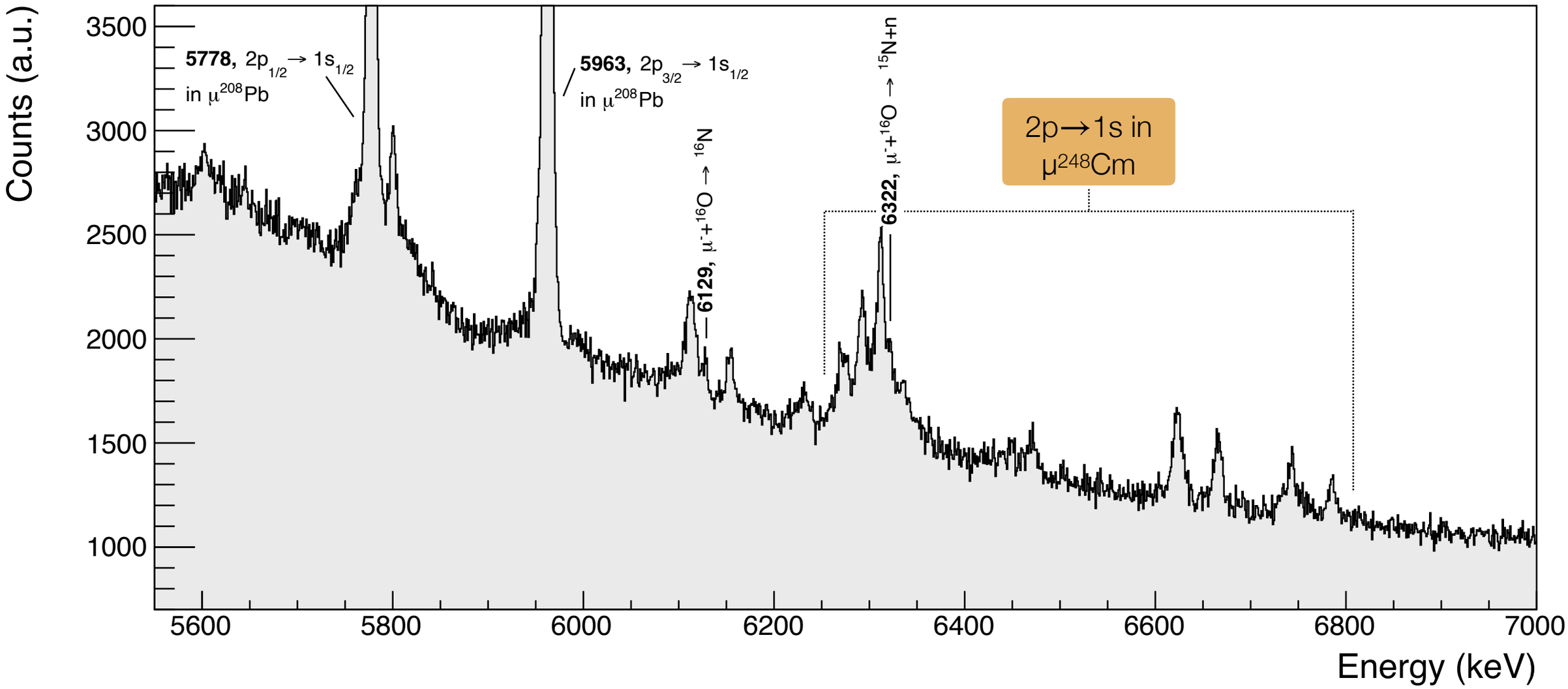

^{248}Cm 2p1s analysis

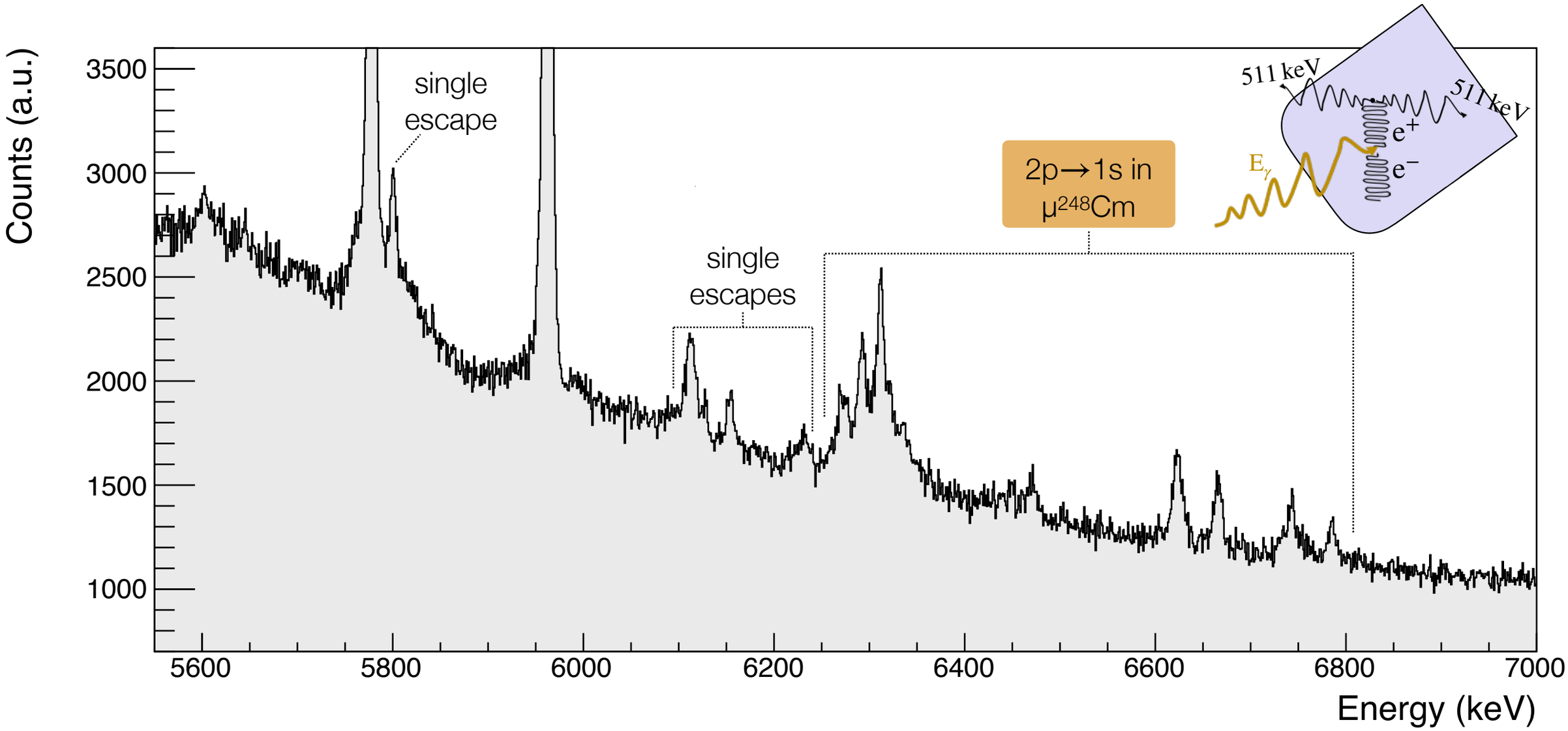

^{248}Cm 2p1s analysis

Theoretical calculations are performed by
N. Oreshkina & I. Valuev, MPIK, Heidelberg

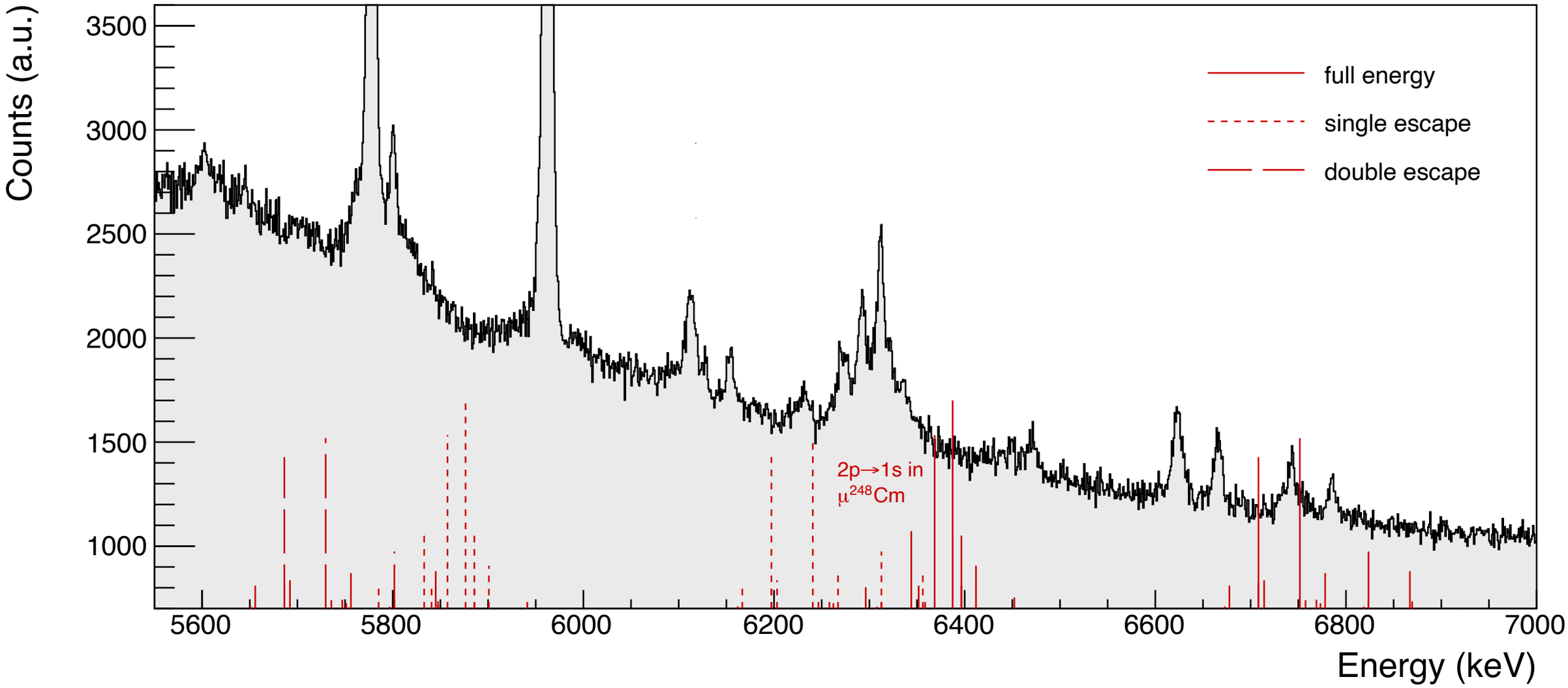

Using the nuclear charge radius prediction by Angeli & Marinova

R=5.8687 fm

^{248}Cm 2p1s analysis

Theoretical calculations are performed by
N. Oreshkina & I. Valuev, MPIK, Heidelberg

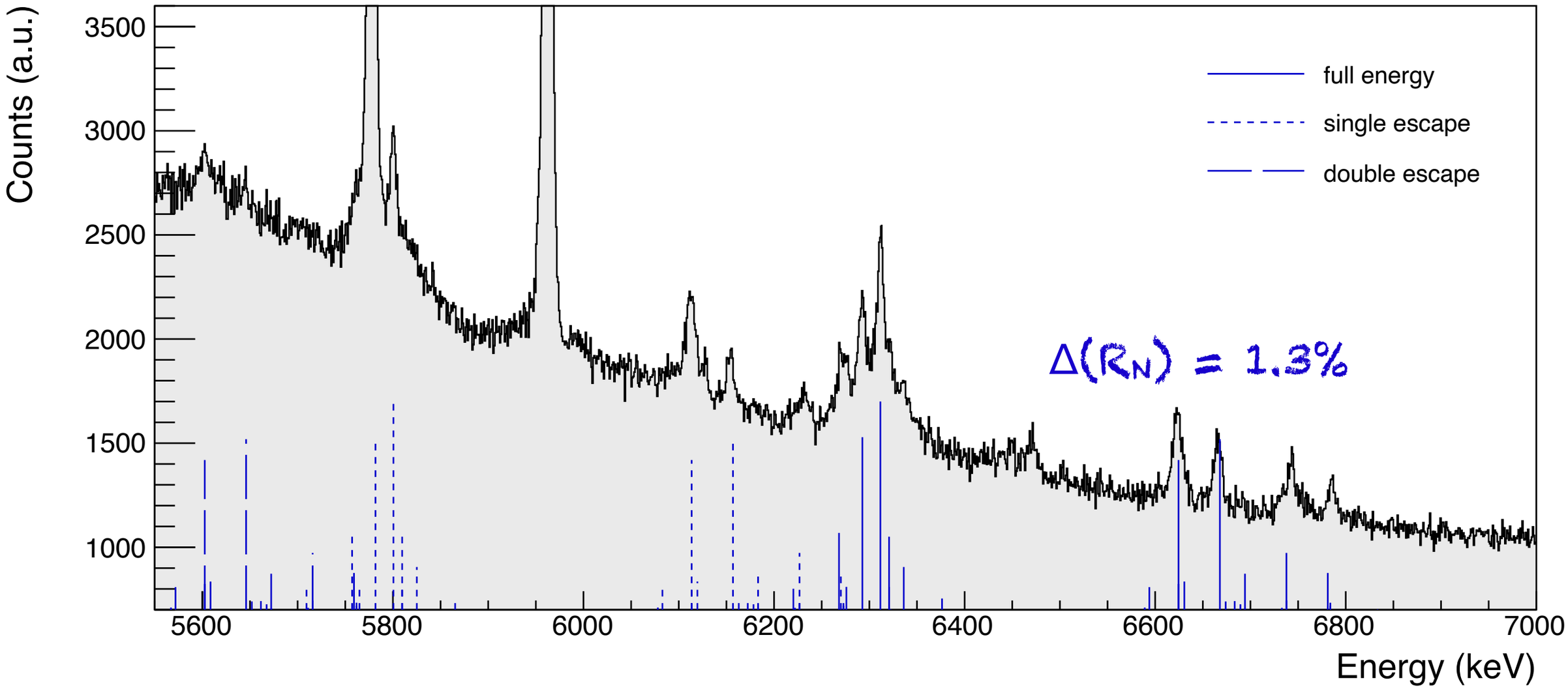

Using the nuclear charge radius prediction by Angeli & Marinova

R=5.8687 fm

^{248}Cm 2p1s analysis

Theoretical calculations are performed by
N. Oreshkina & I. Valuev, MPIK, Heidelberg

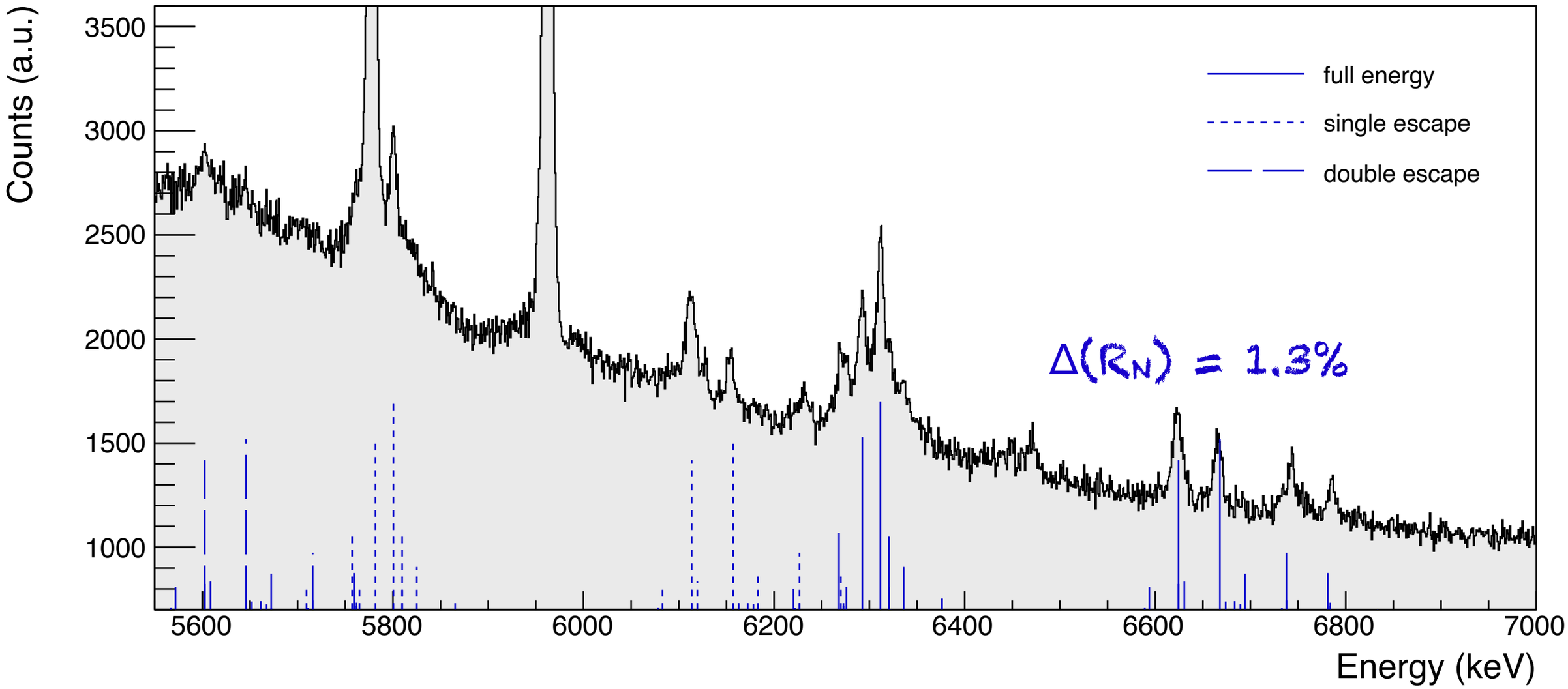

Using the nuclear charge radius prediction by Angeli & Marinova

R=5.8687 fm

Sensitivity on the quadrupole moment Q is also observed

^{248}Cm 2p1s analysis

Transition energy dependence on (R_N,Q)

Theoretical calculations are performed by
N. Oreshkina & I. Valuev, MPIK, Heidelberg

$$dR = \frac{R}{R_N}, \text{ where } R_N = 5.8687\,\text{fm}$$

$$dQ = \frac{Q}{Q_N}, \text{ where } Q_N = 12.04\,\text{b}$$

^{248}Cm is even-even → This is the intrinsic Q calculated as $16\pi B(E2)_{0^+\to 2^+}/5e^2]^{1/2}$, integrated in all possible orientations → spherical density (is that right?)

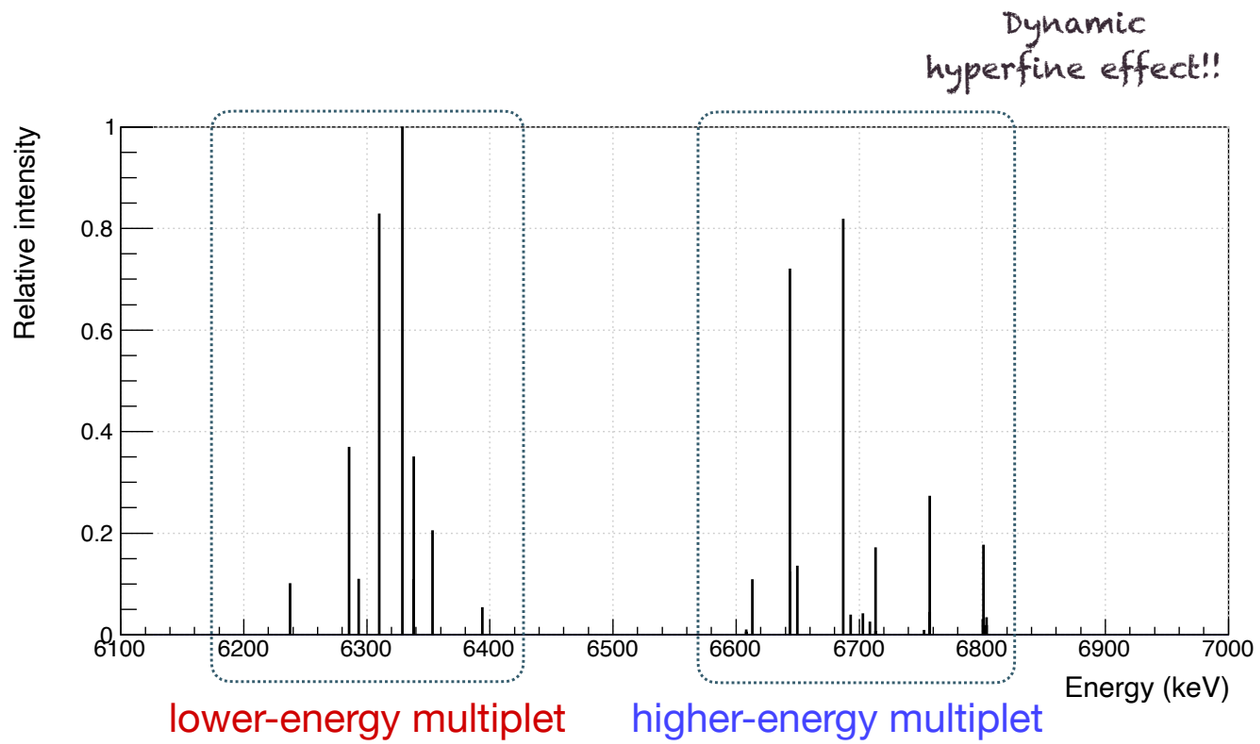

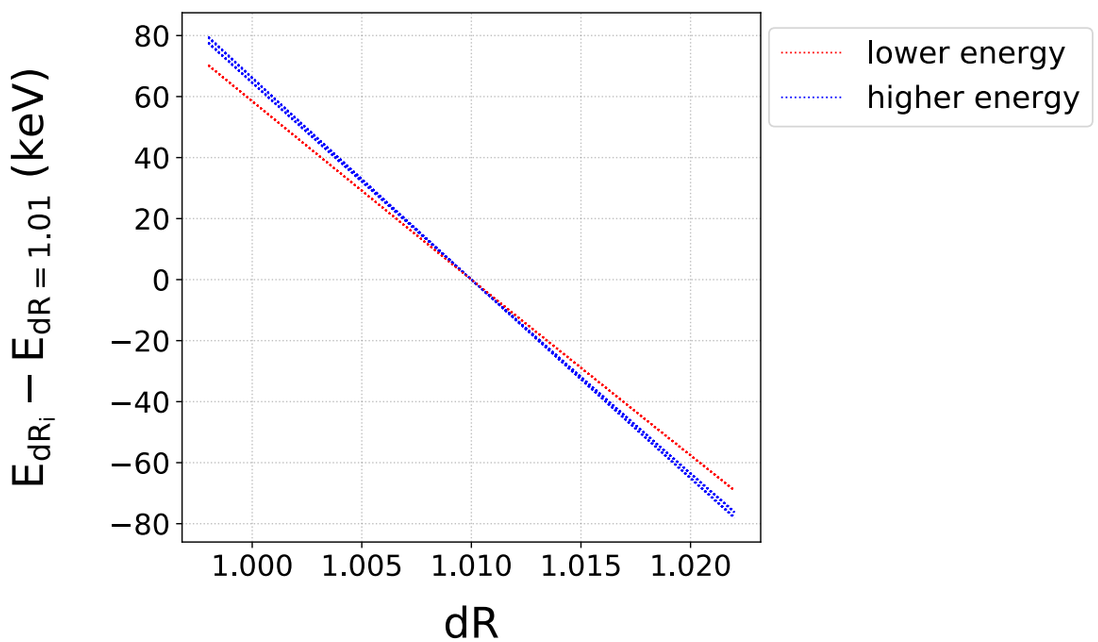

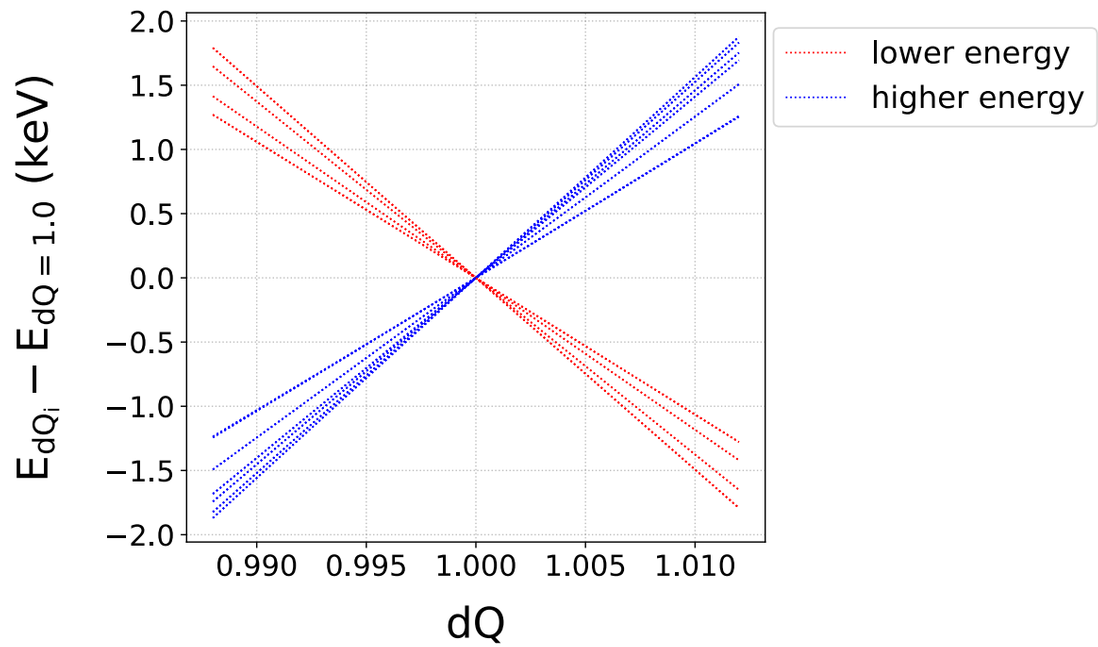

^{248}Cm 2p1s analysis
Nuclear charge radius

$$R = 5.9455(1)_{stat}(117)_{sys}\ fm$$

$$Q = 12.003(8)_{stat}(361)_{sys}\ b$$

Statistical result

My PhD thesis

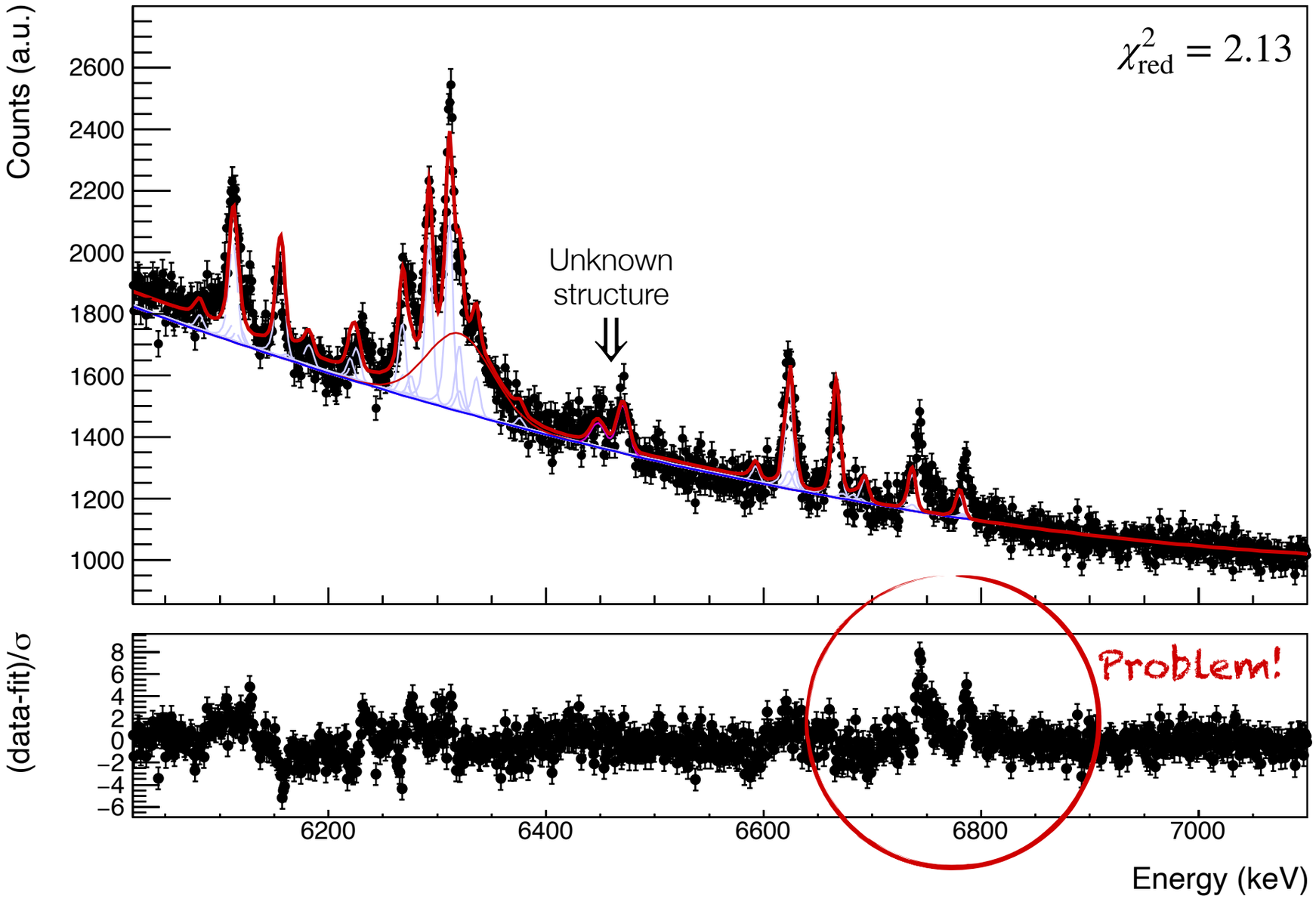

Included corrections:

- Finite size (2-Fermi)
- Vacuum polarisation
- Nuclear polarisation

Not included corrections:

- Magnetic moment (~sub-keV)
- Electron screening?
- Hadronic vacuum polarization
- Recoil effect

Sources of systematic uncertainties
Combined results

		Charge radius		Quadrupole moment	
Systematic effect	Description	Δ(dR)	σ_{dR}	Δ(dQ)	σ_{dQ}
Fitting features	Instrumental line-shape	0	0.000 032	0	0.001 4
	SE/FE ratio	0	0.000 015	0	0.001 3
	Binning	0	0.000 008	0	0.000 8
	Fitting energy range	0	0.000 033	0	0.001 3
	Background model	0	0.000 042	0	0.004 0
	Free intensities fit	0	0.000 028	0	0.000 4
	Combined	0	0.000 070	0	0.004 7
Energy calibration	Wrong energy of ^{16}N line	0.000 12	0.000 04	–0.000 82	0.000 55
	Energy calibration scheme	0	0.000 007	0	0.000 67
	Uncertainty of literature energy	0	0.000 018	0	0.002 25
	Line-shape for energy calibration	–0.000 068	0.000 038	0	0
	Combined	0.000 052	0.000 058	–0.000 82	0.002 4
Theory	Uncertainty of nuclear polarization correction	0	0.000 20	0	0.000 11
Charge distribution model	Change of the skin thickness parameter	0	0.002 2	0	0.001 91
Discrepancies of spectrum and fit	Free Gaussian fits	0	0.000 95	0	0.028 2
Total		0.000 052	0.002 4	–0.000 82	0.028 8

Experimental

Theory

Theory input

Combined result

$R = 5.9455(1)_{stat}(117)_{sys}$ fm

$Q = 12.003(8)_{stat}(361)_{sys}$ b

Needing further theory input

^{226}Ra spectrum in the 2p1s region

No 2p1s structure is observed

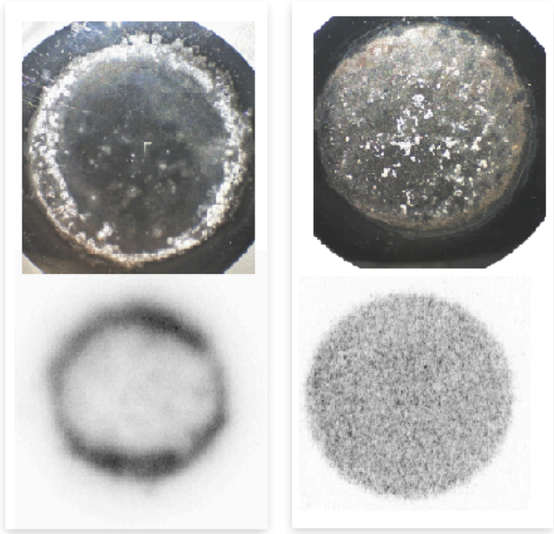

4.37 μg 1.35 μg

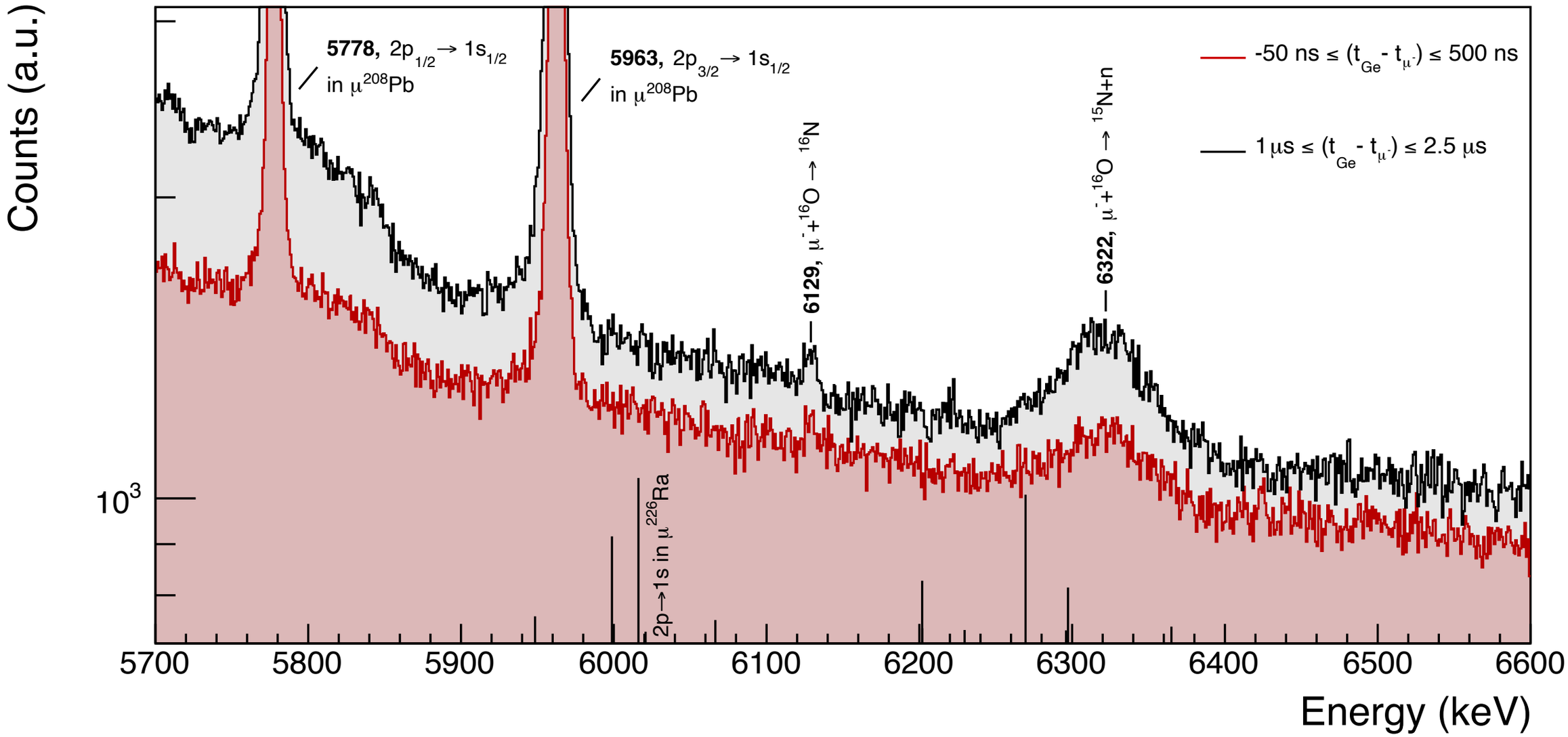

Experimental timeline

Sci Rep 15, 6939 (2025)

2022 — Assessing the target fabrication techniques

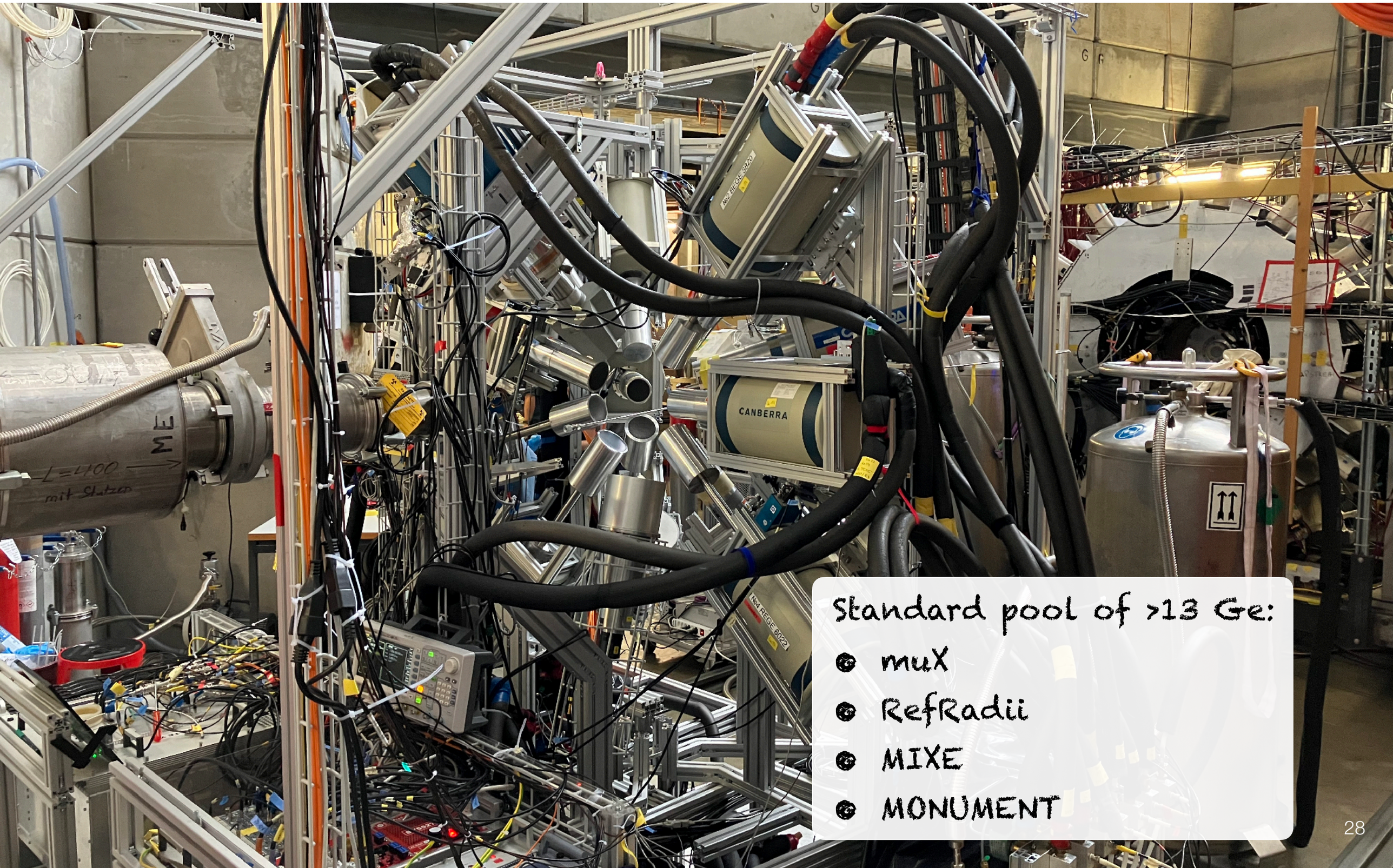

Standard pool of >13 Ge:

- muX
- RefRadii
- MIXE
- MONUMENT

Experimental timeline

2023 — ^{35,37}Cl & ^{39,40,41}K & ^{107,109}Ag (𝒪(mg to g) & 7.5 µg)

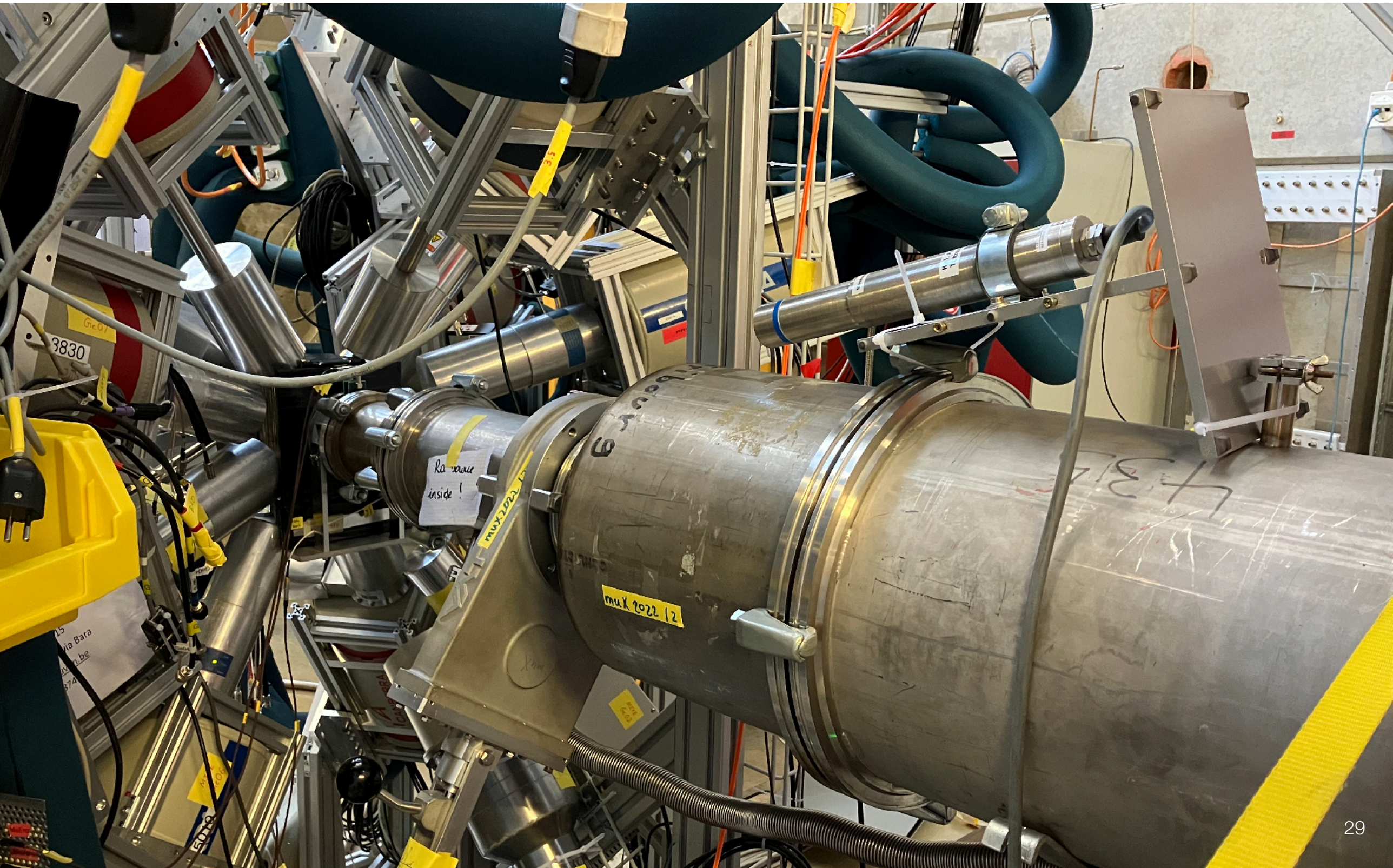

^{35}Cl 2p1s analysis (200 mg)
Nuclear charge radius

Publication in progress;
^{35,37}Cl, ^{39,41}K

Analysis of data and image courtesy of **Michael Heines**

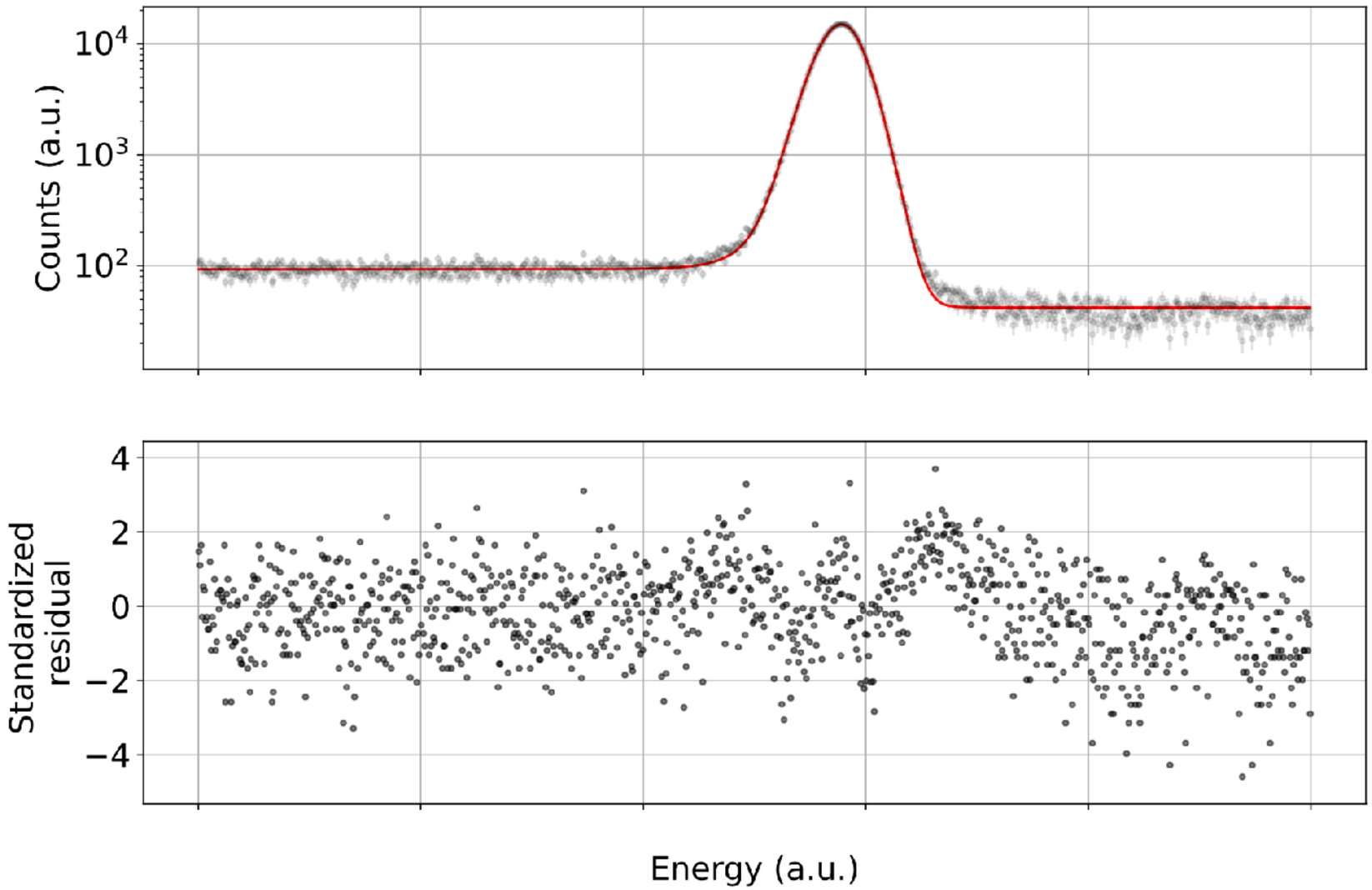

Bunch of corrections for quality data analysis pipeline:

- Thorough line-shape investigation
- Gain stabilisation
- Time algorithm correction
- Rise-time correction
- Combined detector analysis
- ....

Extensive analysis note written!

^{40}K 2p1s analysis (7.5 µg)

Nuclear charge radius

$$E_{2p-1s} = 712.xxx(xx)\,\mathrm{keV}$$

Analysis of data and image courtesy of **Michael Heines**

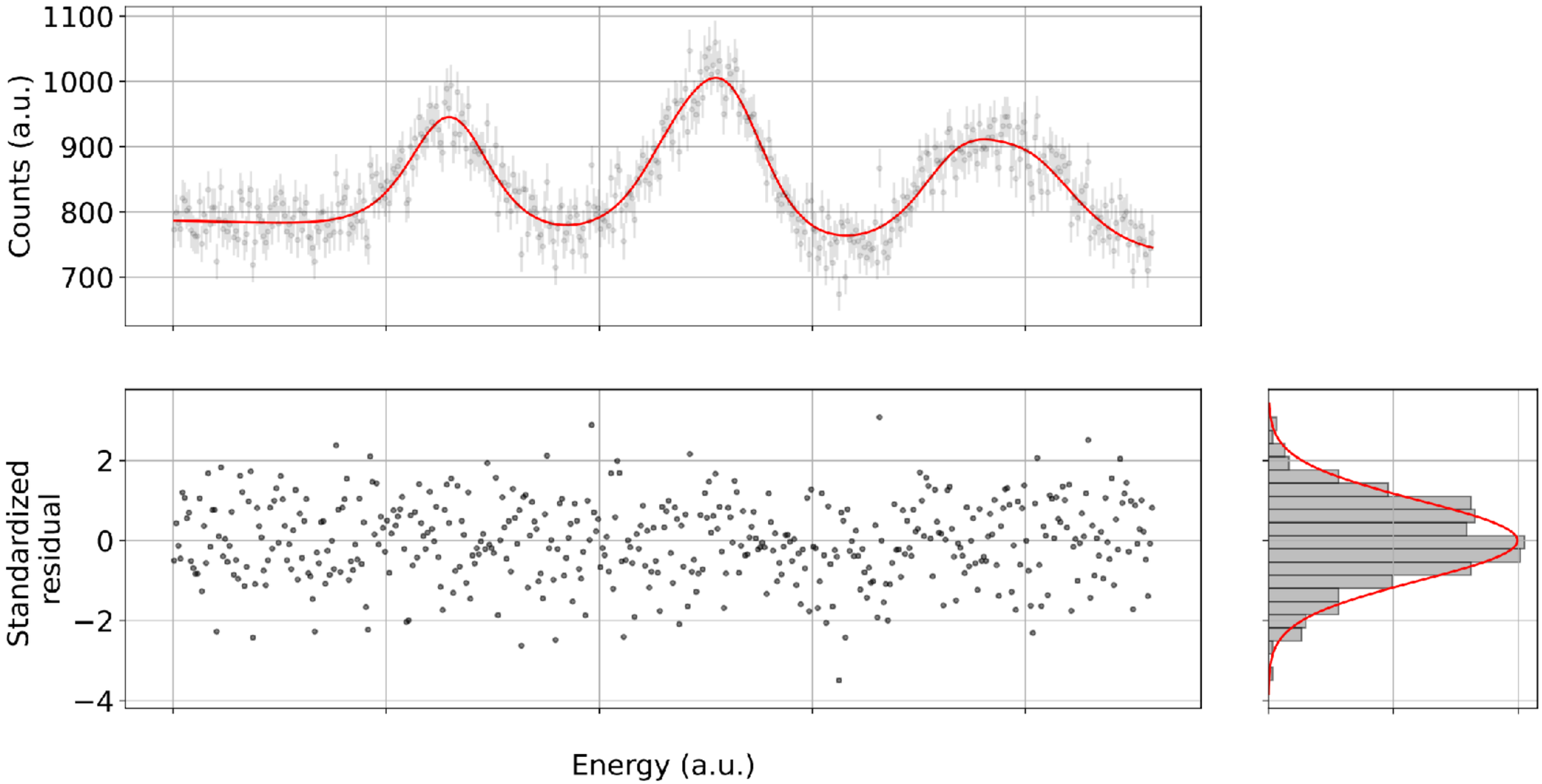

Experimental timeline

2024 — ^{27}Al, $^{28,29,30}Si$, ^{139}La, $^{175,176}Lu$ — $\mathcal{O}$(mg to g)

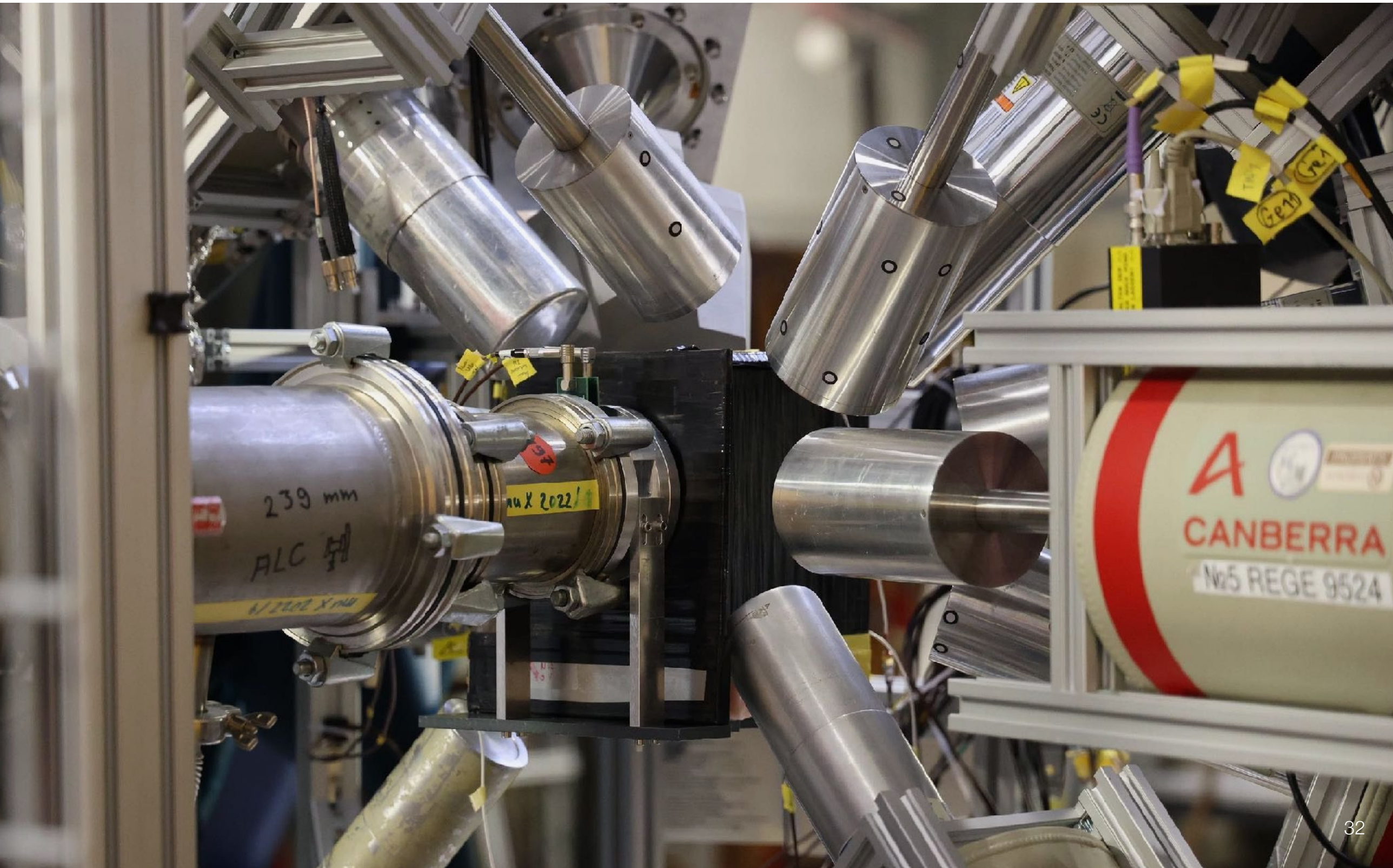

2024 data acquired

Towards nuclear charge radii extraction

Analysis of data by **Marie Deseyn** & **War War Myint Myat Phyo**

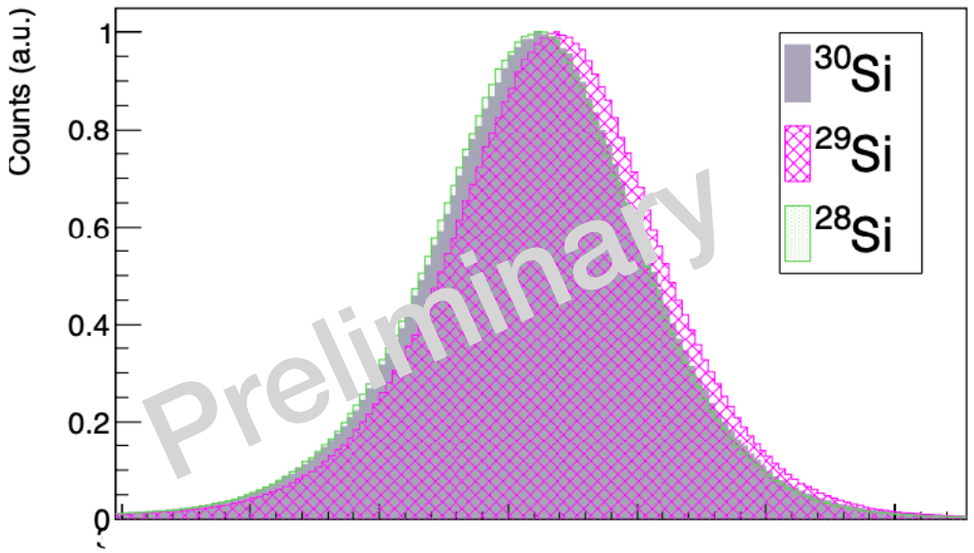

Muonic 2p1s in ^{28,29,30}Si

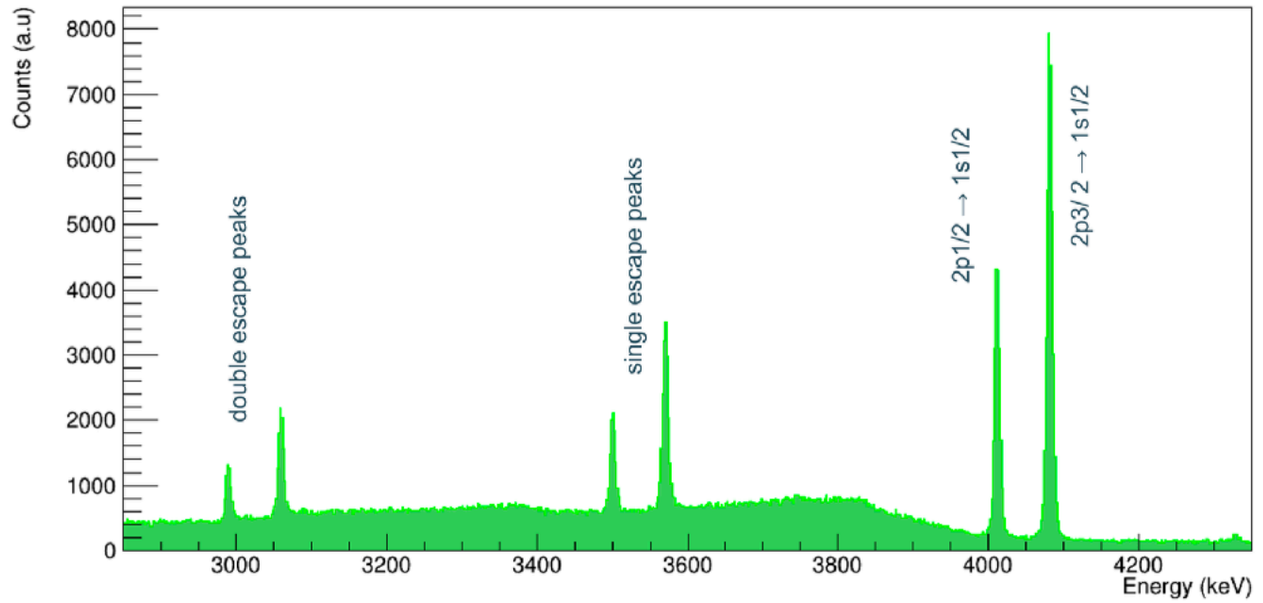

Muonic 2p1s in ^{139}La

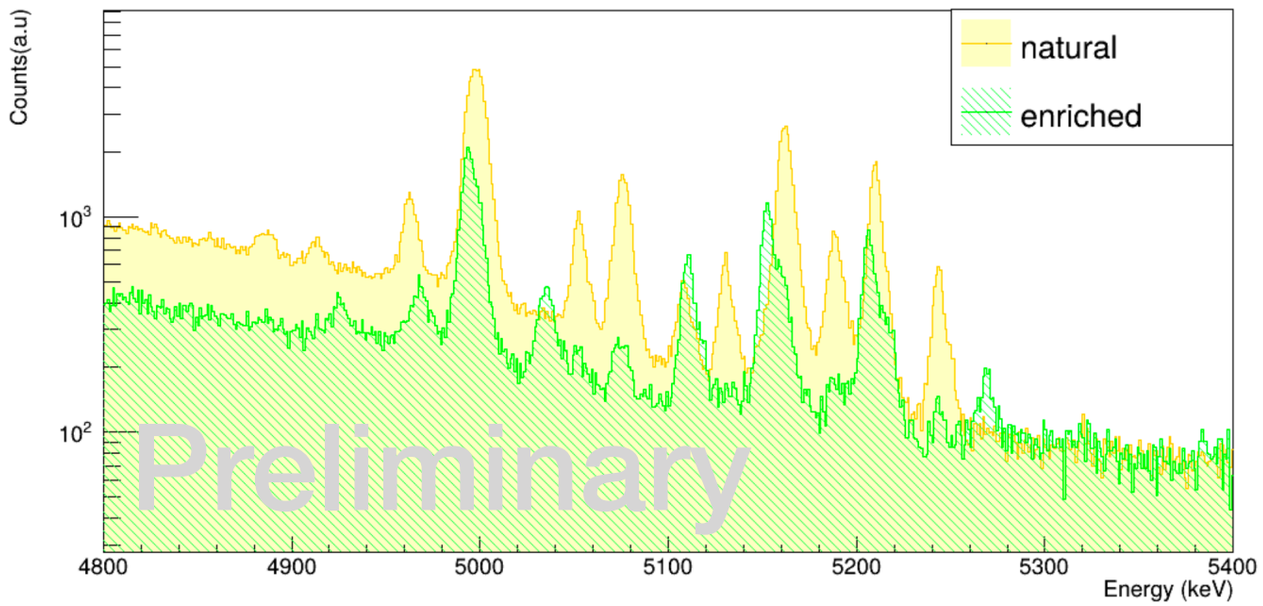

Muonic 2p1s in ^{175,176}Lu

How to tackle the very low-mass regime

QUA*ntum inte****R****rac****T****ions with* ***E****xotic a****T****oms (QUARTET)*

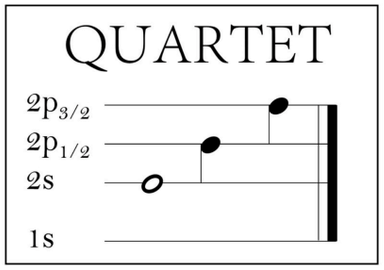

How to tackle the very low-mass regime

QUA*ntum inte****R****rac****T****ions with* ***E****xotic a****T****oms (QUARTET)*

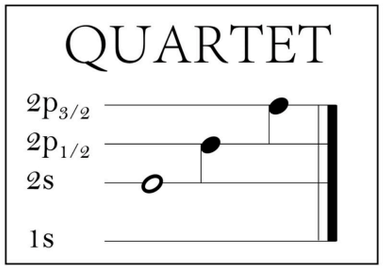

How to tackle the very low-mass regime

QUA*ntum inte****R****rac****T****ions with* ***E****xotic a****T****oms (QUARTET)*

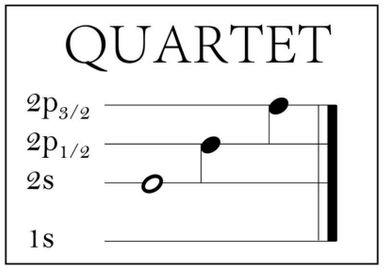

How to tackle the very low-mass regime

QUA*ntum inte****R****rac****T****ions with* ***E****xotic a****T****oms (QUARTET)*

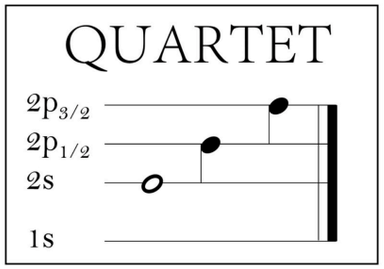

At low masses where the 2p1s muonic x rays are on the order of few tenths of keV, the charge radius extraction suffers from the detection resolution of standard semiconductors.

How to tackle the very low-mass regime

QUA*ntum inte****R****rac****T****ions with* ***E****xotic a****T****oms (QUARTET)*

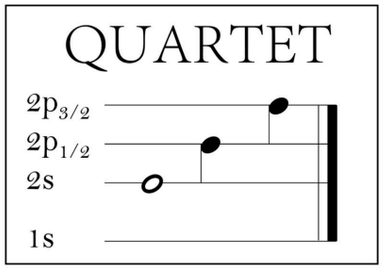

At low masses where the 2p1s muonic x rays are on the order of few tenths of keV, the charge radius extraction suffers from the detection resolution of standard semiconductors.

Expected energy resolution @ 20 keV

HPGe: >0.500 keV (FWHM)

SDD: ~0.200 keV (FWHM)

Probing muonic x-ray energies with high precision with metallic magnetic calorimeters (MMC)

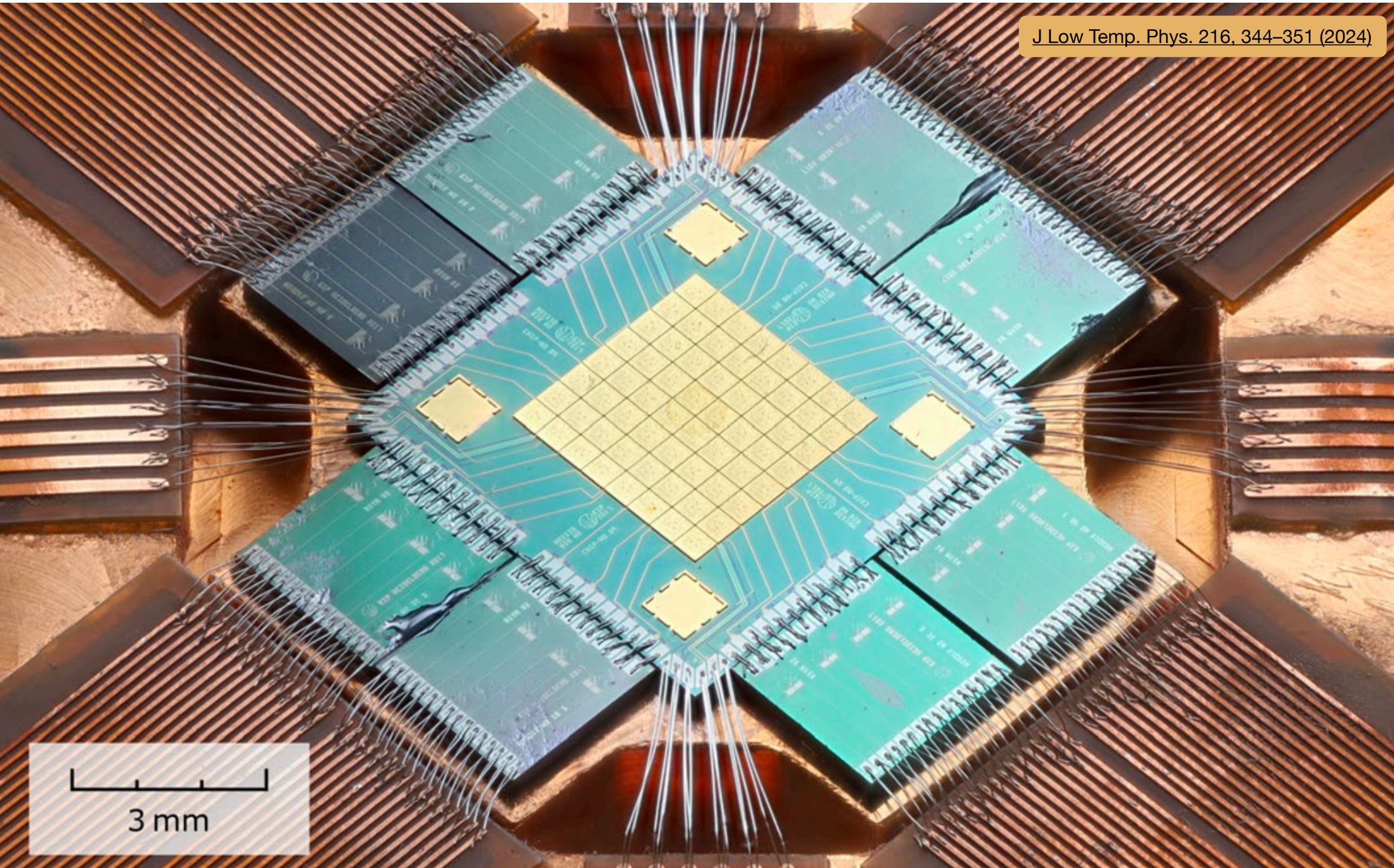

J Low Temp. Phys. 216, 344–351 (2024)

Working principle of MMC
Achieving a high energy resolution

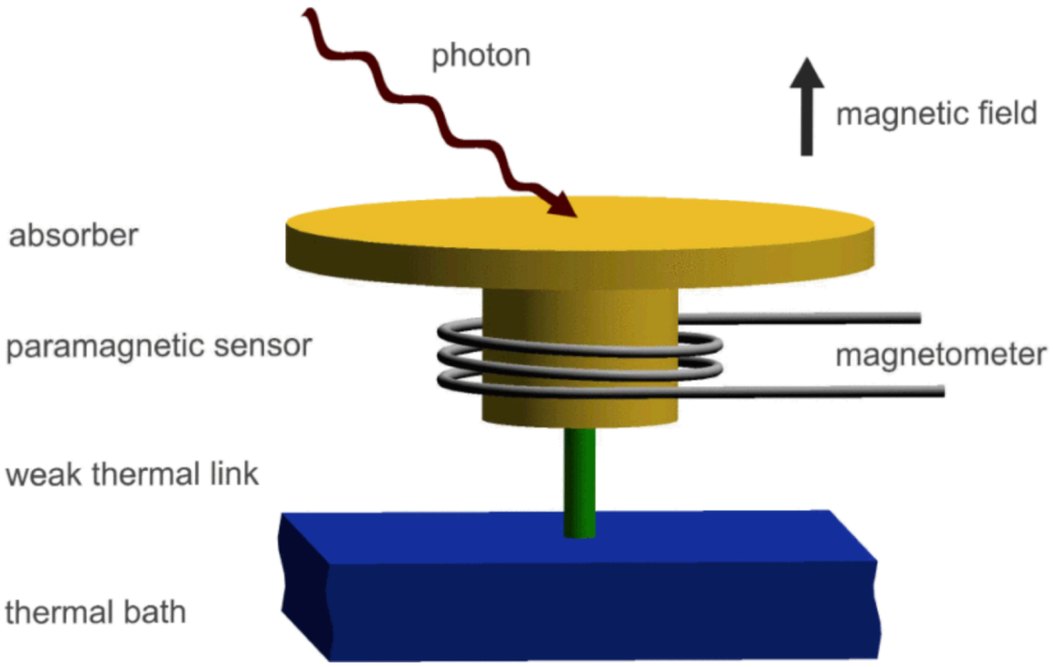

IEEE Transactions on Applied Superconductivity 19, 63 (2009)

- Tiny pixel 500 x 500 um²
- Temperature increase of the detector due to photon's absorption
- Decrease of sensor's magnetization, read by magnetometer (SQUID)
- Connected to thermal bath, the detector operates in a cryostat.

Image courtesy of **Katharina von Schoeler**

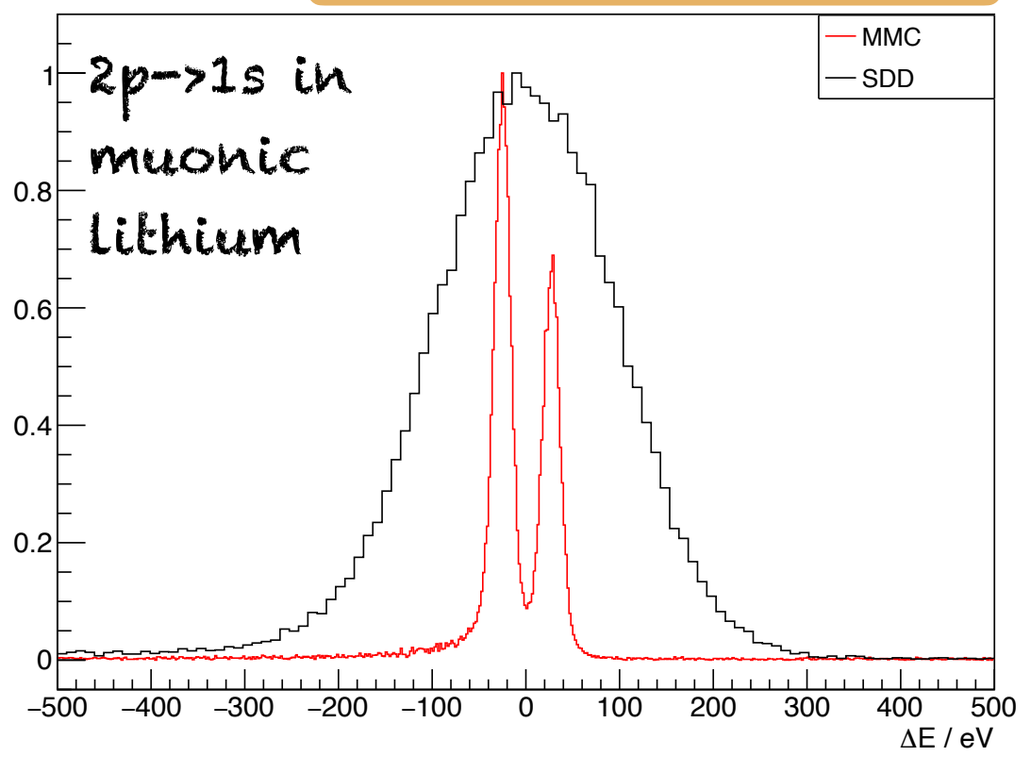

Expected energy resolution @ 20 keV

HPGe: >0.500 keV (FWHM)

SDD: ~0.200 keV (FWHM)

MMC: ~0.010 keV (FWHM)

Measurement demonstration of lithium
Energy spectrum

Analysis of data and image courtesy of **Katharina von Schoeler**

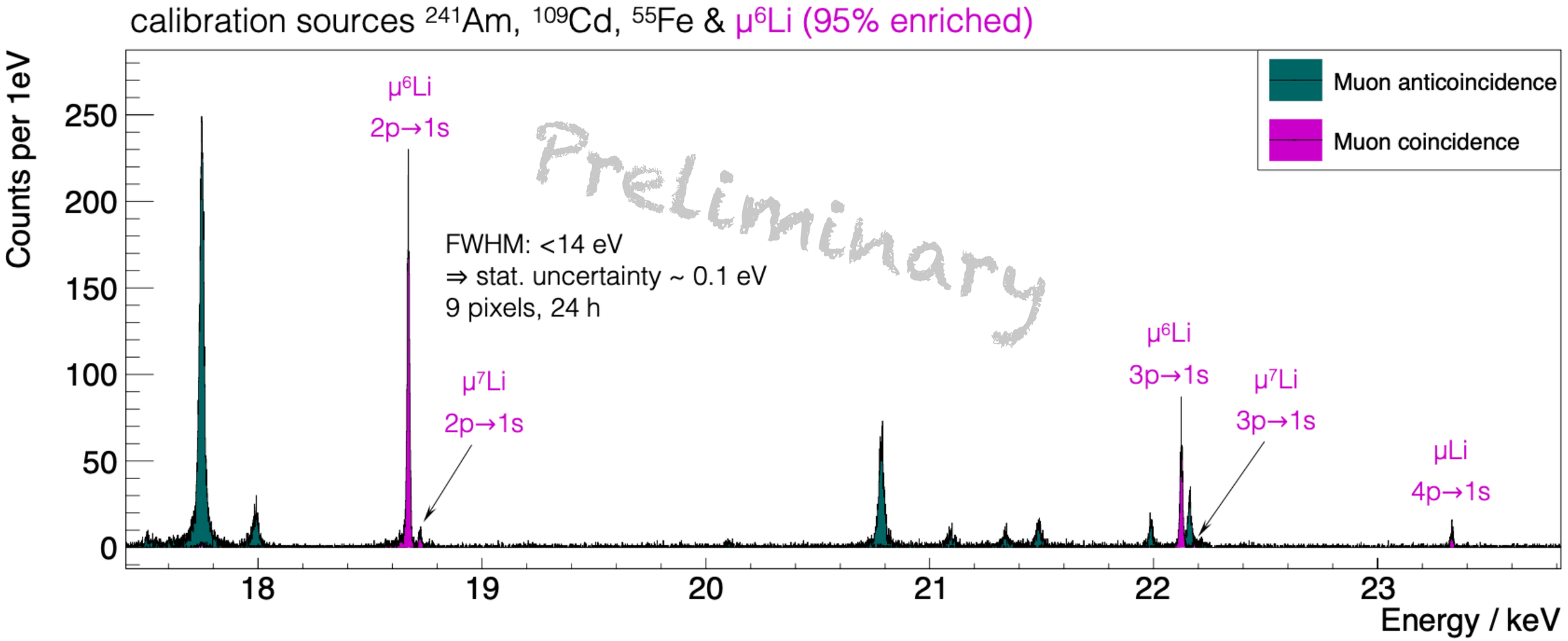

More elements have been measured since then!!

Studying capture rates after muon's nuclear capture

Muon Ordinary capture for the NUclear Matrix elemENTs in ββ decays (MONUMENT)

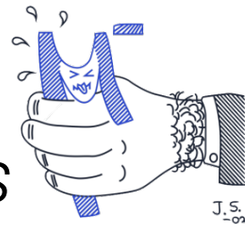

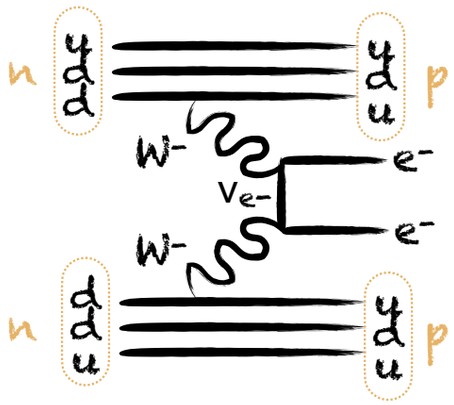

Decay rate of 0νββ

Phase space

$$\Gamma^{0\nu}_{\beta\beta} = \frac{1}{T^{0\nu}_{\beta\beta}} = G^{0\nu} \left| M^{0\nu} \right|^2 \langle m_{\beta\beta} \rangle^2$$

NME squared
→ calculated with large theoretical uncertainty

Square of effective Majorana mass

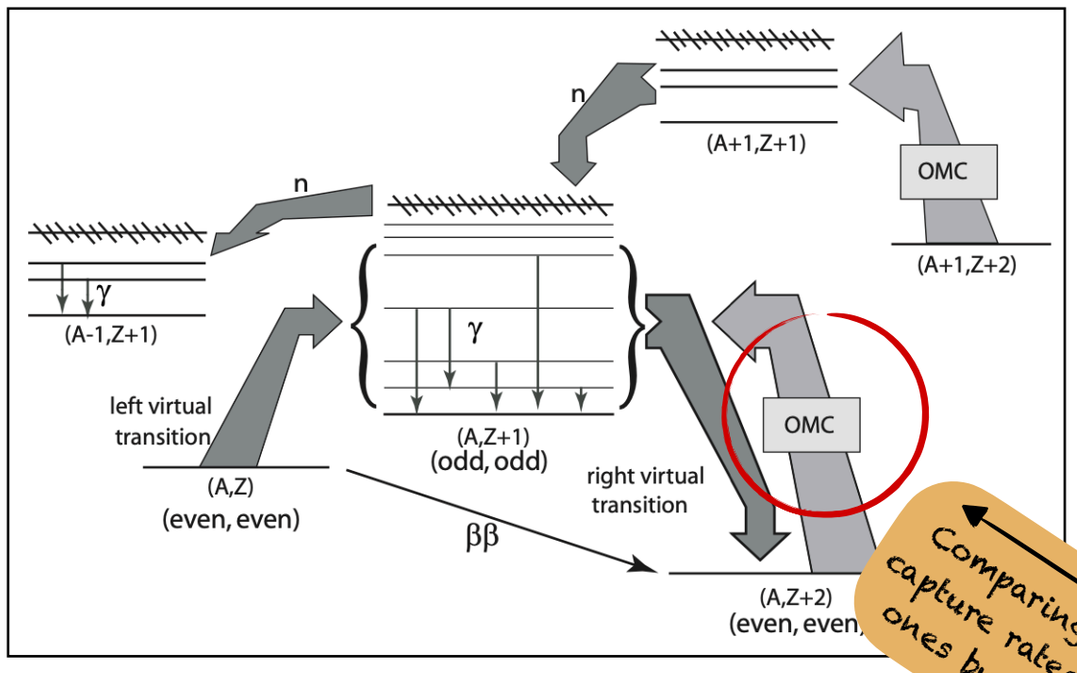

$$\begin{aligned}
\mu^- + (\mathbf{A},\mathbf{Z}) &\rightarrow (A, Z-1)^* + \nu_\mu \\
&\rightarrow (A, Z-1) + \gamma \\
&\rightarrow (A-1, Z-1) + \gamma + n \\
&\rightarrow (A-2, Z-1) + \gamma + 2n \\
&\vdots \\
&\rightarrow (A-2, Z-2) + \gamma + n + p
\end{aligned}$$

Comparing experimental capture rates to calculated ones by the shell model

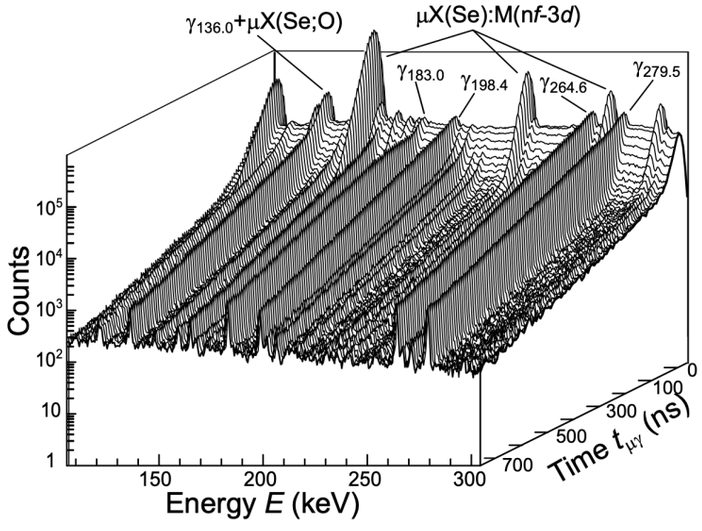

Phys. Rev. C 99, 024327 (2019)
Eur. Phys. J. C 84, 1188 (2024)
EPL 58, 666 (2002)

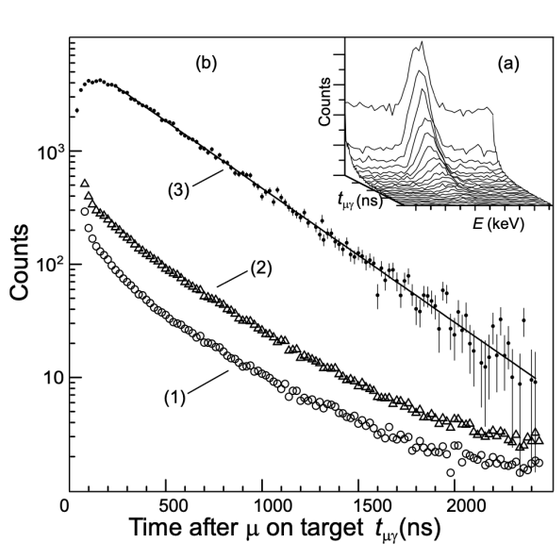

Total capture rate

$\lambda_{total} = \lambda_{decay} + \lambda_{absorbed} = 1/2.2\ \mu s + 1/\tau_{capture}$

Partial capture rate

$\lambda_{capture\text{-}i} = \lambda_{total}\ Y_i$ → Absolue γ-ray yield

Studying samples' elemental composition
***M**uon **I**nduced **X**-ray **E**missions (MIXE)*

- Determining the elemental composition of different samples (such as archaeological artefacts, meteorites, batteries) from the cascade transition yields of the muonic x rays.

- The muonic energies are characteristic of the element.

Arrowhead made of meteoritic iron

Journal of Archaeological Science 157, 105827 (2023)

Knob bow fibula

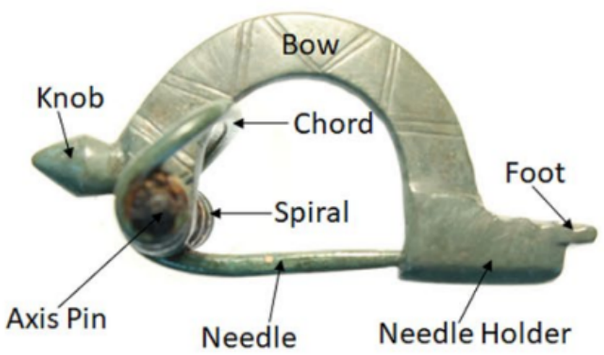

Herit Sci 11, 43 (2023)

Copper (Cu)
Zinc (Zn)
Tin (Sn)
Lead (Pb)

Herit Sci 11, 43 (2023)

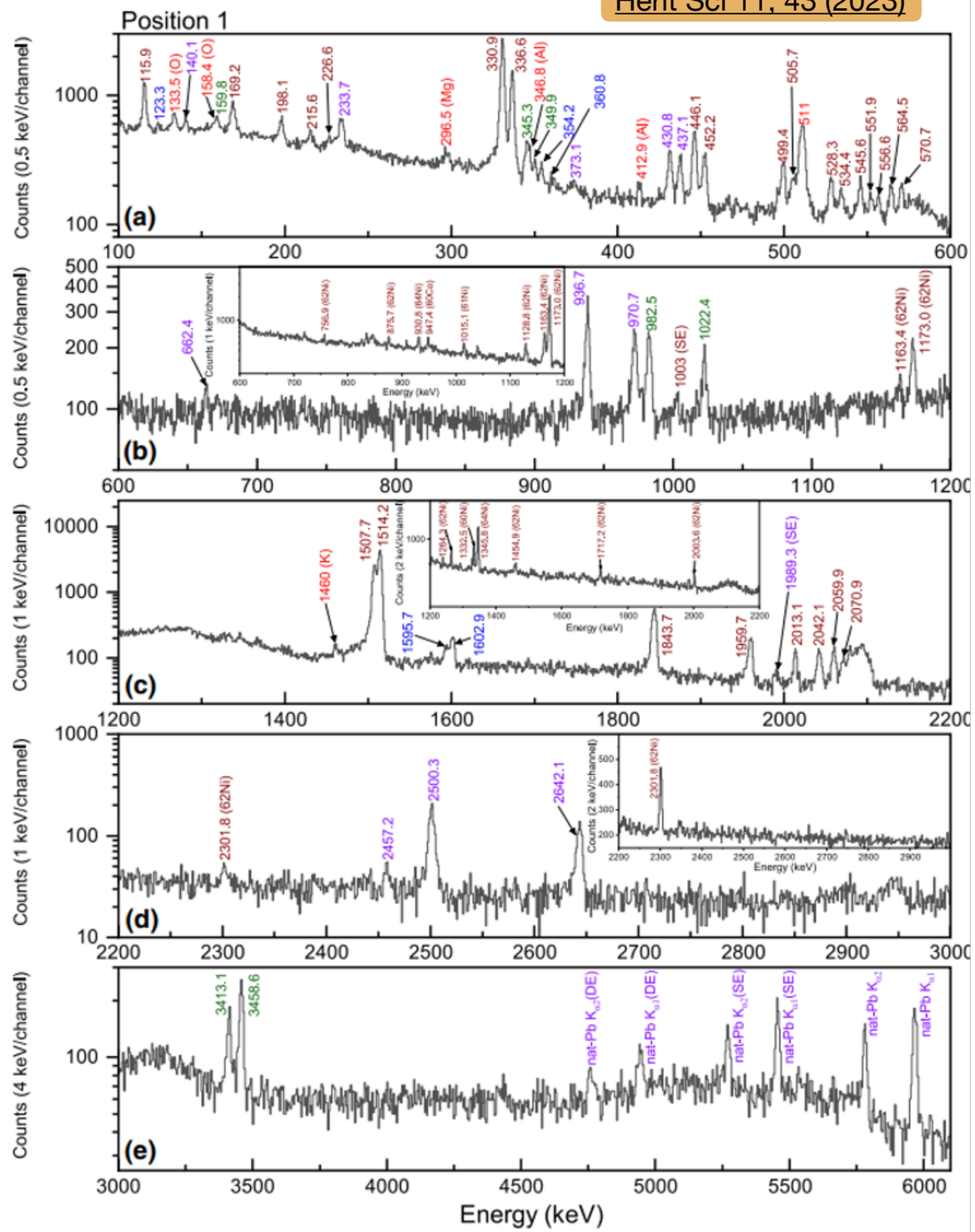

Science case
Summary & Outlook (muX / RefRadii)

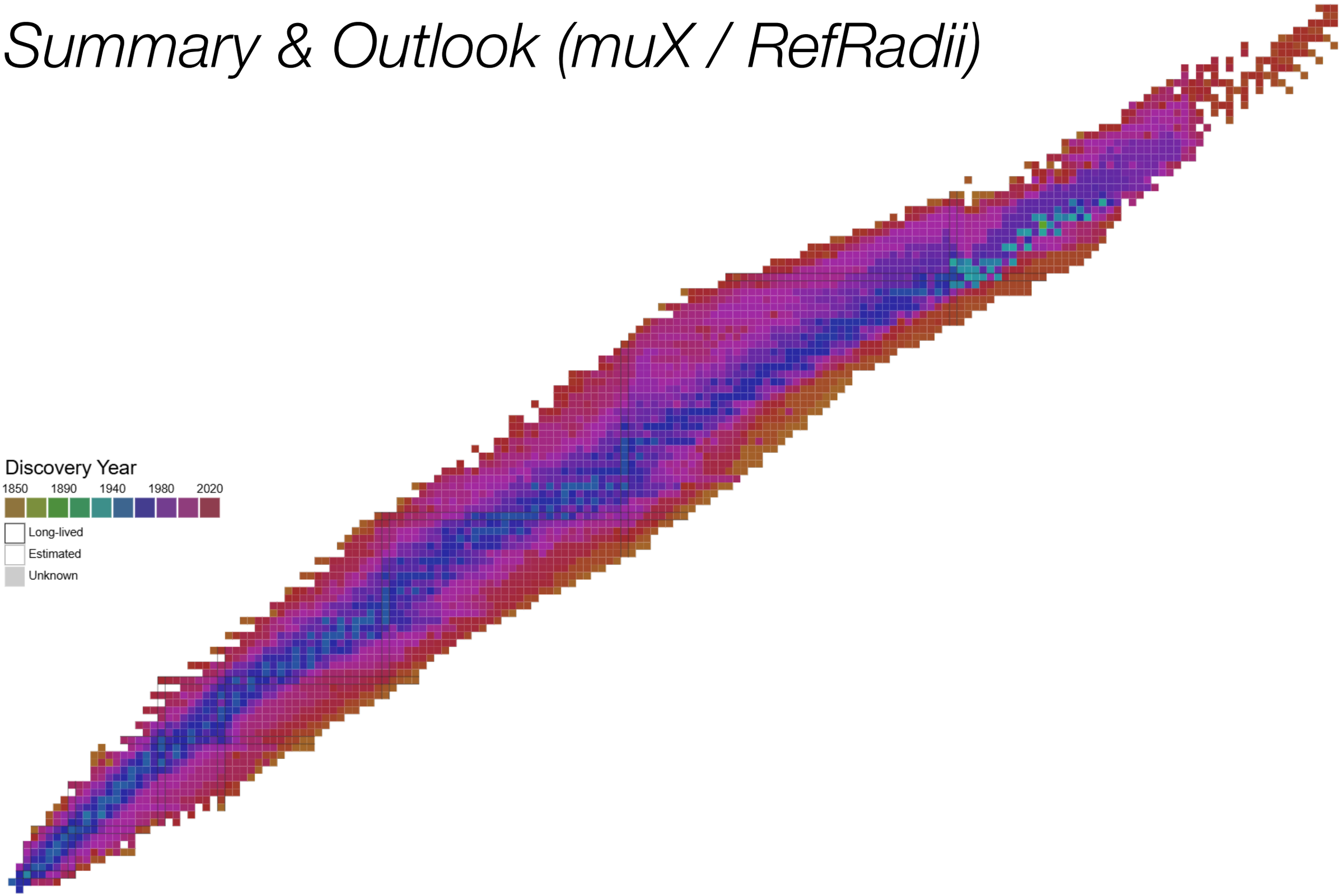

Science case
Summary & Outlook (muX / RefRadii)

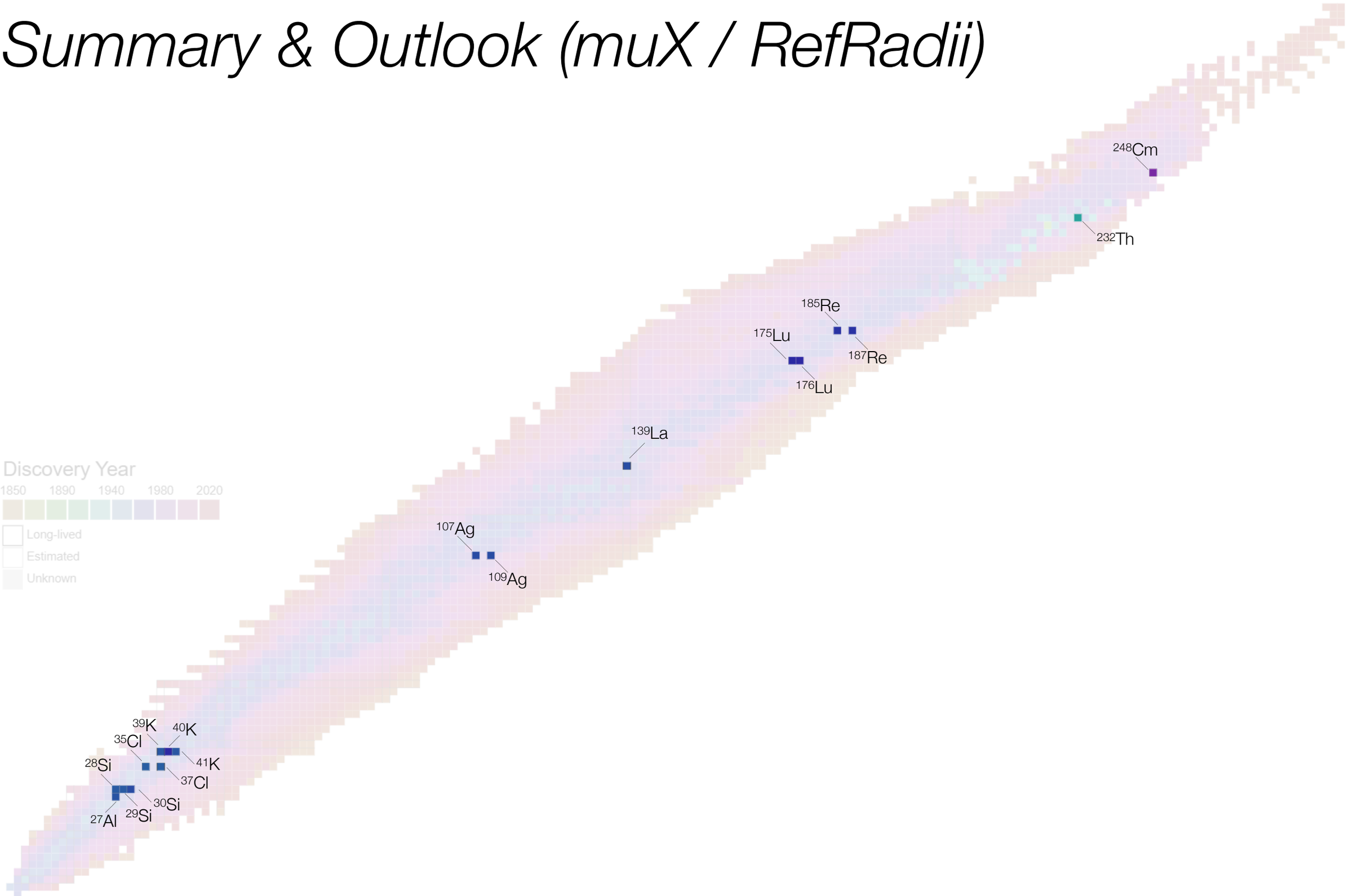

Science case
Summary & Outlook (muX / RefRadii)

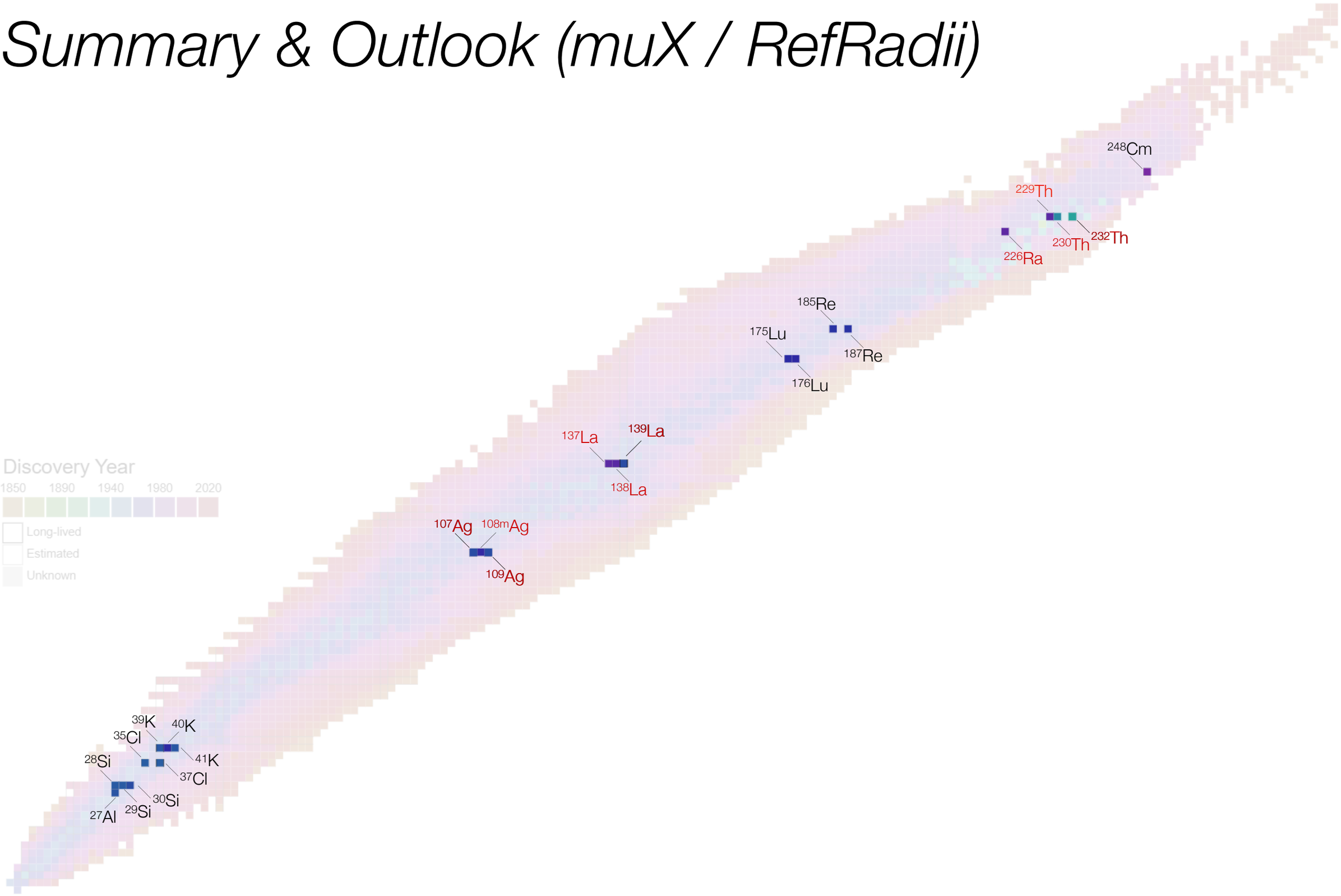

Behind the story told...

Backup Slides

^{185}Re and ^{187}Re 5g4f analysis

Spectroscopic quadrupole moment

The spectroscopic quadrupole moment Q is extracted from the 5→4 transitions being not sensitive to the details of the nuclear charge distribution

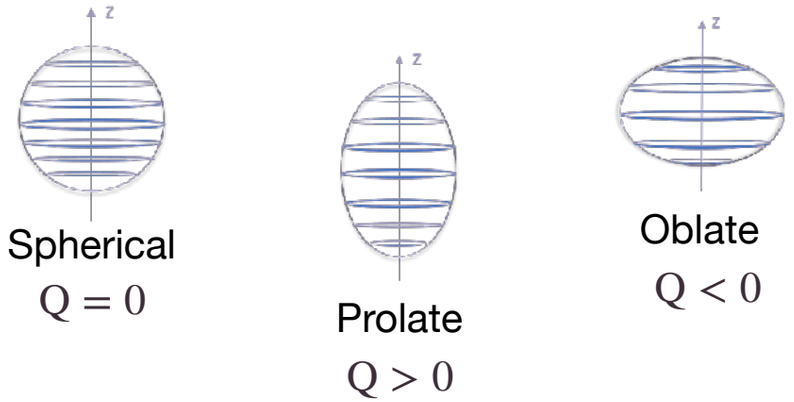

To extract the quadrupole moment:

- Theoretical predictions of hyperfine transitions
- Good knowledge of the instrumental response is required

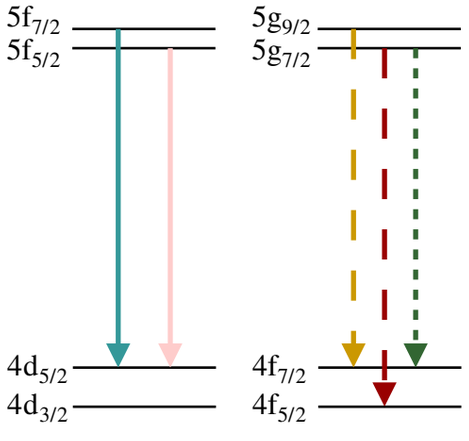

Theoretical calculations by **N. Michel & N. Oreshkina**, MPIK, Heidelberg

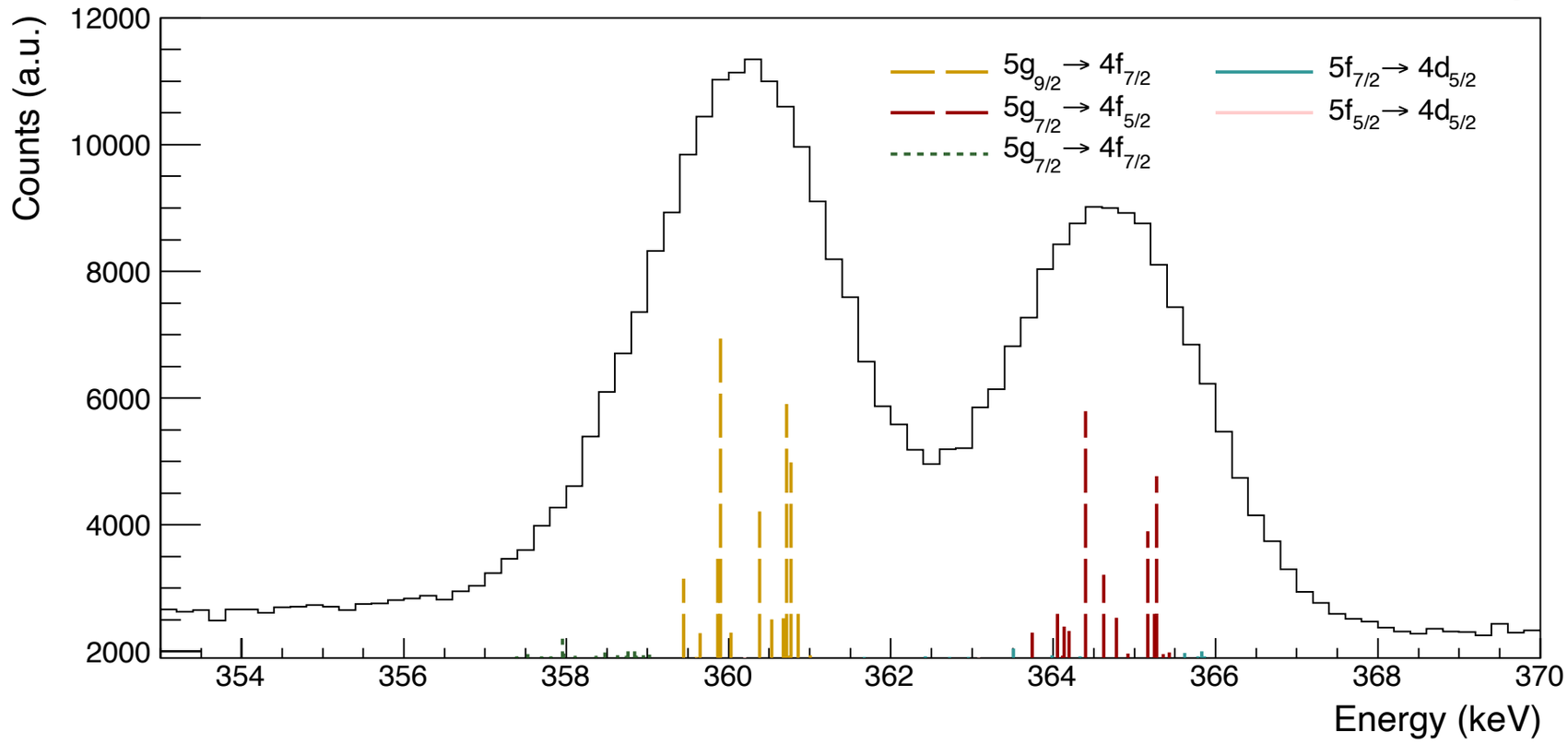

Optimizing the geometry for higher efficiency
Full GEANT4 simulations

- Full GEANT4 simulations of the detectors' position in the frame considering all physical limitations of the setup.
- Angle dependencies on single crystals and combine all HPGe detectors to reach the maximum possible efficiency
- Use wisely the electron veto-ed space for good HPGe detectors

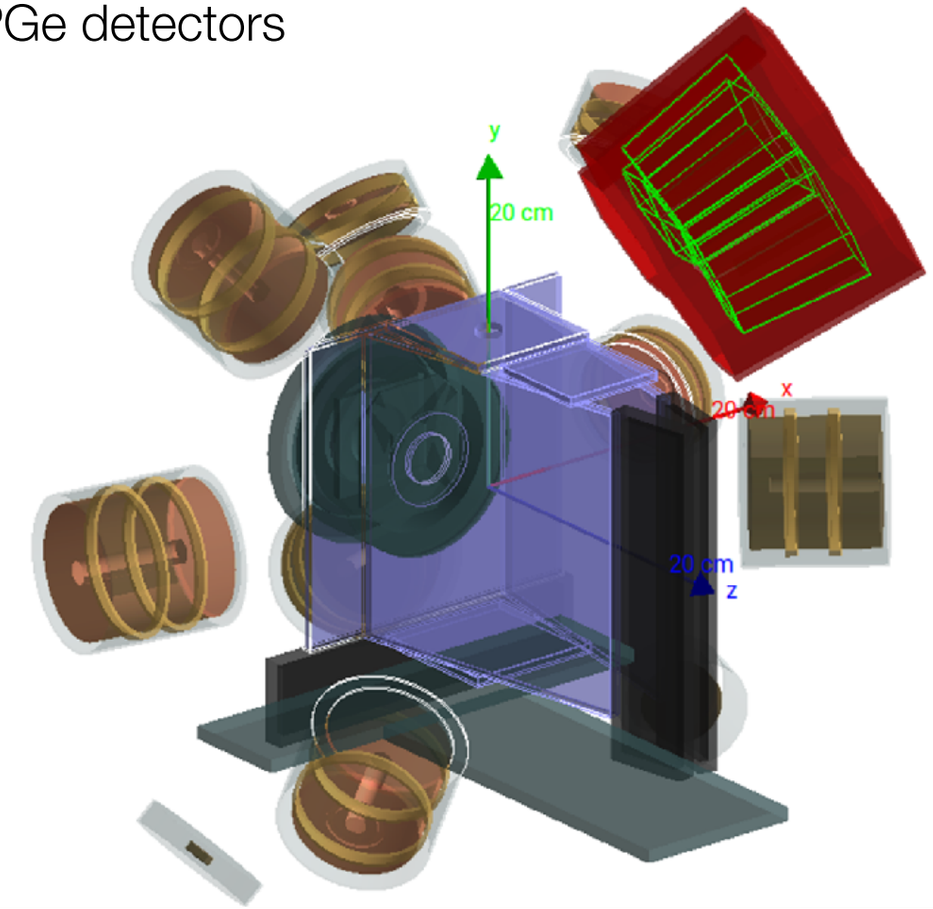

Geant4 simulations and visualisations created by **Marie Deseyn**

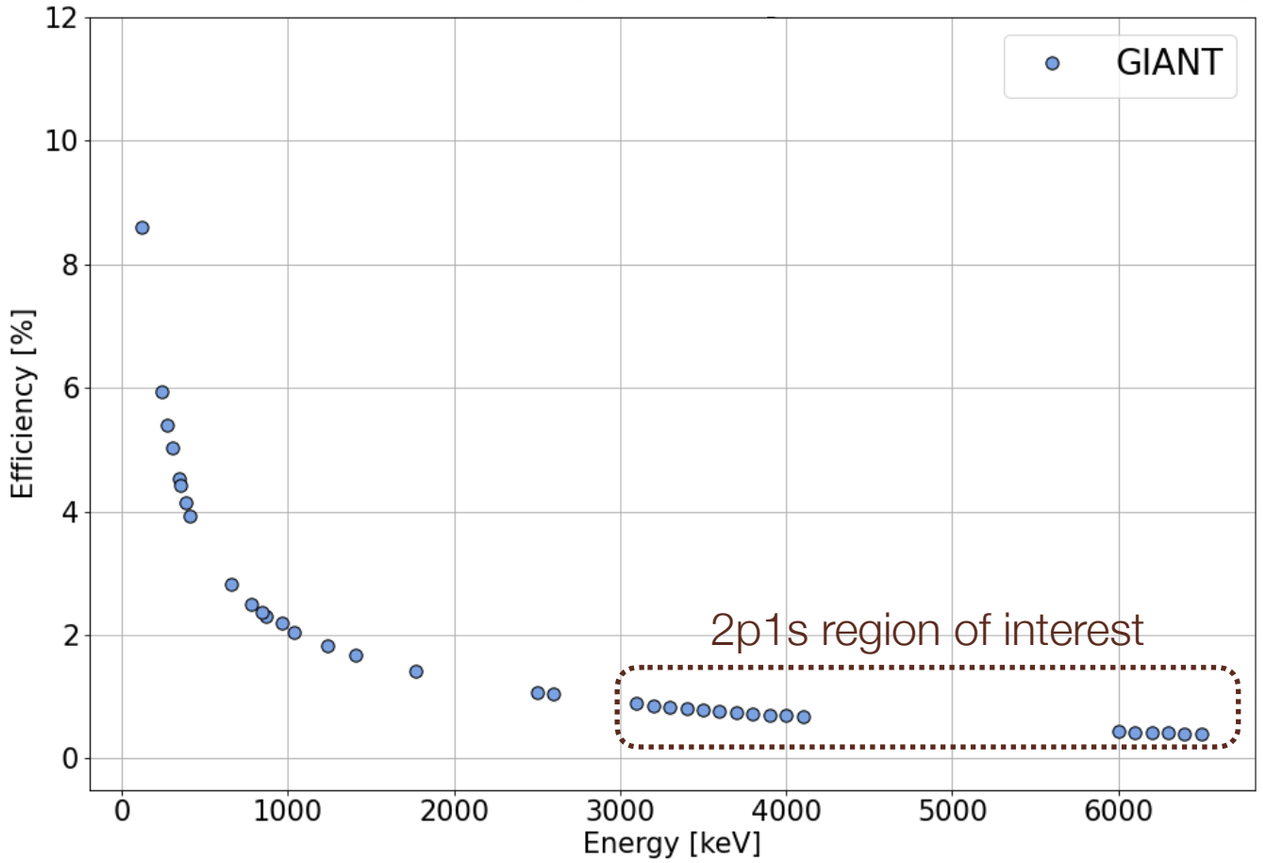

Motivation for ^{226}Ra

Atomic parity violation in radium

Adapted from Nature 557, 207–211 (2018)

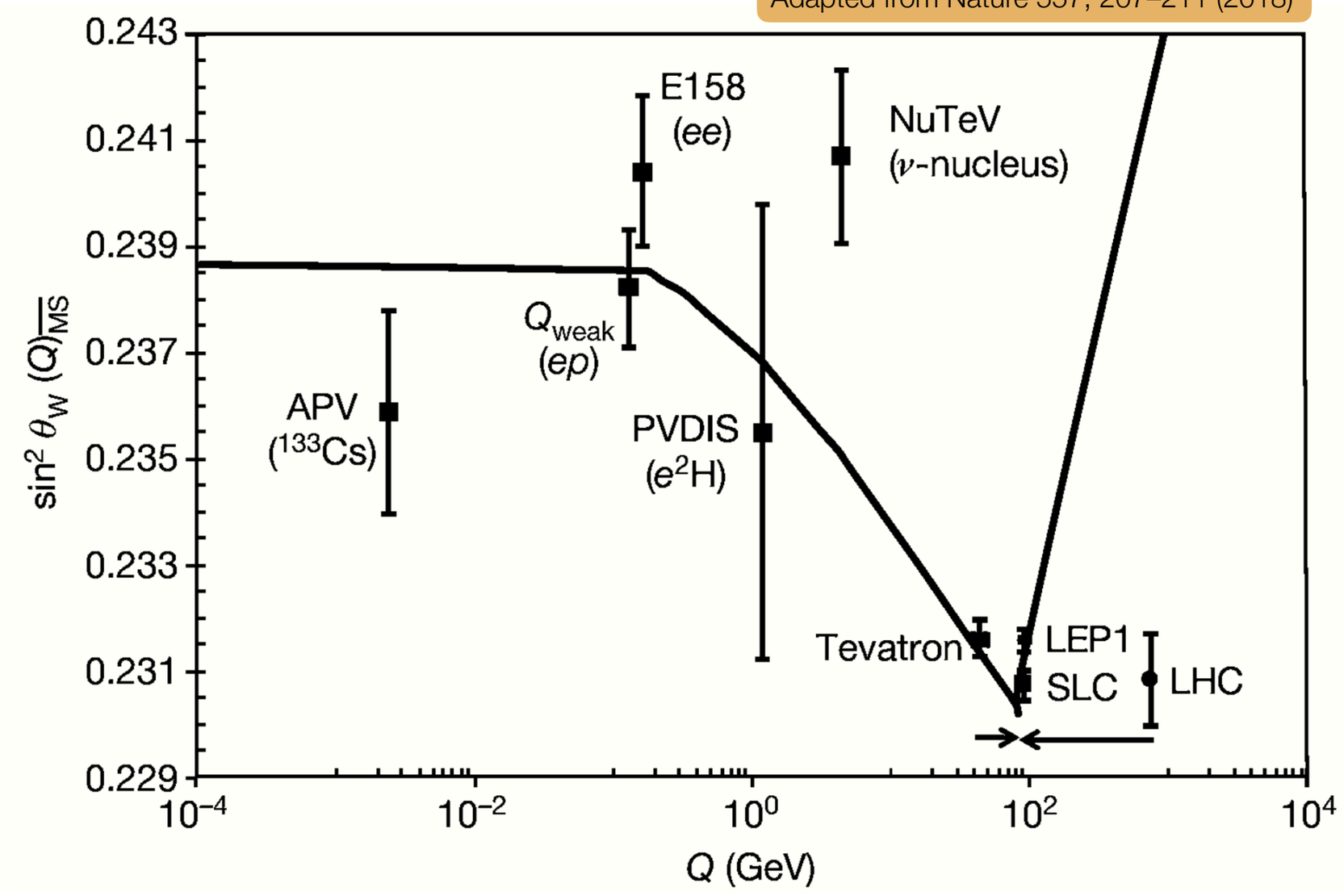

MMC detector
Detection efficiency

J Low Temp. Phys. 216, 344–351 (2024)

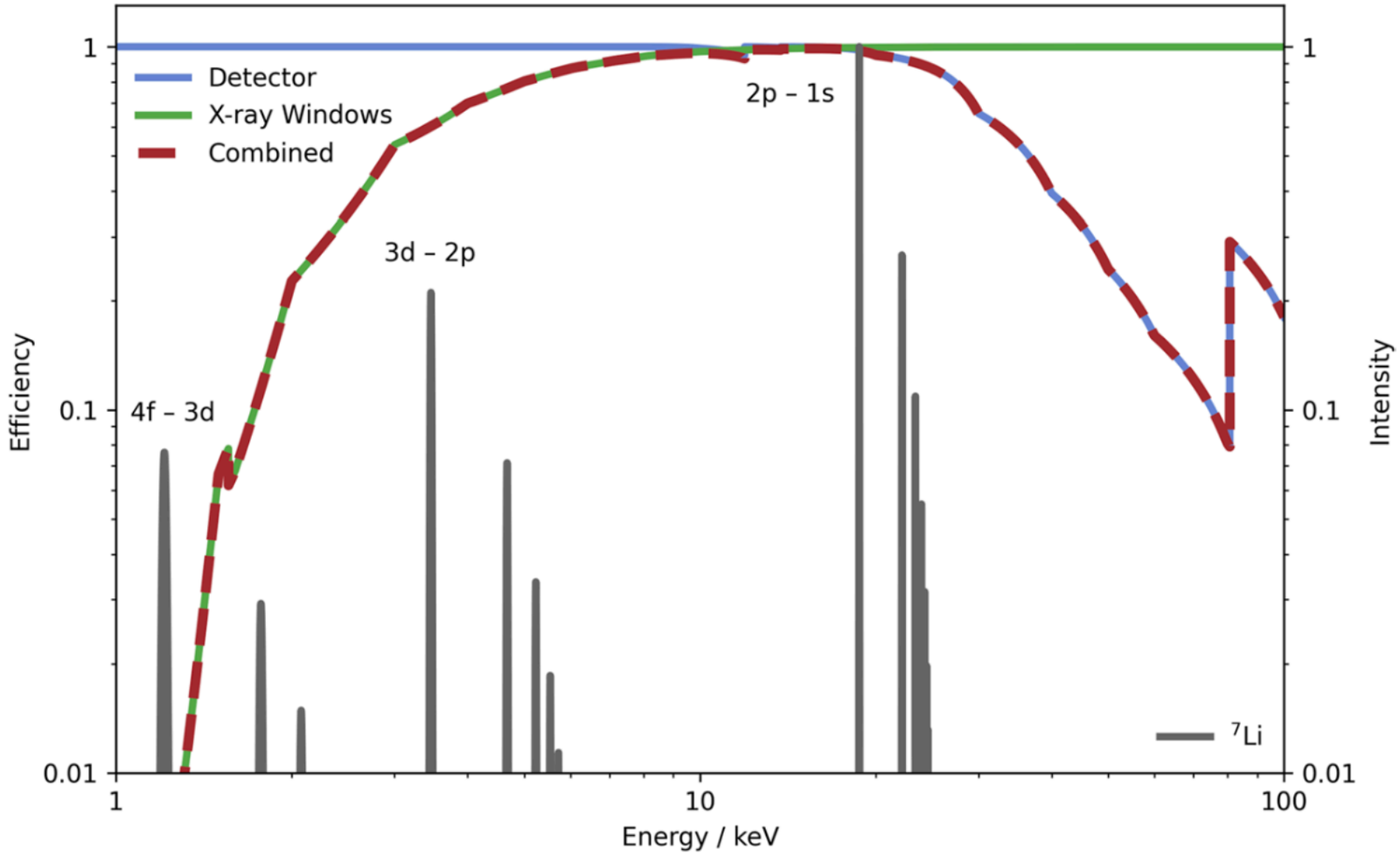

Comparing target fabrication techniques

Graphite targets

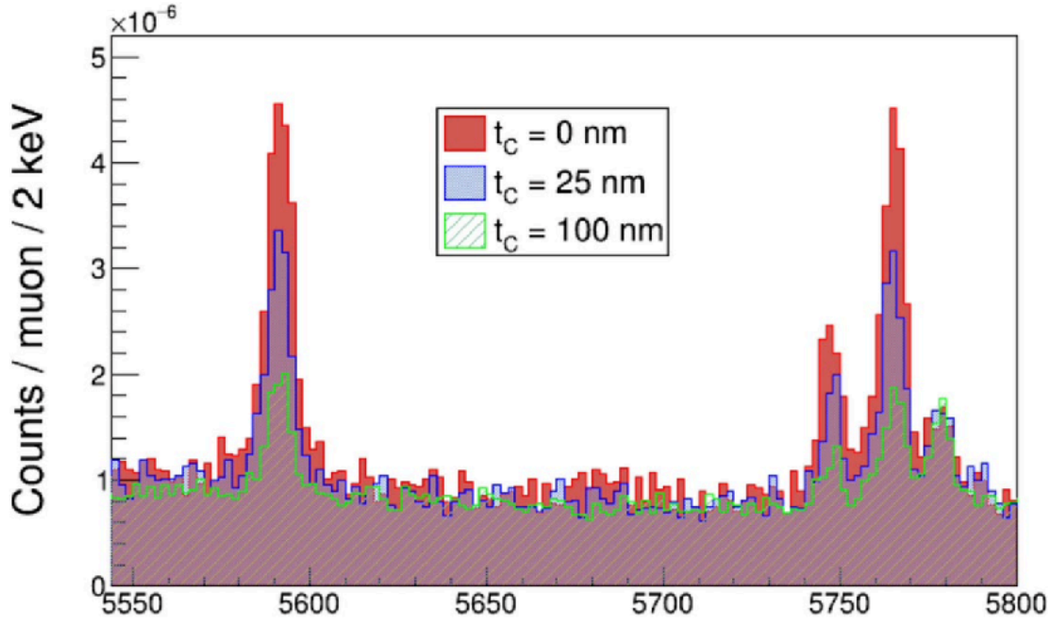

Sci Rep 15, 6939 (2025)

Molecular plating &
Drop-on-Demand

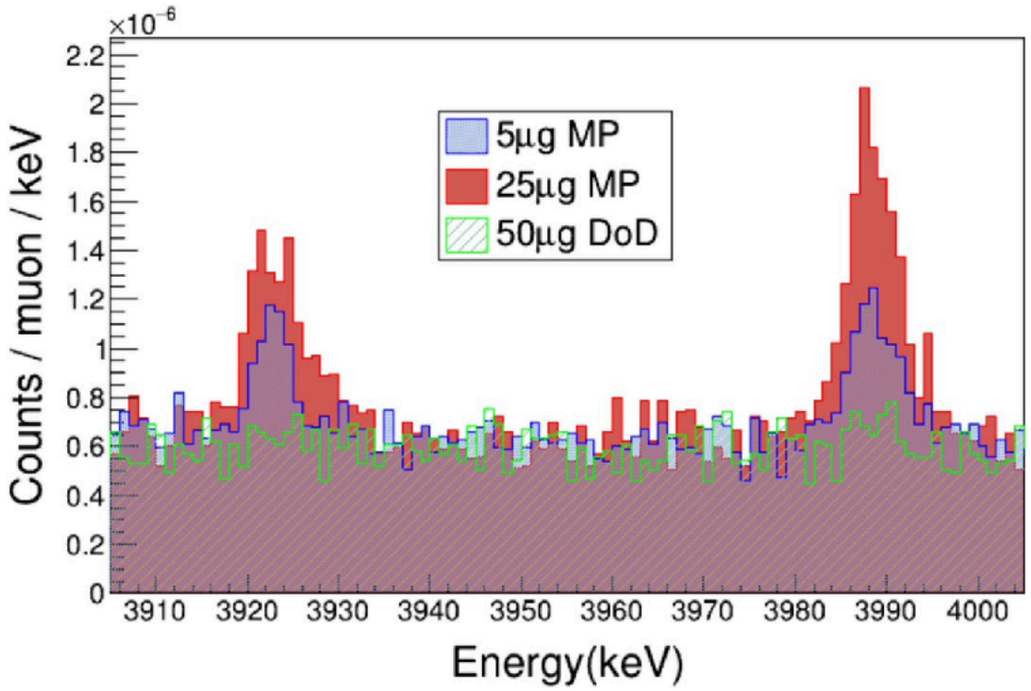

Muonic spectrum in ^{nat}La

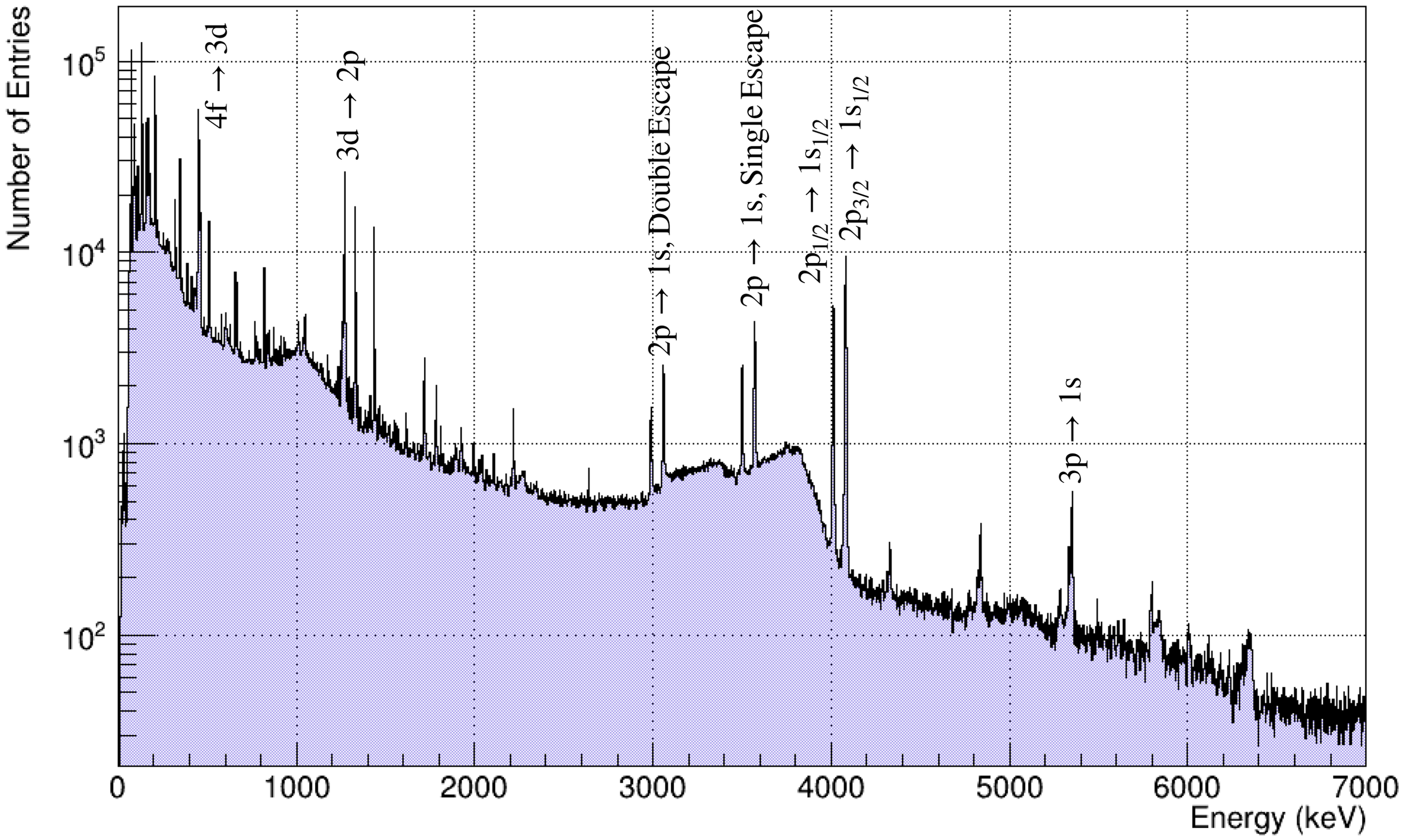

Charge distribution model

Nuclear charge distribution
for spherical nuclei

$$\rho(r) = \rho_0 \left(1 + e^{4 \ln 3 \frac{r-c}{t}}\right)^{-1}$$

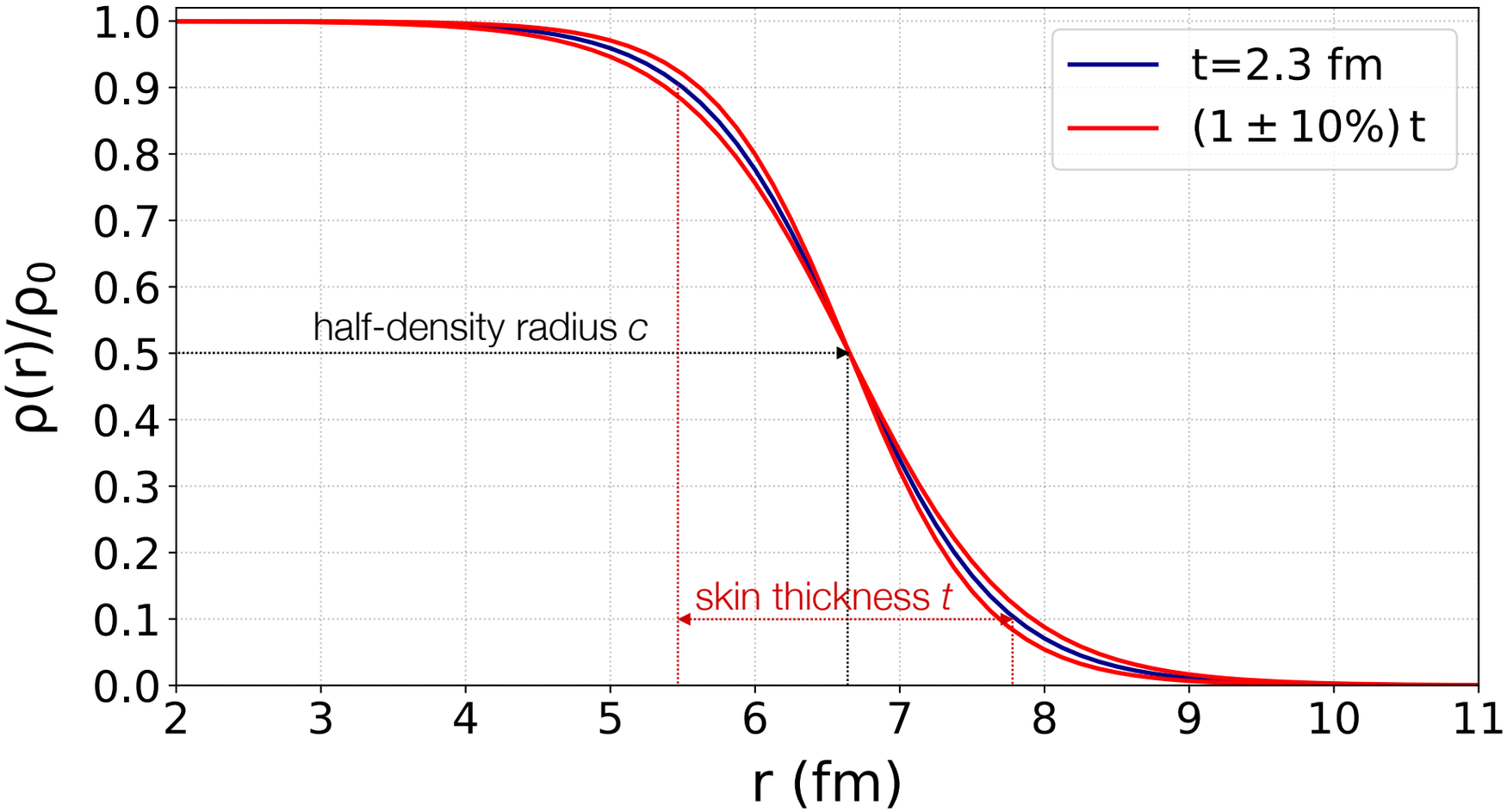

Gas cell structure

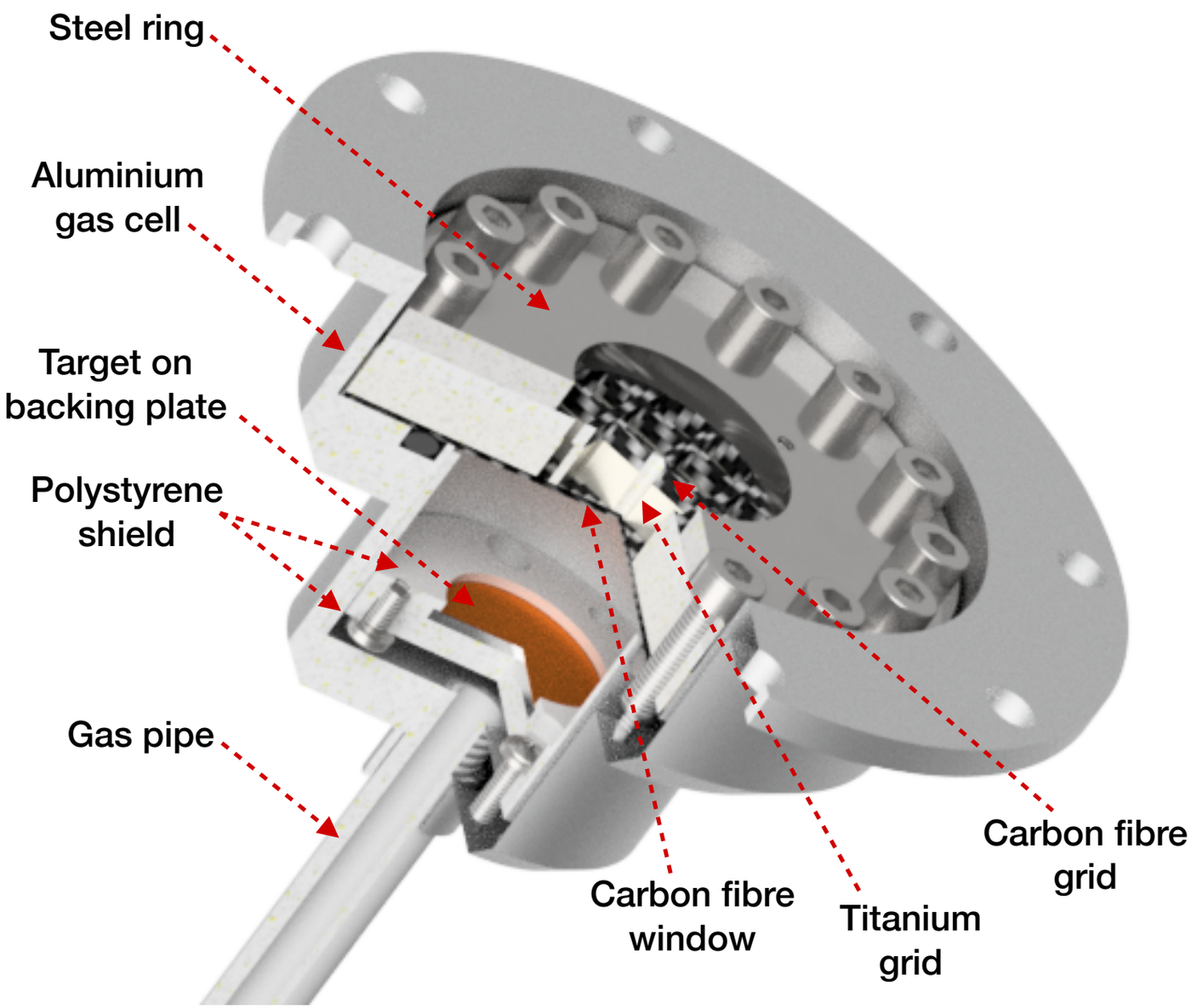

Time distributions after transfer

PhD thesis of A. Skawran
Simulations by J. Nuber

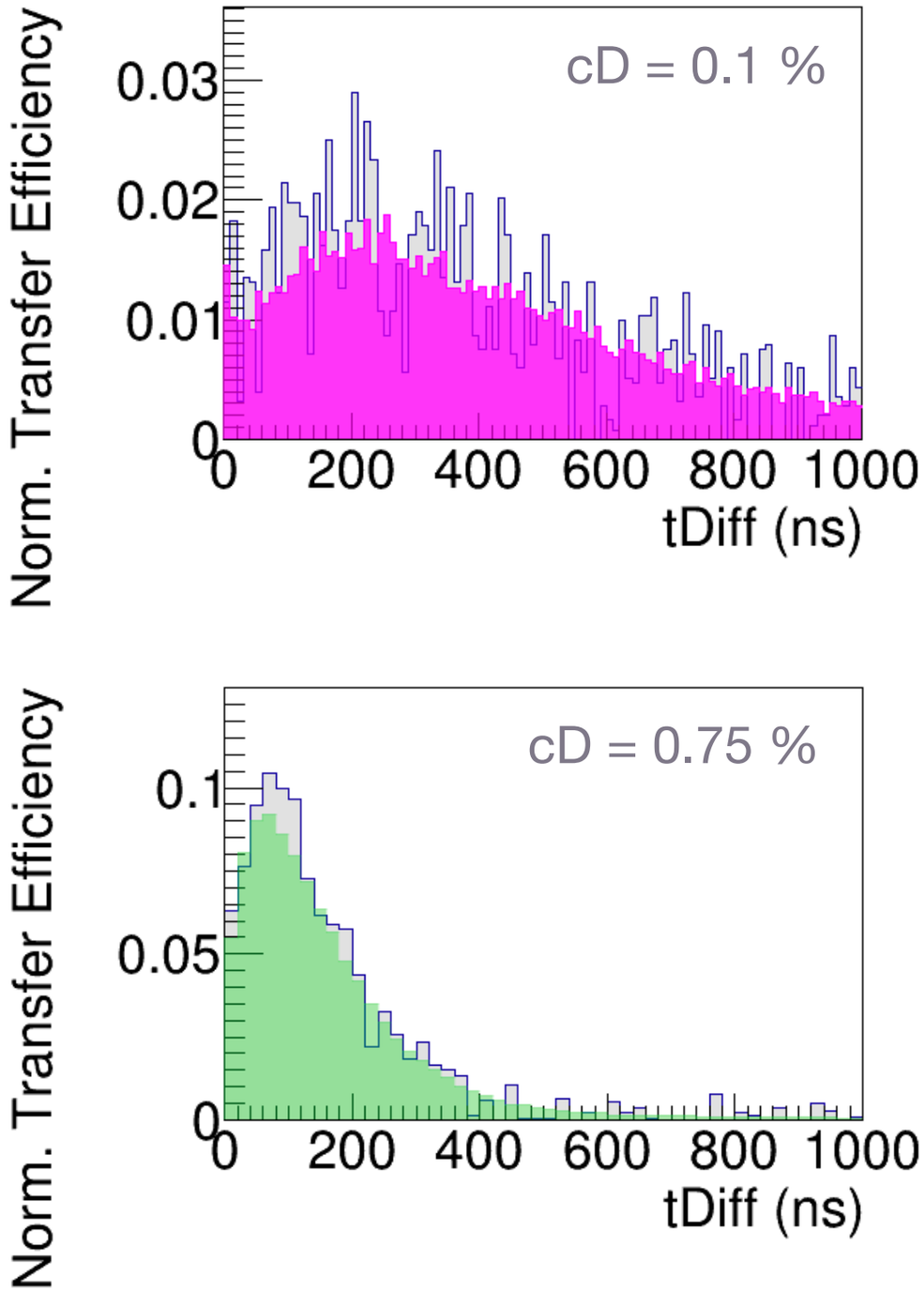

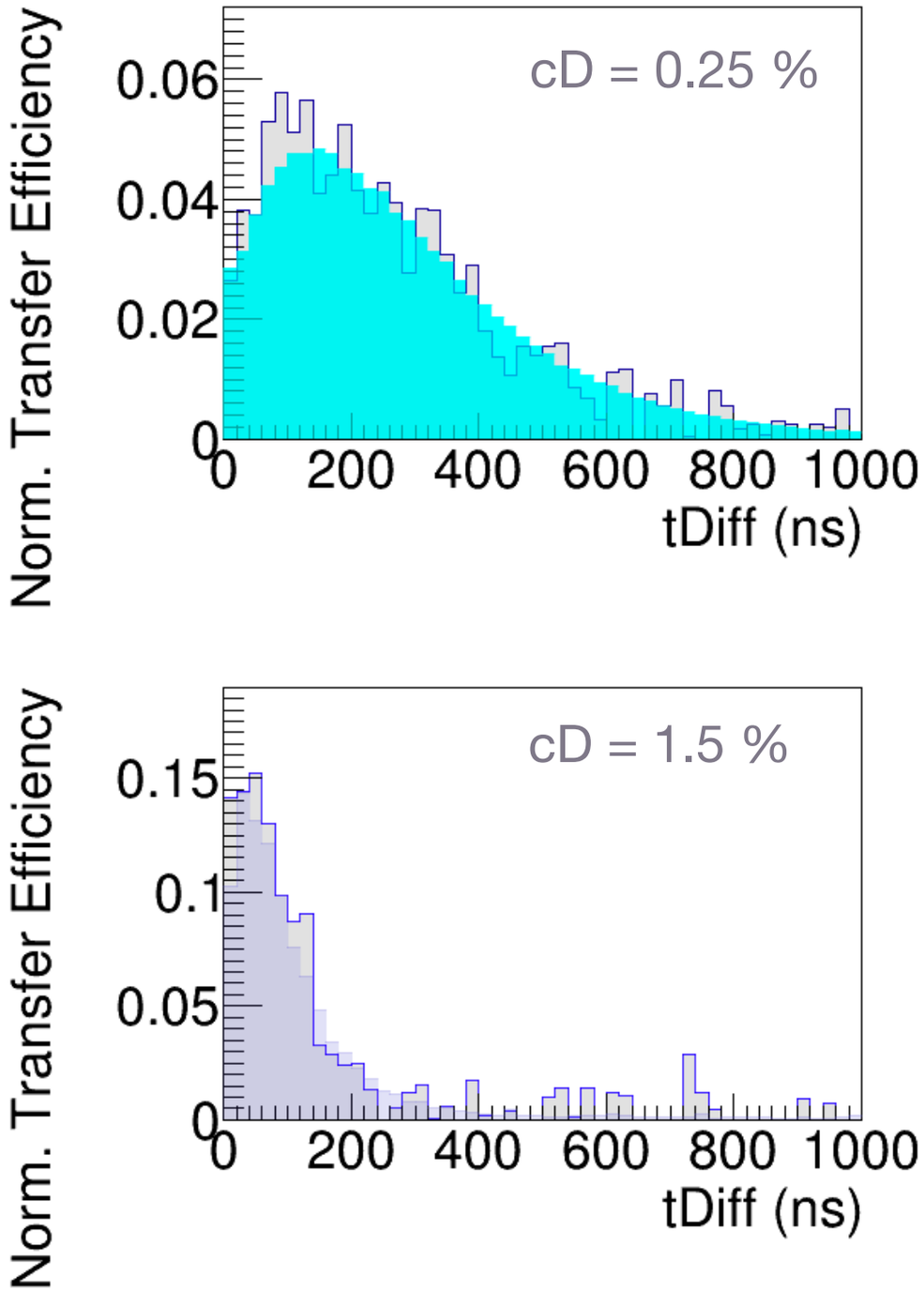

Demonstration of muon transfer reaction

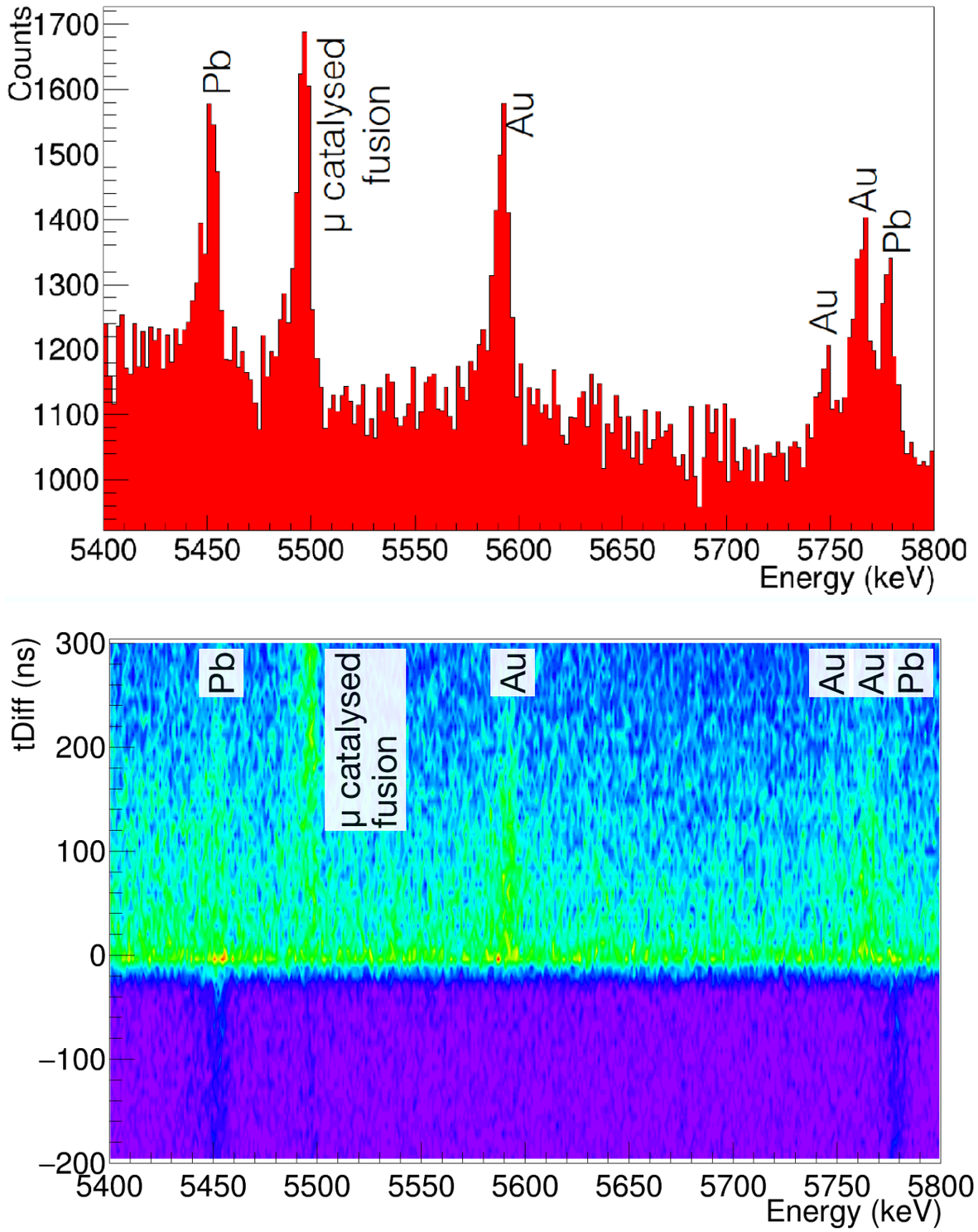

GIANT efficiency comparison
Experimental VS simulated

Image courtesy of **Marie Deseyn**

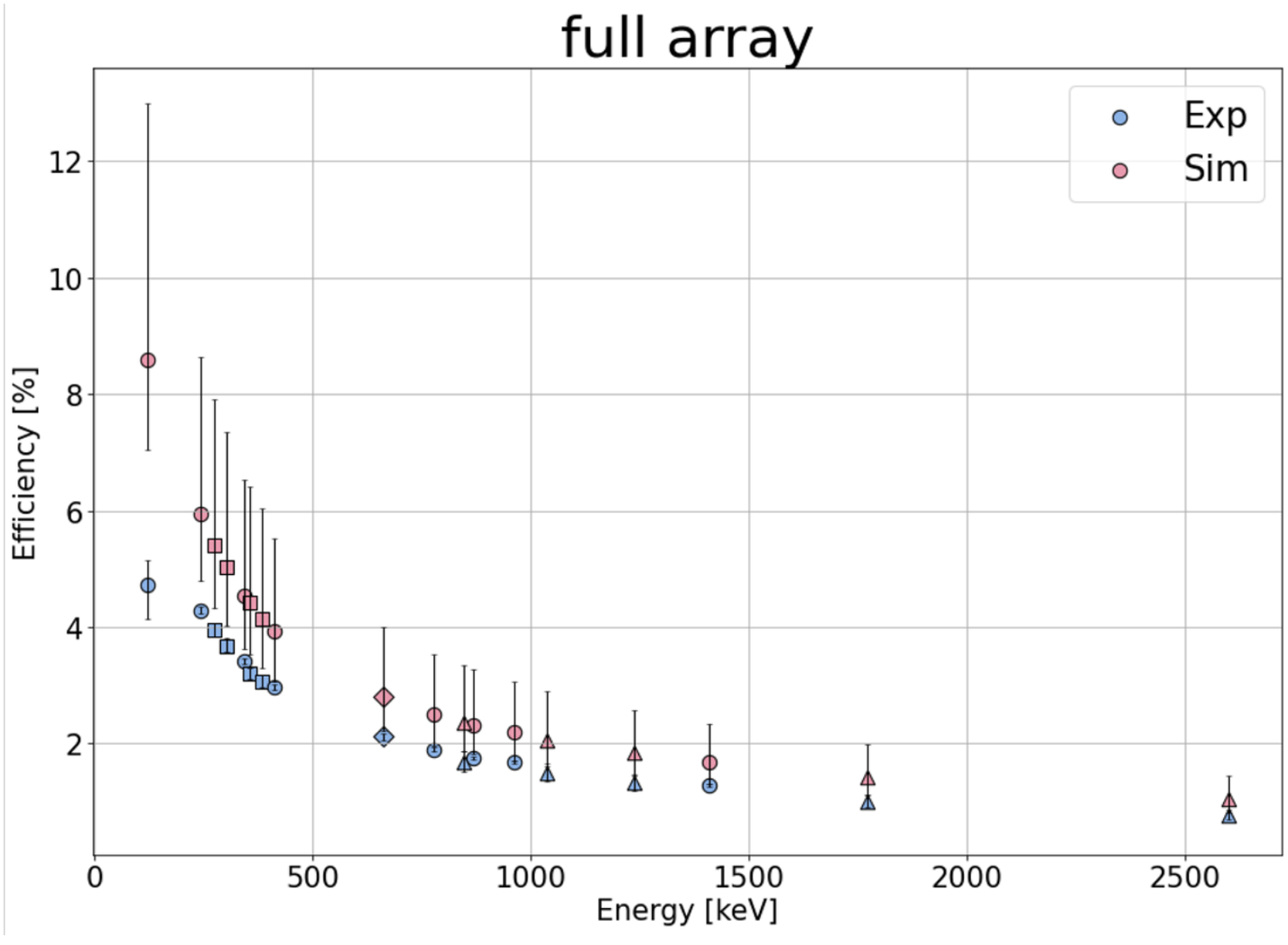

Challenging the microgram targets
Higher efficiency with the IDS array

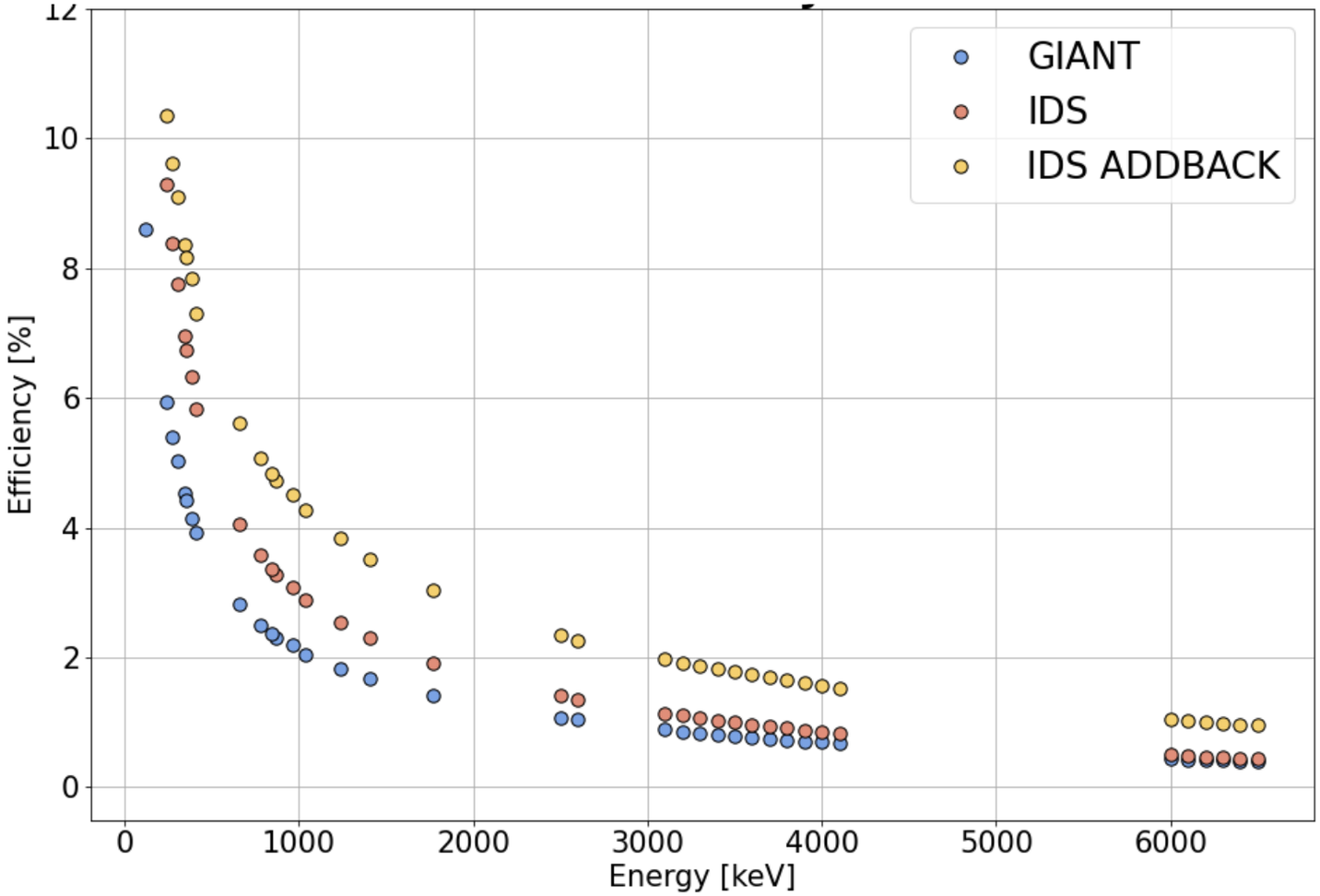

Only 12 IDS clovers are simulated

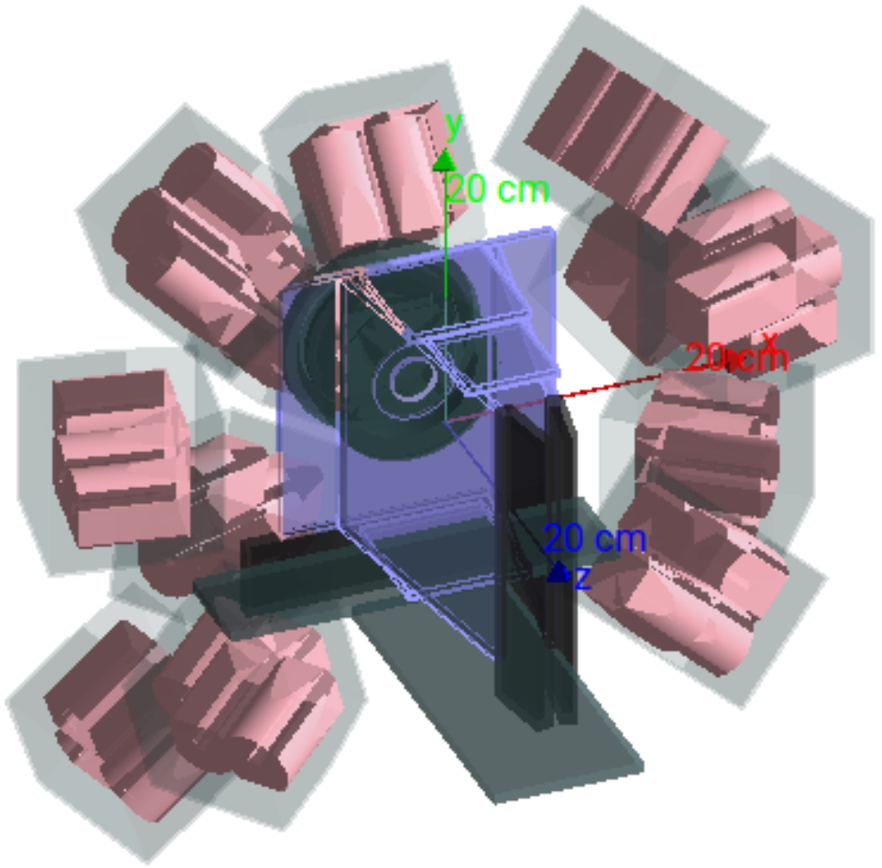

**IDS simulation assumes 20 mm between end cup and all crystals. Efficiency to be increased by ~25% for the corrected gap.

Geant4 simulations and visualisations created by **Marie Deseyn**.
IDS detectors' geometry by **War War Myint Myat Phyo**.

Science case
What's next?

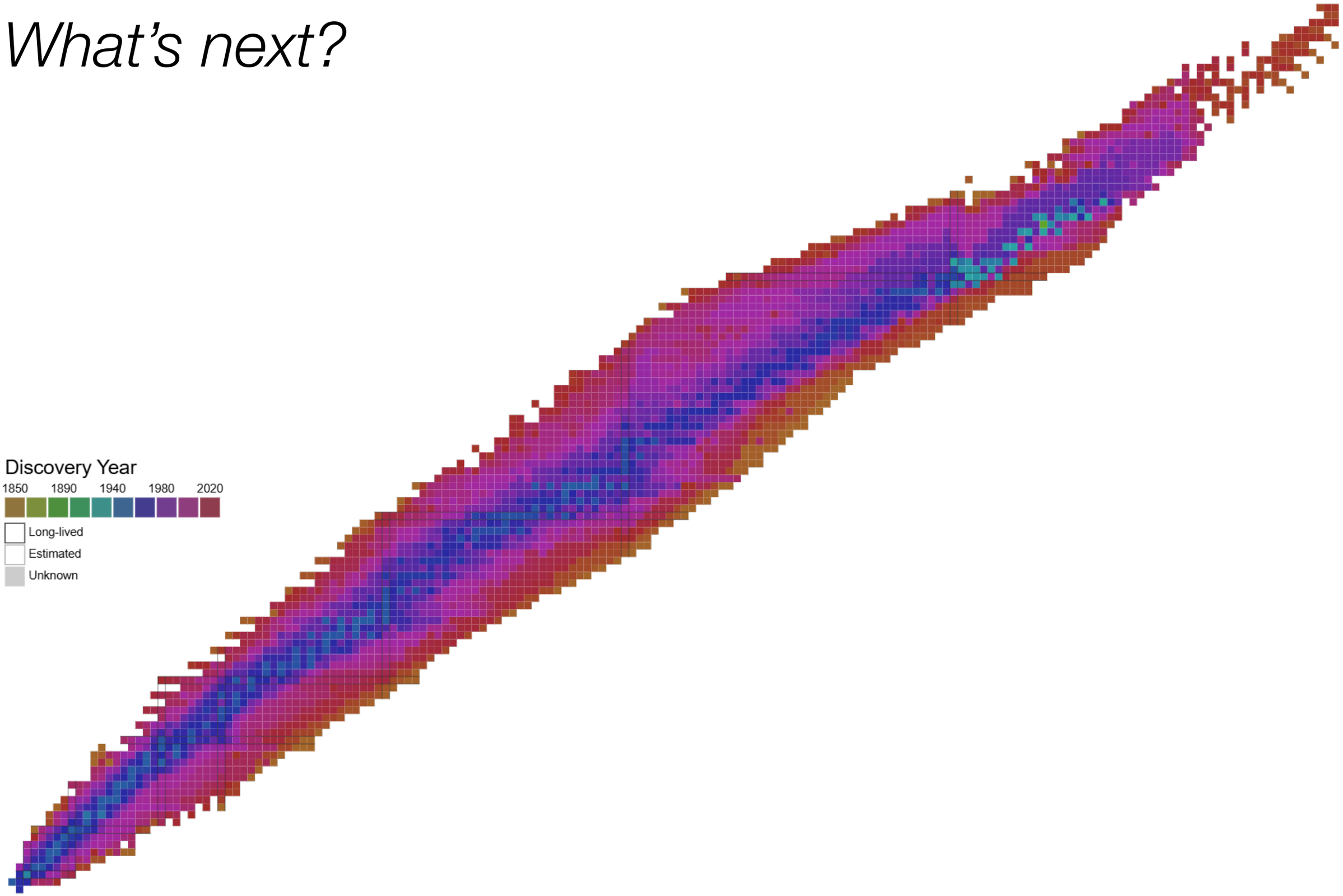

Science case
What's next?

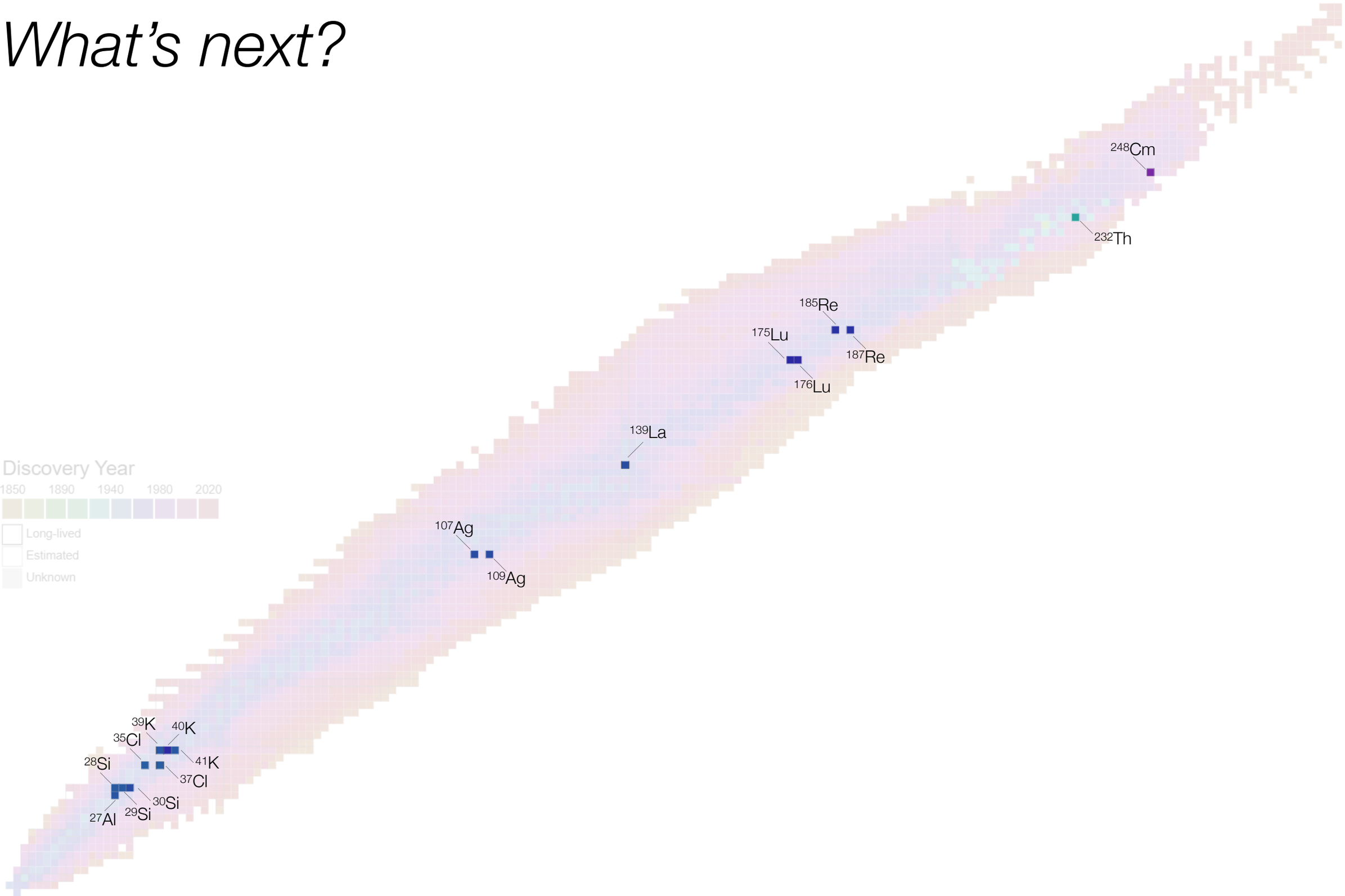

Science case
What's next?

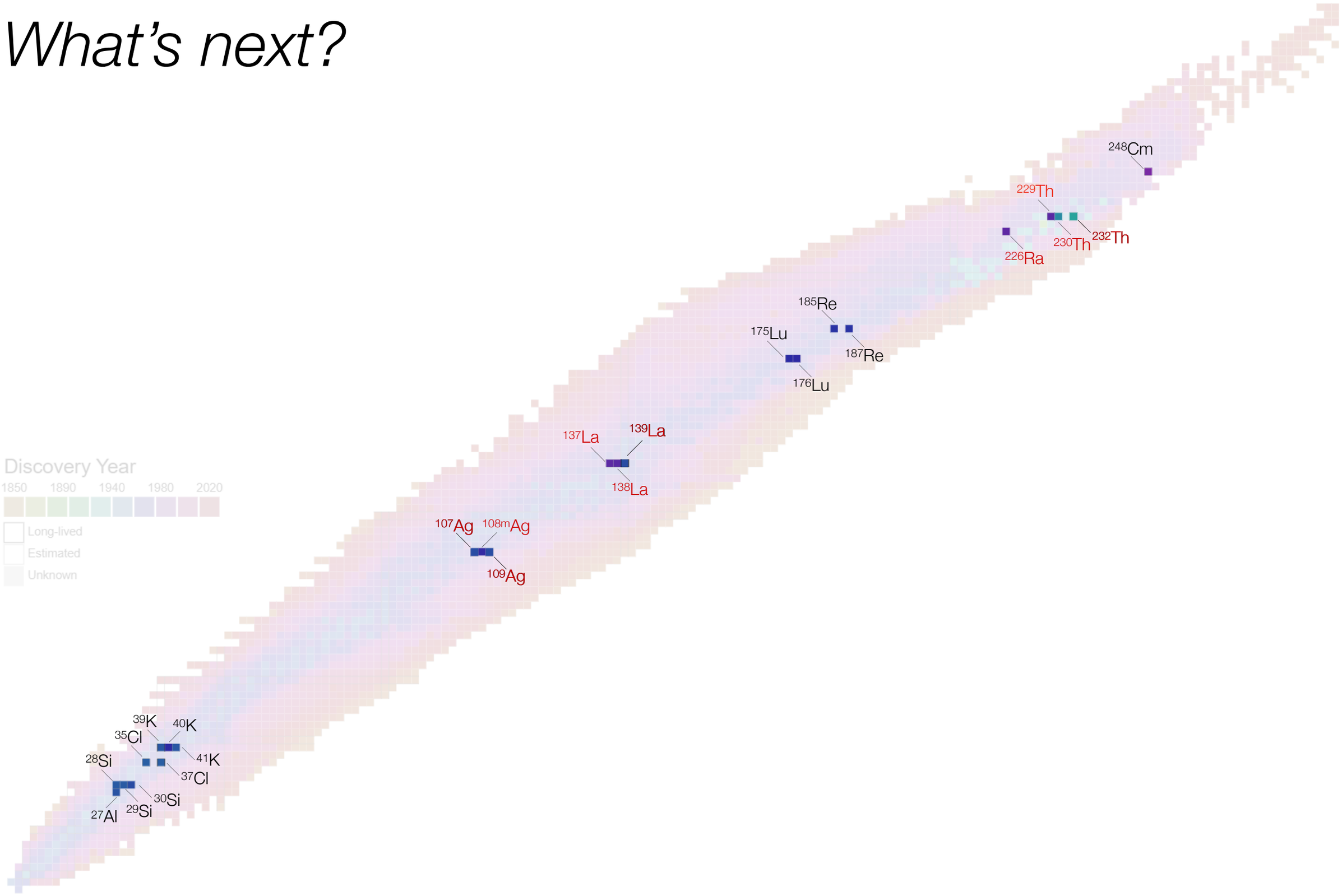

Science case
What's next?

Benchmarking the laser spectroscopy results & test state-of-art nuclear models

Image courtesy of Marie Deseyn

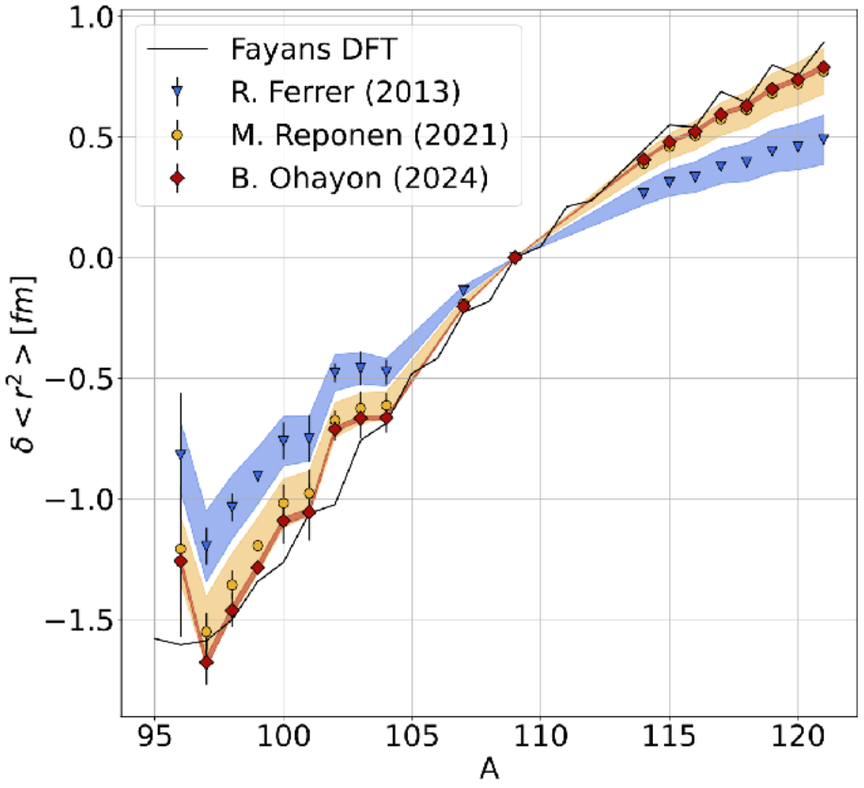

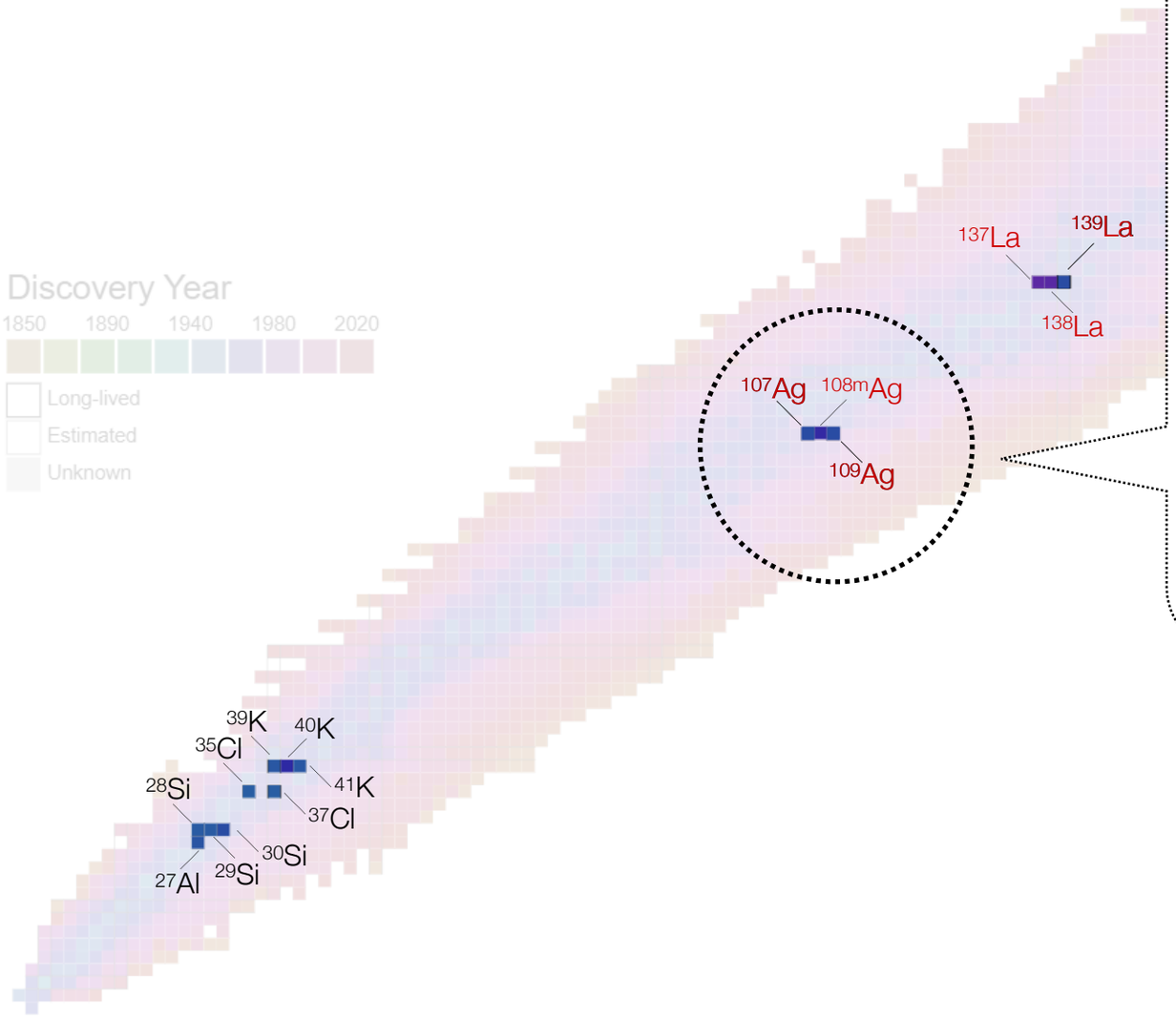

Phys. Rev. Research 6, 033040 (2024)
Nat. Commun. 12, 4596 (2021)
Phys. Lett. B 278, 191 (2014)

Science case
What's next?

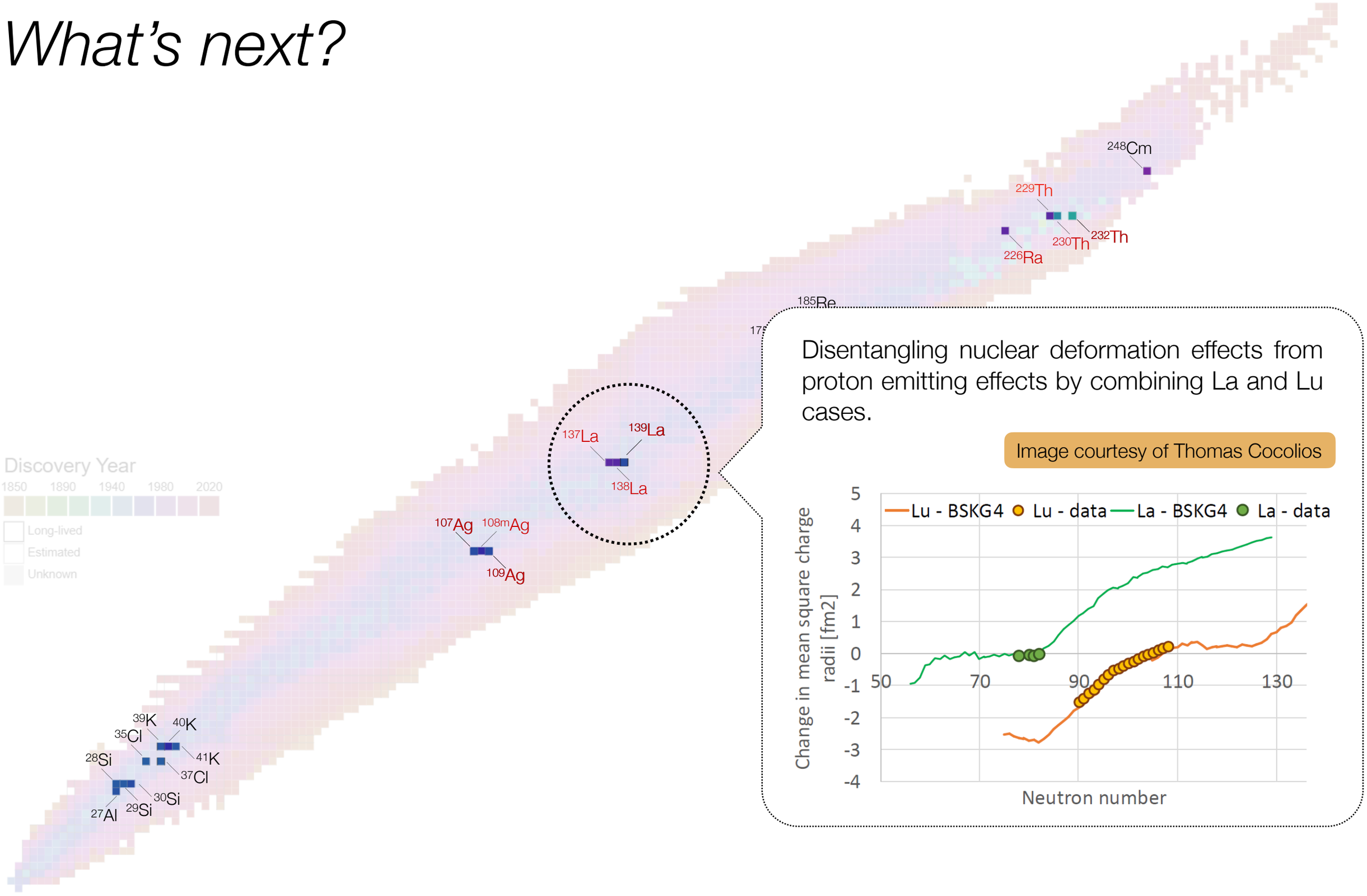

Disentangling nuclear deformation effects from proton emitting effects by combining La and Lu cases.

Image courtesy of Thomas Cocolios

Science case
What's next?

Extracting the Weinberg angle a low Q and probing new physics.

Adapted from Nature 557, 207–211 (2018)

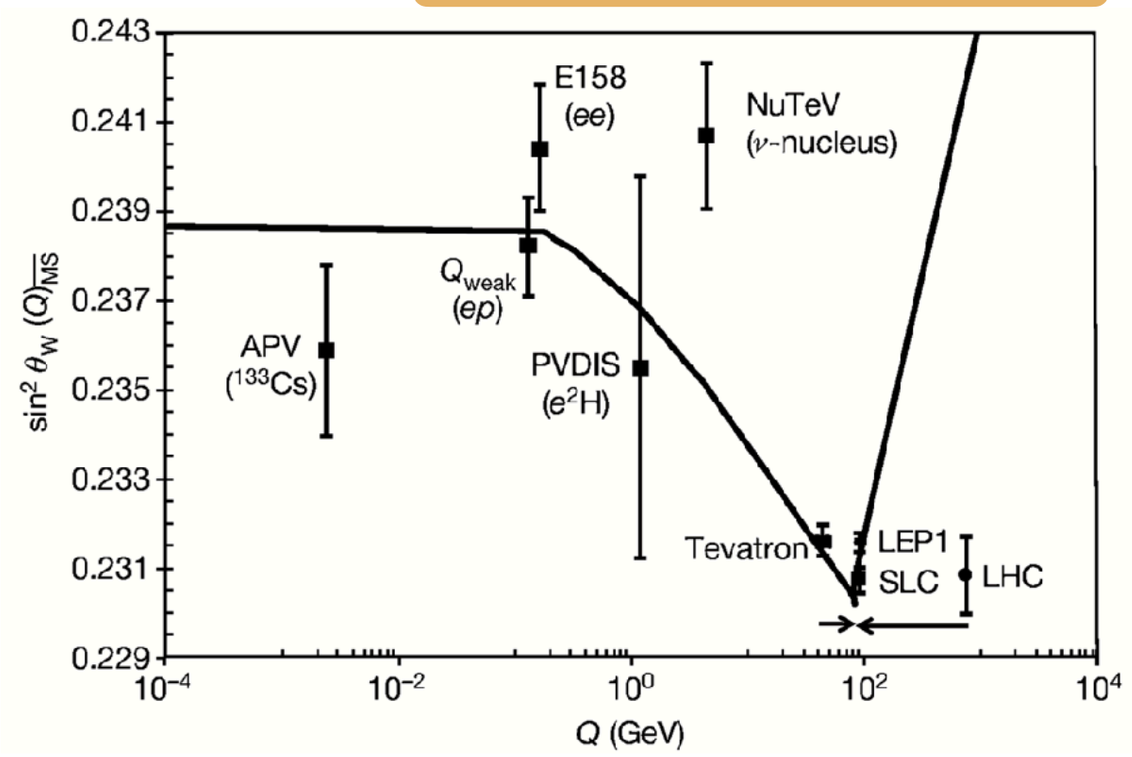

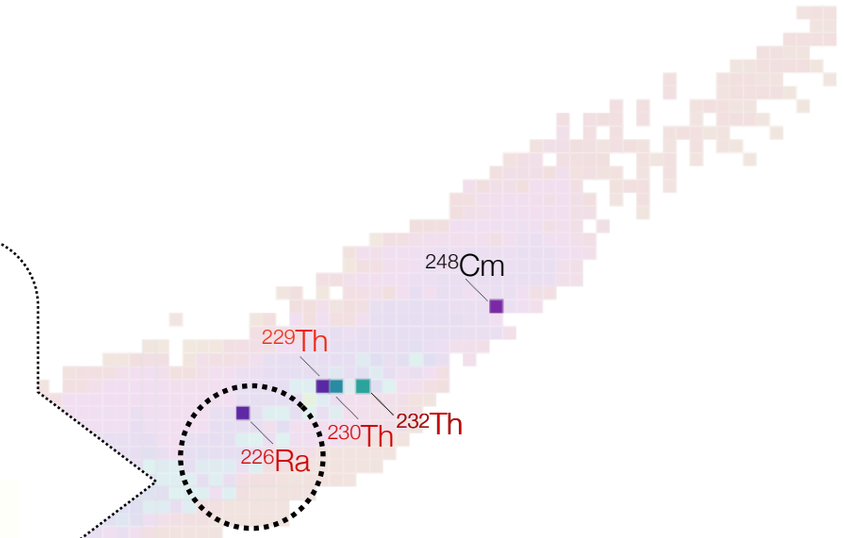

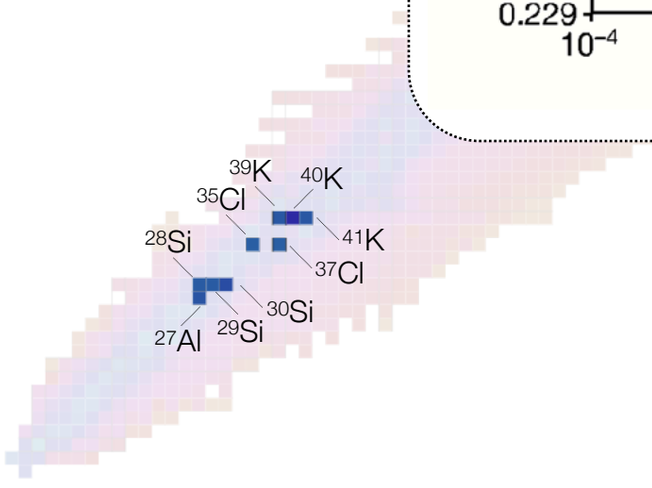

Science case
What's next?

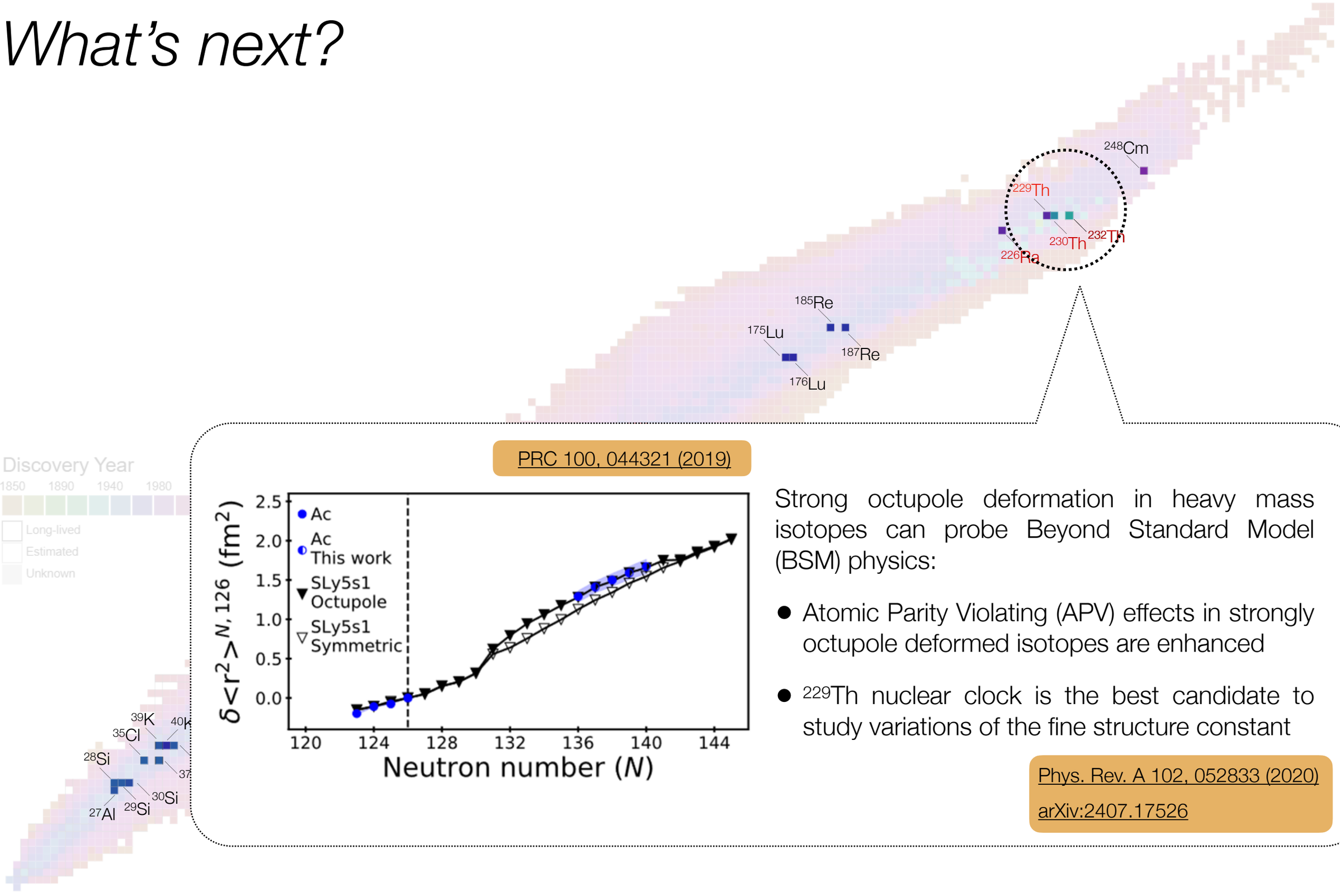

PRC 100, 044321 (2019)

Strong octupole deformation in heavy mass isotopes can probe Beyond Standard Model (BSM) physics:

- Atomic Parity Violating (APV) effects in strongly octupole deformed isotopes are enhanced
- ^{229}Th nuclear clock is the best candidate to study variations of the fine structure constant

Phys. Rev. A 102, 052833 (2020)

arXiv:2407.17526

Science case
What's next?

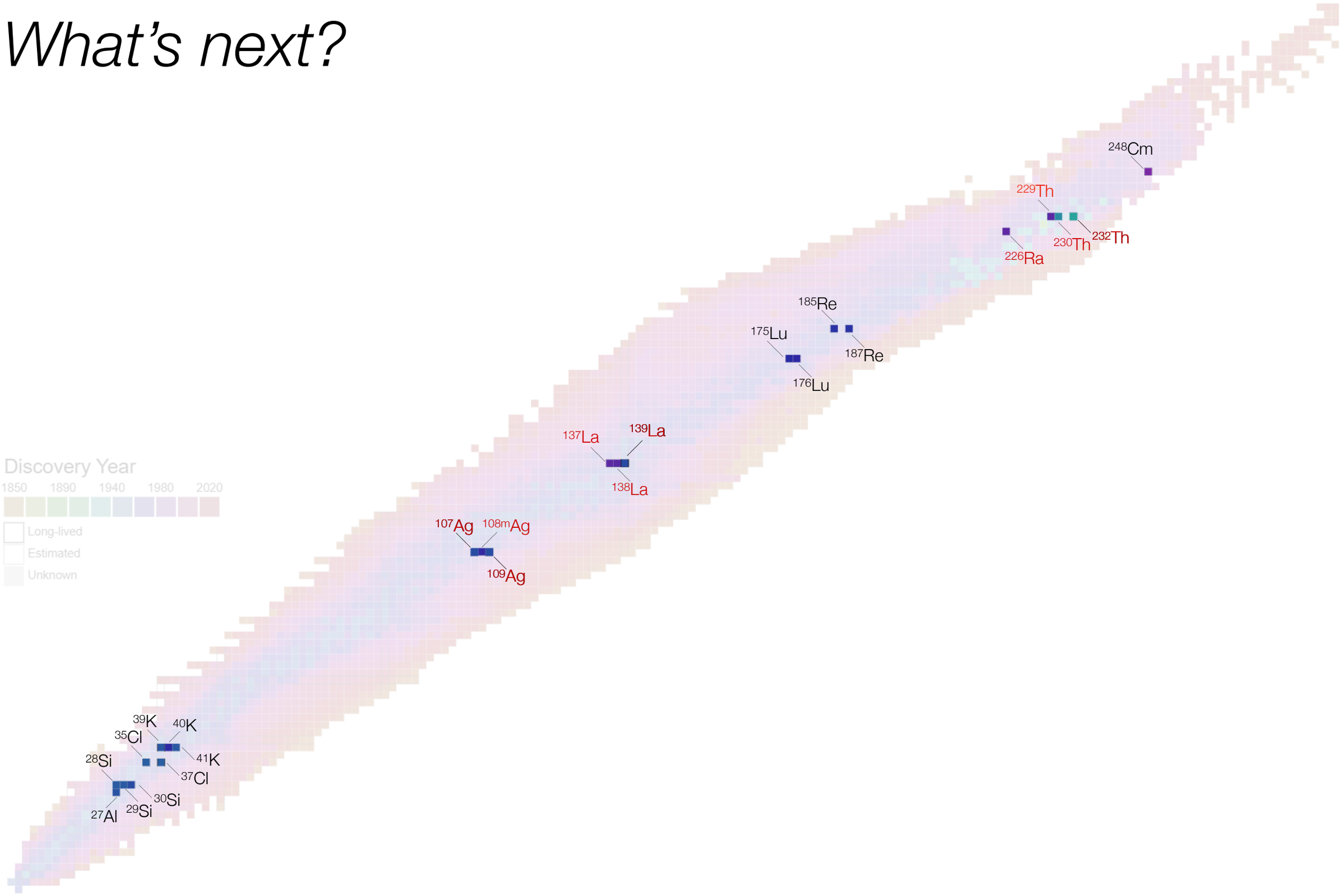

Science case
What's next?